Development of a high-speed capillary electrophoresis assay for the analysis of branched chain amino acids released from 3T3-L1 adipocytes

A THESIS
SUBMITTED TO THE FACULTY OF
UNIVERSITY OF MINNESOTA
BY

Rachel Kay Harstad

IN PARTIAL FULFILLMENT OF THE REQUIREMENTS
FOR THE DEGREE OF
DOCTOR OF PHILOSOPHY

Michael T. Bowser, Advisor

August 2016

Acknowledgements

I would like to start by thanking my graduate school research advisor, Dr. Michael T. Bowser, for the inspiration and guidance that he has provided throughout my career as a graduate student. Joining his research group was the best choice I made entering graduate school and I am so very thankful for the opportunity to be a part of the exciting research going on in the Bowser Lab. Through this research, I was able to develop skills and learn life lessons that are needed to for success in the future—not only as a scientist, but in everyday life. Thank you.

I would like to thank my fellow Bowser group members that I've had the pleasure of working with over the past 5 years, especially Jing Yang, Thane Taylor, Amy Stading, Matt Geiger, Sarah Anciaux, Megan Weisenberger, Kailey Soller, Alex Johnson, and Sean Dembowski. Thank you all for all of the meaningful (and not so meaningful) conversations we've had over the years. Thanks for making the lab a place that I want to come back to everyday.

I would like to thank my professors at the University of Minnesota that I've had the pleasure of interacting with during my time as a student here. I would also like to thank the labs of Dr. Edgar Arriaga and Dr. Christy Haynes, for guidance early on in my graduate career, with techniques our lab was unfamiliar with at the time.

I would like to thank my friends that have always been there for me, whenever I needed a listening ear or a break from reality. All of you have helped shape who I am as a person and I thank you for all the memories we have created over the years.

And last, but certainly not least, I would like to thank my parents, Tom and Sue, for your never ending support and encouragement. Without your support, especially while growing up, I wouldn't have learned to strive to always do my best, and do my best no matter what. Thank you for showing me that hard work does pay-off; without this valuable skill, graduate school would have been nearly impossible to get through. I am forever grateful for your love and support.

Dedicated to my parents and sister:
for their love and support throughout my education.

Abstract

We have developed a high-throughput assay for monitoring branched chain amino acid (BCAA) uptake and release dynamics in 3T3-L1 cells using microdialysis coupled to high speed capillary electrophoresis (CE). Isoleucine, leucine, and valine are important indicators of lipogenesis, as are alanine, glutamate, and glutamine, which are by-products produced through the catabolism of BCAAs. The major focus of this work will be on the development and optimization of a high-speed (high-throughput) CE assay for the separation of fluorescently labeled amino acids; particularly the BCAAs and their downstream metabolites. Development of this assay allows for us to ask important biological questions related to lipogenesis using an *in vitro* cell model. In combination with bulk culture, release and uptake rates of BCAAs were monitored and assessed as a function of various biological stimuli, including several concentrations of glucose, circulating concentrations of BCAAs, as well as insulin and artificial sweeteners. Changes in release profiles were also monitored as cells progressed through the differentiation cycle in order to see if development stage affects lipogenesis.

Table of Contents

List of Figures

List of Abbreviations

2D	Two-Dimensional
3D	Three-Dimensional
Ace K	Acesulfame K+
ANOVA	Analysis of Variance
ATCC	American Type Culture Collection
BAT	Brown Adipose Tissue
BCA	Bicinchoninic Acid
BCAA	Branched Chain Amino Acid
BCKA	Branched chain keto acids
BSA	Bovine Serum Albumin
CAPS	N-Cyclohexyl-3-Aminopropanesulfonic Acid
CE	Capillary Electrophoresis
CoA	Coenzyme A
DMEM	Dulbecco's Modified Eagle Medium
DNP	2,4-dinitrophenyl
EDTA	Ethylenediaminetetraacetate Acid
FBS	Fetal Bovine Serum
FITC	Fluorescein Isothiocyanate
GABA	gamma-Aminobutyric Acid
GC	Gas Chromatography
HPLC	High Performance Liquid Chromatography

HP-β-CD	Hydroxypropyl-β-cyclodextrin
IBMX	3-Isobutyl-1-methylxanthine
LC	Liquid Chromatography
LIF	Laser Induced Fluorescence
LOD	Limit of Detection
MD	Microdialysis
MPER®	Mammalian Protein Extraction Reagent
MS	Mass spectrometry
mTOR	Mechanistic target of rapamycin
MWCO	Molecular Weight Cutoff
NBD-F	4-Fluoro-7-Nitro-2,1,3-Benzoxadiazole
NCS	Newborn Calf Serum
NDA	2,3-Naphthalenedicarboxaldehyde
OPA	O-Phthalaldehyde
PBS	Phosphate Buffered Saline
PMT	Photomultiplier Tube
RFU	Relative Fluorescence Units
RSD	Relative Standard Deviation
SDS	Sodium Dodecyl Sulfate
SEM	Standard Error of the Mean
T-25	Tissue Culture Flasks sized 25 cm^2
TCA	Tricarboxylic acid

WAT	White Adipose Tissue
α-ABA	alpha-Aminobutyric Acid
α-CD	alpha-cyclodextrin
α-KG	alpha-ketogluterate
β-ABA	beta-Aminobutyric Acid
β-CD	beta-cyclodextrin
γ-CD	gamma-cyclodextrin
μFFE	micro-Free Flow Electrophoresis

Chapter 1: Introduction

1.1 Motivation and Cell Models

1.1.1 Obesity

Obesity rates worldwide have more than doubled since 1980; more than 1.9 billion adults are overweight and over 600 million adults are obese as of 2014.[1] Because this disorder has reached unprecedented levels, recent research has focused on understanding how obesity develops and progresses. For many overweight patients, a simple change in energy flux is not enough to reverse the acquired problems. Once basic principles about how obesity develops are understood, we can work to develop methods for prevention and treatment, when diet and exercise are not enough to counteract negative symptoms. Understanding connections between our daily energy intake and development of obesity will also offer insight into the mechanisms of disease development.

The role of adipose tissue in obesity has been scrutinized over the past several decades. For many years, adipose tissue was thought to act only as a storage depot for excess energy taken in during meal consumption.[2,3] Recently, however, it was discovered that adipose tissue acts as an endocrine organ, signaling to other organs to give information about energy balance, appetite, and inflammation.[4-9] In order to understand this signaling mechanism and how it contributes to the development of obesity, it is important to understand the role of adipose tissue throughout the body.

There are two types of adipose tissue found in the body—brown and white (BAT, WAT, respectively).[10,11] Both BAT and WAT store excess energy as triglycerides in lipid vesicles; however, they are much different in appearance. BAT typically has a single,

large lipid vesicle, while WAT has many smaller lipid vesicles. BAT's role in the body is much different than WAT. BAT is the source of thermogenesis,[12,13]while WAT is traditionally thought to be primarily used for longer term storage, housing triglycerides until they are mobilized for use in gluconeogenesis.[2,3] Recently, WAT been shown to release small molecule messengers that play an important role in signaling throughout the body including signaling to the pancreas, muscle, and the brain.[14-16]

Those who are overweight or obese have an increased percentage of WAT throughout the body as compared to lean muscle mass. This increase can be attributed to expansion of adipocytes from increased lipid storage, as well as an increase in the number of total adipocytes. Humans who are obese have a higher total adipocyte number than lean individuals.[5,17,18] Recently, it was discovered that new adipocytes can be formed throughout life,[17] however, it is not well understood what contributes more to obesity, adipocyte size or number.

Due to expansion of the adipose tissue, the cells undergo molecular changes in metabolism. These changes include physical expansion of the adipocytes, increased free fatty acid release from adipocytes, and increased production and release of inflammatory and other energy regulating hormones.[5] Physical expansion of both individual cells, as well as adipose tissue, may play a critical role in the development of disease and cellular dysfunction.[5] Excess adipose tissue, as seen in those who are obese, has been linked to type-2 diabetes, heart disease, high blood pressure, and can lead to increased risk of development for many types of cancers, including breast cancer and colon cancer.[5]

Adipocytes secrete many hormones and cytokines that serve as signaling messengers throughout the body.[4,8,9,19,20] Having excess adipose tissue oftentimes causes patients to develop resistance to insulin and leptin, two hormones important for regulation of energy balance.[4,5,8,21,22] Dysregulation of the secretion of these hormones, along with the small molecules released, may play an important role in the development of obesity and other metabolic diseases.[23]

1.1.2 **Branched Chain Amino Acids**

The branched chain amino acids (BCAAs), isoleucine, leucine, and valine (Figure 1.1) are important signaling molecules throughout the body. BCAAs have been identified as an important group of small molecules regulated by adipocytes. These BCAAs are essential amino acids and not easily metabolized by the liver.[24] There is evidence to suggest that these amino acids in particular, play a role in the development of obesity and obesity related diseases.[25] BCAA receptors can be found throughout the body and BCAAs are highly regulated in adipose tissue. Adipose tissue regulates whole body BCAA concentrations as a signal to other organs about the state of energy balance in adipose.[26-29]

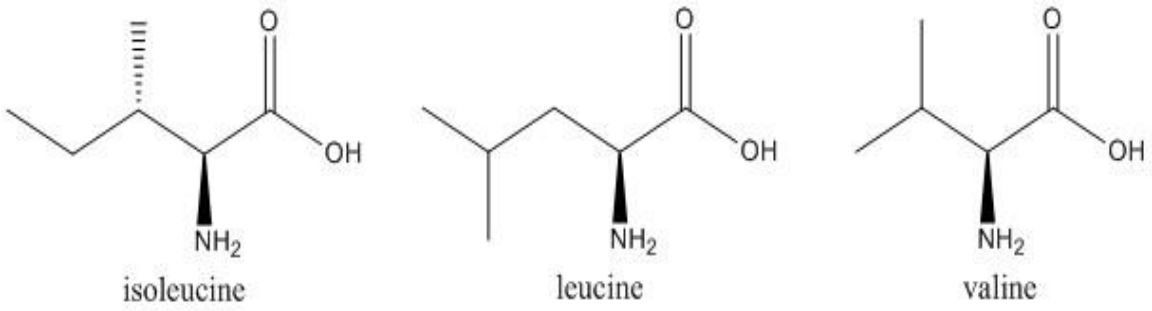

Figure 1.1. Molecular structures of the branched chain amino acids.

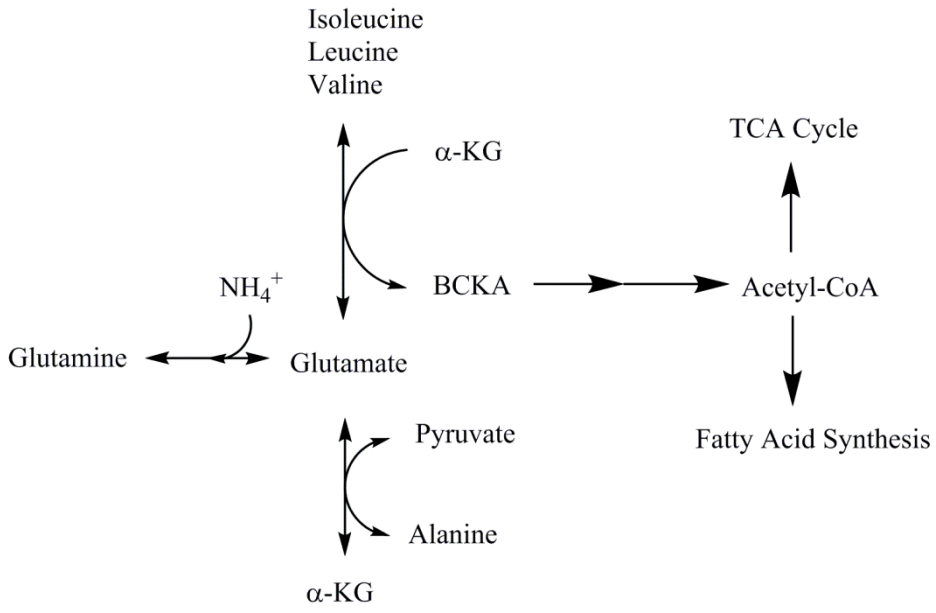

Figure 1.2. Pathways involved in the catabolism of BCAAs. BCAAs + α-ketoglutarate (α-KG) produces branched chain keto-acids (BCKAs) and glutamate. The BCKAs are further metabolized to acetyl-CoA, where it either goes to the TCA cycle or fatty acid synthesis pathways, depending on the cell's energy needs.

BCAAs are controlled in adipose tissue through catabolism, which feeds into the lipogenesis cycle and the production of tricarboxylic acid (TCA) cycle or fatty acid synthesis intermediates (Figure 1.2).[26-29] Recent studies have shown that 3T3-L1 cells catabolize isoleucine and leucine to generate nearly one-third of the acetyl-CoA used in the TCA cycle.[30] When energy is readily available, excess energy is stored as triglycerides in lipid vesicles, where it can be easily mobilized when cellular energy is low.

It is known that BCAAs are found in higher concentrations in those who are overweight and obese.[26-28] It has also been shown that leucine stimulates the release of leptin from adipocytes.[31-33] Overstimulation of the adipocytes, thus, increased release of

leptin from adipocytes, may lead to the development of resistance to this important hormone. In addition to leucine, it has also been shown that high concentrations of glucose and L-alanine influence leptin release from adipocytes.[25,32]

1.1.3 **Obesity Models**

Obesity can be studied *in vitro* or *in vivo*, using many different cell and animal models, including human patients.[34-37] While both *in vitro* and *in vivo* models have their distinct advantages and disadvantages, an *in vitro* design is simple and allows for basic knowledge discovery. 3T3-L1 and 3T3-F442A cell lines are the two most popular models used for studying obesity *in vitro*.[38] The 3T3-L1 cell line was isolated from parent mouse 3T3 cultures after identifying colonies with a lipid accumulating phenotype once cells reached confluency.[39] Previously, Thomson et al. used 3T3-L1 cells to study the development of insulin resistance,[40] while Tremblay et al. used 3T3-L1 cells to study activation of the mammalian target of rapamycin (mTOR) pathway and its effects on insulin signaling.[41] More recently, 3T3-L1 cells were used to study the catabolism of BCAAs and their corresponding contribution to odd or even-chain fatty acids.[42] Differentiation is fairly straightforward and has been optimized in order to achieve full differentiation into mature adipocytes.[43,44]

1.2 **Microdialysis**

1.2.1 **Microdialysis Probe Design and Function**

Microdialysis probes are created by sealing two capillaries inside of a regenerated cellulose, hollow fiber dialysis membrane, in either a side-by-side, concentric, loop, or

linear arrangement.[45] Figure 1.3 shows the side-by-side configuration of a microdialysis probe. The hollow fiber tubing is porous and acts as a membrane that filters out large, complex biological samples, only allowing molecules with molecular weights less than the molecular weight cut off (MWCO) to diffuse through. Hollow fiber dialysis tubing is available with various MWCO thresholds, in order to be used with a wide variety of target substrates.

Figure 1.3. Side-by-side microdialysis probe. Perfusate is pushed through capillary A. Small molecules diffuse from the extracellular space through the membrane into the perfusate. The perfusate is then pushed out through capillary B, as dialysate.

This probe is most often inserted into the tissue of interest and perfused with a solution that closely matches the surrounding extra-cellular matrix, called perfusate. The perfusate flows in through the inlet capillary (Figure 1.3, A). Analytes present in the tissue diffuse across the dialysis membrane, and are recovered. Perfusate flowing in through the inlet capillary pushes the solution out of the sampling region and out through the outlet capillary (Figure 1.3, B). This outlet stream, termed dialysate, is moved out of the capillary and contains a fraction of the molecules present in the extracellular matrix and can be used for analysis. Perfusate is pushed through the capillaries at very

low flow rates to ensure small molecules move across the membrane based on the concentration gradient.[46]

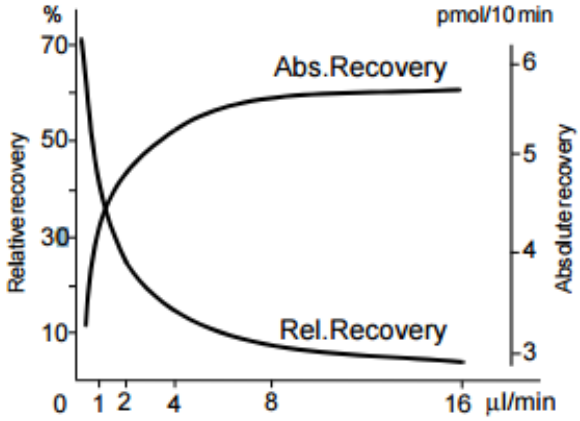

Figure 1.4. Relative and absolute recoveries for a microdialysis probe, plotted as a function of flow rate. Adapted from Reference 51.

1.2.2 **Recovery and Resolution**

Absolute quantification of analytes in tissues is difficult when using microdialysis sampling. Equilibrium between the perfusate and surrounding cellular matrix is never established because the perfusate is constantly being pushed through the microdialysis probe, even at typical, slow flow rates (0.1-1 µL/min). Thus, concentrations of recovered analytes collected are proportional to each other, but are a fraction of the actual concentrations found in the tissue matrix.[45,47-49]

In order to quantitatively determine analytes present in the tissue matrix, recovery rates for each probe must be established. Under the assumptions that the concentration outside of the probe is proportional to the concentration in the dialysate, the recovery can be determined under a set of experimental conditions. There are two types of recovery commonly associated with microdialysis: relative recovery and absolute recovery.[50] Absolute recovery is a rate indicating how much analyte is recovered per a given amount of time. Relative recovery compares the concentration of analytes in a solution that have diffused through a probe to the concentration of analytes in the same solution when that solution is pumped directly into the analytical detection method. These recoveries are

sensitive to the flow rate of perfusate through the microdialysis probe. As higher flow rates through the microdialysis probe are used, absolute recovery increases, while relative recovery decreases, as shown in Figure 1.4.[51] Peak heights of each analyte are compared to determine the relative recovery of the corresponding analyte.[52] The extraction efficiency is the ratio between gain of analytes in the dialysate and loss of analyte from the surrounding matrix:

$$Extraction\ Efficiency = \frac{C_d - C_i}{C_e - C_i} \qquad (1.1)$$

where C_d is the concentration of analyte in the dialysate, C_i is the concentration in the perfusate, and C_e is the concentration in the surrounding matrix. C_i=0 (essentially) when performing recovery experiments, and thus, the extraction efficiency becomes identical to the relative recovery. The following equation (1.2) has been widely accepted as the mathematical expression used to describe relative recovery:[53]

$$Relative\ Recovery = 1 - exp^{\left(\frac{1}{Q_d(R_d + R_m + R_e)}\right)} \qquad (1.2)$$

where Q_d is the flow rate of the perfusate, R_d, R_m, and R_e are the resistances of the dialysate, cellulose membrane, and extracellular matrix space, respectively. The resistance of the cellulose membrane is dependent on probe dimensions, including sampling region, the molecular weight cut-off of the membrane, and the diffusion coefficient of the analytes of interest. R_d and R_m account for the diffusion of the analytes in the dialysate and membrane, respectively, while R_e takes into consideration the diffusion rate of analytes in the extracellular space.[53-56]

Relative recovery of analytes depends on many factors including flow rate, diffusion coefficient of the analyte across the membrane; length and diameter of the membrane, diffusion coefficient of analyte within the dialysis membrane; and chemical interactions between the analytes and the membrane.[45,57,58] The length and diameter of the membrane can affect a probe's relative recovery since probes with larger sampling regions have more area for the analytes to diffuse through, which increases the recovery of analytes.[59-61]

Relative recovery of microdialysis probes must be determined to obtain quantitative analyte information. To do so *in vitro*, the probe can be calibrated by immersing the probe in solutions of known concentrations, obtaining the signal, and subsequently creating a calibration curve. This would be compared with the signals that are obtained through direct injection of the same concentration of analytes into an analysis system, without using microdialysis.[47,62,63] However, this *in vitro* calibration method may not be representative of the recovery actually attained *in vivo*, so using *in vivo* calibration methods may be necessary to accurately describe probe recovery.[64-66] *In vivo* probe recoveries are typically lower than those obtained *in vitro.* This is most likely due to the complexity of the tissue and extracellular matrix, which includes fewer direct paths to the microdialysis probe as well as release and uptake of molecules during the sampling period.[67]

In order to more accurately calibrate probes *in vivo,* several methods have been developed, including: variation of perfusion flow rates[66] ("zero flow"),[68] no-net-flux,[69] and retrodialysis.[37, 38] The no-net-flux method is the most commonly used calibration

method used *in vivo*.[60,70] These experiments take a long time to perform because the probe is perfused with different concentrations of the analyte of interest, until there is no change in concentration of the analyte between the perfusate and dialysate. To determine the relative recovery, the change in dialysate concentration is plotted versus the initial perfusate concentration, and the slope of the line is the relative recovery, while the x-intercept is the extracellular concentration of the analyte of interest.[60] Because the no-net-flux experiments take so long to conduct, a retrodialysis method can be used instead. This is a delivery experiment where an analyte that is of no interest is added to the perfusate. This analyte should have similar properties to the analyte of interest in order to get accurate recovery data.[60] The perfusate with this molecule is then flushed through the microdialysis probe and concentration of the dialysate is measured.

Other factors limiting the capabilities of microdialysis are the temporal and spatial resolutions that can be attained. The spatial resolution is determined by the size of the sampling region on the probe (1-5 mm typically, *in vivo*). Probes are oftentimes operated at slightly higher flow rates to increase absolute recovery. This is leads to depletion of compounds in areas directly around the probe at a more rapid rate, inducing a concentration gradient that can extend for several millimeters away from the probe, decreasing the spatial resolution.[65] Spatial resolution is a serious factor *in vivo*, because of damage to surrounding tissue upon implantation of the probe.

Temporal resolution is defined as the time it takes an analytical system to respond to step changes in in analyte concentrations. Temporal resolution affects both *in vivo* and *in vitro* studies, as well as online and offline coupling of microdialysis to an analytical

system. Overall, the temporal resolution that can be attained is affected by factors related to capabilities of the analytical system being used, as well as flow rates through the microdialysis probe.[46] Using slower flow rates increases relative recovery, however, slows down the rate at which sufficient sample volume can be collected, thus decreasing temporal resolution. If biological processes are slower than the sampling and analysis time, it is possible to detect changes in abundance as a function of time; however, it may not accurately represent dynamics of the system. When this is the case, the temporal resolution is defined as the time required for the signal to increase from 10-90% of the maximum signal intensity.[70]

1.2.3 **Microdialysis Coupled to Analytical Systems**

In order to couple microdialysis to the analytical system, offline samples can be collected or the probe can be directly coupled to the system for online analysis. Despite many of the limitations mentioned previously, microdialysis is widely utilized to as a sampling method and has been coupled online to CE, LC, and MS, along with other analytical methods.[54]

CE is an analytical separation method that separates molecules based on their mobility in an electric field. The mobility of a molecule is determined by a molecule's charge to size ratio.[71] Jorgenson *et al.* were the first group to report using CE for analytical separations.[72] In their work, they used glass capillaries that were 80-100 cm in length and were moved manually from buffer to sample containing reservoirs. Separations of fluorescently labeled amino acids, amines, and dipeptides were accomplished in 10-30 min. Since that paper, there have been many advances in the field

of CE in order to automate sample injection, improve temporal resolution, and decrease separation time.

Hogan and Lunte were the first to report direct, online coupling of CE to microdialysis.[47] This report was the first to show how coupling microdialysis to CE can improve temporal resolution and used an interface that created samples from a continuous sampling method. In order to accomplish this, Hogan *et al.* designed an interface on a microscope slide. They aligned the separation and reaction transfer capillaries in a reservoir containing the run buffer. This set-up allowed for discrete samples to be injected into the separation capillary, allowing for online analysis. Temporal resolution of 90 s was achieved for measuring the pharmacokinetics of 3-amino-1,2,4-benzotriazine 1,4-di-N-oxide *in vivo.*[47]

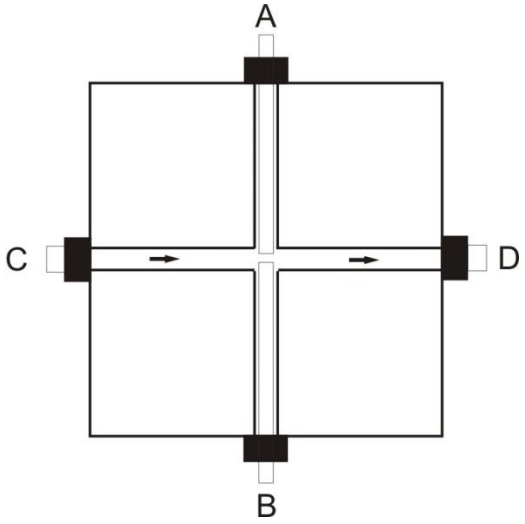

Figure 1.5. Flow gate interface developed by Jorgenson. Dialysate from the microdialysis probe enters through capillary A, which is the reaction capillary, B is the separation capillary, C is the inlet of buffer flow, and D is the outlet that goes to waste.

In order to further improve temporal resolution, Jorgenson and Hooker designed a transparent flow gate in 1997, as depicted Figure 1.5, for use as a routine and reproducible interface between micro-HPLC and capillary zone electrophoresis (CZE).[73] The transparent design allowed for alignment of capillaries in the polycarbonate block. The flow gate holds the reaction (A) and separation capillaries (B), with an

approximately 50 μm gap between them. Separation buffer flows across this gap. During a separation, the separation buffer flows through the flow gate and carries any sample from the reaction capillary to waste. To perform an injection, flow across the flow gate is stopped by a pneumatically actuated valve, and a sample plug fills the gap between the capillaries. An injection voltage is applied, which draws the sample plug into the separation capillary. After the injection is completed, flow of the separation buffer across the flow gate resumes, and a separation voltage is applied.

This design allowed for coupling of microdialysis with high-speed analytical methods, and its usefulness has been demonstrated in various applications.[46,74-76] The flow gate interface allows for discrete sample plugs to be injected into the separation capillary for CE separation.[47,73] Using this set-up, fast separations (~30 s) with high temporal resolution can be achieved, even with low flow rates during microdialysis.[73]

CE is an ideal separation technique to couple with microdialysis because it is especially powerful when analyzing biological samples, which typically have very small sample volumes. Online CE coupled to microdialysis can provide great temporal resolution of analytes in samples because smaller volumes used for separations allow for slower flow rates to be used during the sampling.[77,78] Temporal resolution is also improved when microdialysis is coupled to CE because rather than the resolution of analytes being dependent on the injection volume and flow rate of perfusate, it is dependent on analysis time.[47,54,79]

Lada and Kennedy were able to improve temporal resolution (from 3 min to 45 s), while still achieving high recovery of a number of analytes. The improved temporal

resolution was accomplished by coupling microdialysis to CE with laser induced fluorescence detection and online derivatization. The flow rate used during these experiments was 79 nL/min, compared to a typical flow rate 0.1-1 µL/min, of which allowed for higher relative recoveries than had been attained previously.[80]

1.2.4 **Detection of analytes**

Small concentrations of analytes are often collected when sampling a biological matrix using microdialysis because only a fraction of analyte is collected. Because concentrations are so small, a sensitive detection platform needs to be incorporated into the analysis scheme.[81] Laser induced fluorescence (LIF) is used for the detection of fluorescent molecules. LIF works by exciting a molecule to a higher energy state using laser light. This causes the spontaneous emission of light, which is detected by a photo multiplier tube (PMT) or other detector. LIF is a very sensitive detection method and is therefore useful when trying to detect small amounts of analytes.[82] Previously, Chen and Dovichi were able to detect 50 yoctomoles of rhodamine 6G, using LIF detection, showing the sensitivity of the technique.[83]

Molecules oftentimes need to be derivatized with a fluorescent tag because they are not natively fluorescent. Many fluorescent tags have been developed for the detection of amino acids and other small molecules, including 2,4-dinitrophenyl (DNP), napthalene-2,3-dicarboxyaldehyde (NDA), o-phthaldialdehyde (OPA), and FITC.[84-86] The fluorescent labels each selectively bond to a moiety on the analytes of interest. This allows for the detection and analysis of a particular class of analytes, while eliminating interference from unwanted signals. Reducing these interferences improves efficiencies,

gives higher plate counts, and lower limits of detection.[87] The limit of detection is defined as the smallest amount of analyte that produces a signal significantly different than a blank solution. That value corresponds to three times the standard deviation of the baseline signal.[87]

OPA, and NDA, are compatible for use with microdialysis-CE because they react readily at room temperature, under basic aqueous conditions, within 1 minute.[88] At one time, OPA was the most commonly used labeling reagent for microdialysis-CE assays, however, OPA labeling is unstable and photobleaching occurs readily.[85] OPA requires a

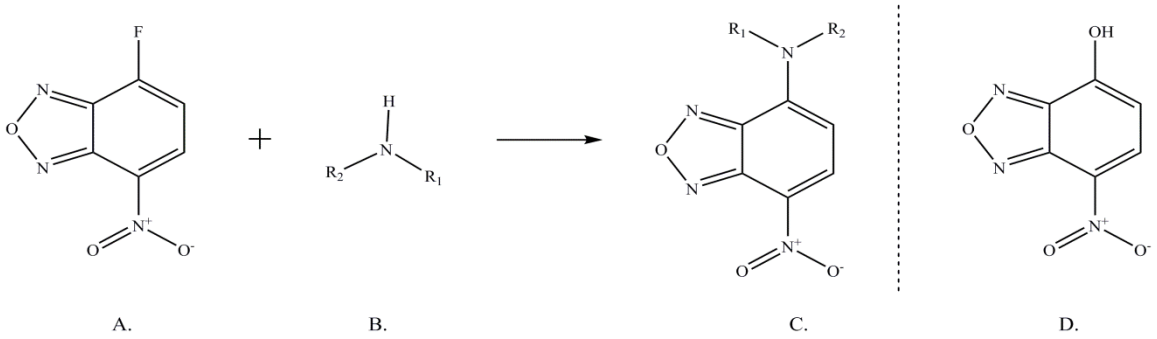

Figure 1.6. NBD-F labeling reaction. NBD-F (A) reacts with primary and secondary amines (B) to produce fluorescently tagged analytes(C) are detected using LIF at 488 nM excitation. A by-product (D) is produced by the hydrolysis of NBD-F.

special UV laser due to its absorption in the UV spectrum as well as special optics. In addition, it also has poor limits of detection compared to other reagents.[89] 4-Fluoro-7-Nitro-2,1,3-Benzoxadiazole (NBD-F) was used by early Bowser group members as an alternative to OPA derivatization for detection of neuroamines using microdialysis-CE (Figure 1.6). NBD-F reacts efficiently with primary and secondary amines and has an optimum excitation wavelength of ~ 470 nM, compatible with common 488 nM lasers.

Optimization of the derivatization conditions has been previously reported for use in assays using microdialysis-CE.[90]

Although this method has proven successful for derivatization of amines, it is not without its drawbacks. One major disadvantage to this derivatization method is the reaction by-product that is produced. The reaction by-product produces a large peak in the middle of the electropherograms and without optimization of the separation, may obscure analyte peaks. Experimentally, the derivatization step in our experimental set-up occurs when the dialysate is allowed to react with an NBD-F solution in a reaction tee prior to the flow gated interface. This derivatized sample then flows in a heated reaction capillary to push the reaction to completion and passes through the flow gate interface for injection into the separation capillary and detection in the sheath flow cuvette.[90]

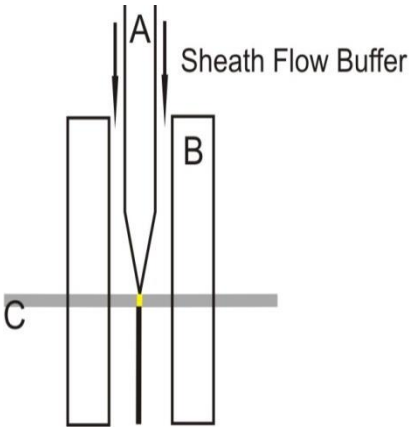

Figure 1.7. Sheath flow cuvette used to improve sensitivity of LIF detection. Fluorescent (native or derivatized) sample flows through the separation capillary (A) and into the sheath flow cuvette (B). Sheath flow buffer flows around the capillary, through the cuvette. A laser line (C) is focused just past the exit of the capillary exciting the sample.

As a way to improve sensitivity, sheath flow cuvettes can be used (Figure 1.7). The sheath flow cuvette houses the exit of the separation capillary and sheath flow buffer flows through the cuvette and around the capillary. Sheath flow cuvettes are designed based on cuvettes used in flow cytometry.[91] Typical dimensions of cuvettes are 2 mm square with a 400 µm × 400 µm square inner bore. The cuvette is made from fused silica and the buffer flowing

through the cuvette matches the refractive index so that the sample is hydrodynamically focused as it exits the separation capillary.[92] It is important that flow out of the separation capillary and through the sheath flow cuvette maintain a laminar profile so that detection can be performed just past the tip of the separation capillary. The fluorescently labeled sample is excited with a laser line and is collected through a microscope objective, passed through a series of filters, and is then focused onto a PMT. Using a sheath flow cuvette reduces light scattering that normally occurs with on-capillary detection. This advantage, plus the optical set-up which uses a pinhole filter, which eliminates background signal, allows for very low detection limits[92,93]. Using this technique, Chen and Dovichi were able to analyze picomolar solutions, corresponding to attomoles injected, of amino acids.[86,93] Amino acids were labeled using FITC (fluorescein isothiocyanate) and were then injected into the CE system. Mass detection of arginine was 9×10^{-21} moles.[93] This detection limit shows the power of using the sheath flow detection system because it allows for the detection of small analyte concentrations found in biological samples.

1.2.5 **Biological applications of Microdialysis**

Microdialysis is one of the most commonly used sampling methods for *in vivo* analysis and has been used for monitoring small molecule flux in the brain for decades.[94-101] Recently, microdialysis has been more broadly used to study other tissues, including adipose, liver,[102] heart,[103] stomach,[104] and ears.[105] Microdialysis experiments allow for the study of pharmacokinetics, metabolism,[96-98] toxicology,[106,107] and drug delivery,[99-101] in various tissues because of the intrinsic small sampling size and quick sampling rate.

Typically, microdialysis is coupled to fraction collection, followed by offline analysis, giving temporal resolutions of 10 – 30 min.[46,47,108] When microdialysis is directly coupled to an analytical system, these temporal resolutions can be dramatically improved.[46] When coupled to an online analysis method, the temporal resolution is only limited by analytical separation speed, sample volume requirements, and the limits of detection for the system. Coupling microdialysis to capillary electrophoresis (CE) is ideal due to the small volumes required for CE separation and analysis. 5-10 second sampling rates paired with 10-30 second temporal resolution has been achieved after coupling microdialysis to a CE system.[74,109,110] The ability to monitor analytes on this timescale is something that very few instrumental set-ups can achieve and the near real-time analysis of low concentration analytes makes this instrumental combination ideal for *in vivo* studies.

CE is one of only a few analytical systems able to monitor 20+ analytes on a 30 second time scale. This type of temporal resolution allows for *in vivo* events to be monitored at near real-time. Furthermore, chemical release events, such as a response to a stimulus, can be easily performed and monitored using microdialysis. Although microdialysis has had such success for *in vivo* studies, *in vitro* applications have not been utilized to their full extent. Previously, microdialysis has been used with cell suspensions[111] or with tissue slices,[112-114] however, dilution of analytes was problematic and results in temporal resolutions of 10-20 min.[16,17,20] More recently, Hogerton and Bowser, successfully cultured C8-D1A astrocytic cell clones on the surface of microdialysis probes in order to eliminate the need for fraction collection and improving

temporal resolution.[115] This allowed for near real-time analysis of the cellular response to potassium stimulations, while simplifying a full, *in vivo* model to a cellular model.

1.3 **Scope of Thesis**

Obesity has become a worldwide epidemic and little is understood about the development of the disorder. It is understood that adipose tissue regulates whole body BCAA levels. Dysregulation of this process has been linked to the development of obesity. BCAAs are also known to be important signaling molecules, involved in many energy related biological processes. In order to understand what biological factors influence the development of obesity, a high throughput MD-CE assay was developed. Development of this assay allows for the collection of large amounts of experimental data. This is highly important so that we can push the knowledge barrier in biological systems, such as 3T3-L1 adipocytes and other obesity models, where basic knowledge is lacking.

In this work, we describe a novel separation assay, capable of monitoring 25+ amines, many of which were previously unable to be separated. Chapter 2 describes the optimization of this high-speed CE separation assay for analysis of BCAAs released from 3T3-L1 cells. Optimization of all separation conditions allows for the detection of changes in BCAA release in adipocytes, as well as downstream lipogenesis metabolites, over various lengths of time. These experiments proved to be useful not only as a proof of concept, but provided temporal information about the cellular processes we were interested in, namely lipogenesis.

Once this temporal information was established, further experiments were performed to investigate how local concentrations of BCAAs affect lipogenesis as the cells mature from a pre-adipocyte state to fully differentiated adipocytes. This information is presented in Chapter 3.

Investigation of how local glucose concentrations affect lipogenesis at various cell differentiation stages was investigated in Chapter 4. This allows us to see the influence that each energy substrate (glucose or BCAAs) has on 3T3-L1 adipocytes throughout differentiation. Cellular preference toward one particular energy substrate may indicate or give insight about other cellular processes the cells are undergoing as they mature into full adipocytes.

Chapter 5 presents preliminary work into the investigation of how insulin affects lipogenesis in 3T3-L1 adipocytes. Additionally, preliminary work investigating the influence of various sweeteners found in our everyday diets is presented.

Chapter 6 provides a summary of the work and presents opportunities for future directions using the developed technology.

Chapter 2: High-Speed Microdialysis - Capillary Electrophoresis Assays for Measuring Branched Chain Amino Acid Uptake in 3T3-L1 cells

2.1 **Summary**

We have developed a high-throughput microdialysis-capillary electrophoresis (MD-CE) assay for monitoring branched chain amino acid (BCAA) uptake/release dynamics in 3T3-L1 cells. BCAAs (i.e., isoleucine, leucine, and valine) and their downstream metabolites (i.e., alanine, glutamine, and glutamate) are important indicators of adipocyte lipogenesis. To perform an analysis, amino acids were sampled using microdialysis, fluorescently labeled in an online reaction, separated using CE, and detected using laser induced fluorescence (LIF) in a sheath flow cuvette. Separation conditions were optimized for the resolution of the BCAAs isoleucine, leucine, and valine, as well as 13 other amino acids including ornithine, alanine, glutamine, and glutamate. CE separations were performed in <30 s and the temporal resolution of the online MD-CE assay was <60 s. Limits of detection (LOD) were 400, 200, and 100 nM for isoleucine, leucine, and valine, respectively. MD-CE dramatically improved throughput in comparison to traditional offline CE methods, allowing 8 replicates of 15 samples (i.e., 120 analyses) to be assayed in <120 min. The MD-CE assay was used to assess the metabolism dynamics of 3T3-L1 cells over time, confirming the utility of the assay.

2.2 **Introduction**

Adipocytes are usually considered as merely storage depots for triglycerides. Recent discoveries have changed this thinking demonstrating that adipose tissue participates as an endocrine organ, actively modulating chemical messengers involved in energy regulation, appetite and inflammation.[4-9] Amino acids act as primary, small molecule messengers in adipose tissue, much like hormones in the endocrine system.[14-16,116,117] Of particular interest are the branched chain amino acids (BCAAs): isoleucine, leucine, and valine. These BCAAs are essential amino acids and not easily metabolized by the liver.[24] As such, their circulating concentrations rise significantly after a high protein meal, signaling that energy is abundant and stimulating growth. BCAA receptors are widespread throughout the body and regulate many energy related functions including insulin secretion in the pancreas, protein synthesis in muscle, and appetite control in the brain.[14-16] The heart and kidney are also known to metabolize BCAAs.[118,119] The BCAAs are necessary precursors for the TCA cycle and adipocytes therefore must uptake isoleucine, leucine, and valine to support lipogenesis.[24,116,117] Recent evidence suggests that adipocytes regulate circulating BCAA concentrations through this uptake, relaying a message to the rest of the body

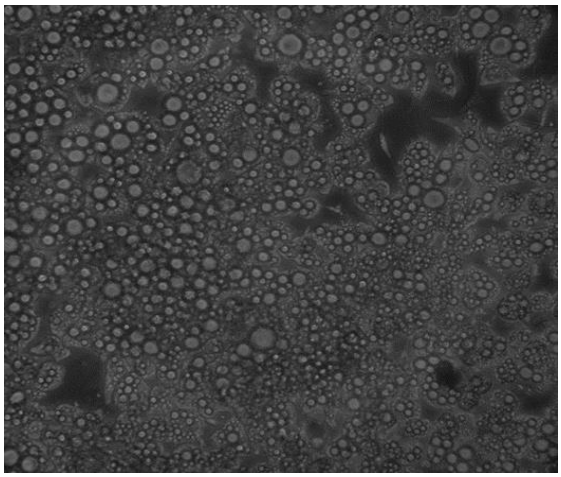

Figure 2.1. Brightfield image of fully differentiated 3T3-L1 cells. Cells show lipid accumulation, confirming successful differentiation.

regarding the state of energy balance in adipose tissue.[26-29] Measuring BCAA uptake therefore provides information regarding both the internal metabolic activity of adipocytes as well as the message they are sending to other tissues involved in energy regulation. The dysregulation of BCAAs has been correlated to obesity, diabetes, and a range of other metabolic disorders.[6,7,116,117,120]

A number of methods have been developed for the analysis of BCAAs. Yang *et al.* developed a two minute LC/MS/MS assay for measuring amino acids in serum.[121] Limits of quantitation were 0.7, 2.6, and 0.3 µM for isoleucine, leucine, and valine, respectively. GC/MS was used by Perez-Cornago for the analysis of amino acids in human serum, with analysis times well over one h per sample.[122] Other methods for the analysis of BCAAs include GC,[123-125] LC,[27,125,126] as well as CE with various detection methods.[127-129] Many of these methods require expensive instrumentation, complicated sample preparation or offline derivatization steps. A simple, high-throughput assay for BCAAs would be beneficial.

Microdialysis is a common technique for sampling small molecules from biological tissues.[54] A microdialysis probe consists of a short length of hollow fiber, semi-permeable membrane connected to two capillary lines in a side-by-side, loop or linear arrangement.[45] Small molecule analytes are able to cross the membrane entering the dialysate while larger molecules and cell fragments are excluded.[46] Typically, the probe is implanted into the tissue of interest and perfused with an electrolyte that mimics the extracellular fluid. Dialysate is collected in fractions and analyzed offline allowing changes in analyte concentrations to be monitored over time. Low perfusion rates and

minimum fraction volumes typically yield temporal resolutions of 10-30 min in offline MD assays.[46-48,76,108] The Lunte and Kennedy groups demonstrated that coupling MD with an online reaction and high-speed CE analysis dramatically improves temporal resolution.[46-48,76] Temporal resolutions as low as 3 sec have been reported for amine neurotransmitters.[74] MD-CE assays have been developed for a range of amines including glutamate, aspartate, GABA, glycine, taurine, glutamine, D-serine and many others.[78,79,90,130-132] To the best of our knowledge no previous MD-CE assay has been reported that is able to resolve the BCAA's. Online MD-CE assays have largely been applied to *in vivo* measurements.[78,131] Our group has demonstrated examples of *ex vivo* (salamander retina and mouse cortical slices)[133,134] and *in vitro* (C8-D1A astrocytes)[115] applications. We have also demonstrated that online MD-CE can be used as a high throughput approach for the analysis of D-serine in tissue homogenates.[130] In this case, the MD probe acts as an efficient mechanism for introducing a series of samples to the high-speed CE for analysis.

In the current manuscript, we describe the development of an online, high-throughput, MD-CE assay for BCAAs and their downstream metabolites. The CE separation resolves isoleucine, leucine, valine, alanine, glutamine, glutamate and 10 other amino acids in <30 sec. BCAA uptake and amino acid release was measured in 3T3-L1 cell cultures to demonstrate the utility of the MD-CE assay.

2.3 Materials and Methods

2.3.1 Chemicals and Reagents

Dulbecco's Modified Eagle's Medium (DMEM), newborn calf serum (NCS), fetal bovine serum (FBS), and penicillin-streptomycin (5,000U/mL) were purchased from Invitrogen Molecular Probes (Eugene, OR). Trypsin solution (0.25% Trypsin/0.53mM EDTA in Hank's Balanced Salt Solution) was purchased from ATCC (Manassas, VA). Phosphate-buffered saline (PBS, 10×) was purchased from Bio-Rad Laboratories (Hercules, CA). Ciglitazone was purchased from VWR International (Radnor, Pennsylvania). α-Cyclodextrin was purchased from CTD Holdings, Inc. (technical grade, Alachua, FL). 3-Isobutyl-1-methylxanthine (IBMX), dexamethasone, insulin (human), and all amino acids were purchased from Sigma-Aldrich (St. Louis, MO). Mammalian Protein Extraction Reagent (M-PER®), Halt Protease Inhibitor Cocktail, EDTA free, Halt™ Phosphatase Inhibitor Cocktail, and sodium borate tetrahydrate were purchased from Fisher Scientific (Pittsburgh, PA).

2.3.2 Buffers and Solutions

All solutions were prepared in deionized water (Milli-Q, 18.2 MΩ; Millipore, Bedford, MA) and filtered (0.22μm) unless otherwise noted. Sheath flow buffer contained 90 mM borate adjusted to pH 9.8. CE separation buffer contained 90 mM borate/35 mM α-cyclodextrin adjusted to pH 9.8. Ringer's solution was prepared with 123 mM NaCl, 1.5 mM $CaCl_2$, and 5 mM KCl, adjusted to pH 7.5; and then autoclaved for sterilization. Derivatization solution was prepared daily by dissolving 4-fluoro-7-nitrobenzofurazan (NBD-F, TCI America, Portland, OR) in methanol and diluting with

equal parts 500 µM HCl and degassing under vacuum, giving a final solution of 20 mM NBD-F/250 µM HCl in 1:1 methanol:water. Stock standard solutions (1 mM) of amino acids were prepared in Ringer's solution.

2.3.3 **Offline Optimamization of CE Separation Conditions**

Optimization of CE separation conditions was performed using a P/ACE MDQ system equipped with a LIF detector (λ_{ex} = 488 nm; λ_{em} = 520 nm) and a 3 mW argon ion laser (Beckman Coulter, Fullerton, CA). A 50 µm i.d. × 40 cm fused silica capillary (Polymicro Technologies, Phoenix, AZ) was used for CE separations. On column LIF detection was performed 30 cm from the inlet. Each day, the capillary was rinsed with 0.1 M NaOH, water, and CE separation buffer for 5 min each at 20 psi before the first separation. Between separations, the capillary was rinsed with 0.1 M NaOH for 1 min (20 psi), followed by 2 min of water and 2 min of separation buffer (20 psi). Amines were fluorescently labeled in an offline reaction by mixing 5 mM NBD-F dissolved in 350 µL MeOH with 350 µL of amino acid standard prepared in Ringer's solution and 300 µL CE separation buffer. The solution was mixed and heated in a water bath at 80 ºC for 5 min. NBD labeled amine standards (20 µM) were injected onto the CE capillary for 10 sec at 0.5 psi and separated using 21 kV (normal polarity) for 10 min

2.3.4 **Cell Culture**

3T3-L1 fibroblasts (ATCC® CL-173™) were cultured in 25 cm^2 tissue culture flasks (T-25 flasks) containing 8 mL of high glucose DMEM supplemented with 10% NCS and 1% penicillin/streptomycin. Cultures were kept in a 37° C incubator (5% CO_2) and were passaged every 3-4 days using a ratio of 1:8, with 0.25% (w/v) Trypsin/0.53

mM EDTA solution. Once a confluent monolayer was established, 3T3-L1 cells were differentiated into mature adipocytes using previously described methods.[44] Briefly, differentiation was induced by adding DMEM containing 10% FBS, 0.5 mM IBMX, 0.25 µM dexamethasone, 2µM ciglitazone, and 170 µM insulin. The IBMX, ciglitazone, and dexamethasone were removed after 48 h, and the insulin was removed after 96 h. Experiments were conducted at this time point (96 h after differentiation induction). Successful differentiation cannot be confirmed visually until lipids have accumulated. We therefore continued the process past the 96 h point to confirm successful differentiation visually by the accumulation of lipid droplets (see Figure 2.1).

2.3.5 *In vitro* Microdialysis

Side-by-side microdialysis probes were constructed in-house, as described previously.[131] Two 40 µm i.d. × 105 µm o.d. fused silica capillaries (Polymicro Technologies, Phoenix, AZ) were inserted into a 200 µm i.d. piece of hollow fiber, regenerated cellulose, dialysis tubing (13 kD MWCO, Spectrum Laboratories, Inc., Rancho Dominguez, CA). The capillaries were offset by 1 cm to create a sampling region and sealed using polyimide resin (Alltech, Deerfield, IL). Probes were conditioned by flushing with ethanol (45 µL/h) for 5 min, followed by 10 min of Ringer's solution (25 µL/h). During analysis, probes were perfused with Ringer's solution at 25 µL/h.

2.3.6 Online Derivatization

Dialysate was carried in a 30-40 cm long × 40 µm i.d. × 360 µm o.d. fused silica capillary (Polymicro Technologies, Phoenix, AZ) to a 250 µm i.d. stainless steel cross (Valco Instruments Co. Inc., Houston, TX) where it was mixed with a 5 µL/h stream of

borate buffer and a 5 µL/h stream of NBD-F derivatization solution (see Figure 2.2). Amino acid derivatization took place as the dialysate traveled through a 90 cm long, 75 µm i.d. × 360 µm o.d., fused silica capillary from the reaction cross to the flow gate interface. A 66 cm portion of the reaction capillary was heated to 80°C to accelerate the reaction by passing the capillary through flexible tubing that circulated water from a water bath (NESLAB EX-7 Digital One heating bath circulator, Thermo, Newington, NH).[90] The length of the reaction capillary and flow rates used resulted in a 5 min reaction time.[90]

2.3.7 **High-Speed Capillary Electrophoresis**

A flow gate interface[73] was used to inject discrete plugs of labeled dialysate into an 8–8.5 cm long, 10 µm i.d. × 360 µm o.d. fused silica CE separation capillary (Polymicro Technologies, Phoenix, AZ). The reaction and separation capillary were aligned coaxially in a polycarbonate flow gate interface block with a gap of ~50 µm. Separation buffer flowing at 40 mL/h was pumped through this gap using a syringe pump (Pump 22 syringe pump, Harvard Apparatus, Holliston, MA). To perform an injection, a pneumatically actuated valve (C2-300A 10 port valve, Valco Instruments Co. Inc., Houston, TX) was used to stop the cross flow for 500 ms allowing the gap between the derivatization and separation capillaries to fill. An injection voltage of -13 kV was applied to the exit of the separation capillary for 200 ms. The cross flow though the flow gate was resumed and a separation voltage of -19 kV was applied at the outlet of the separation capillary. Injections were controlled using an in-house LabVIEW program. CE separations were performed every 30 sec.

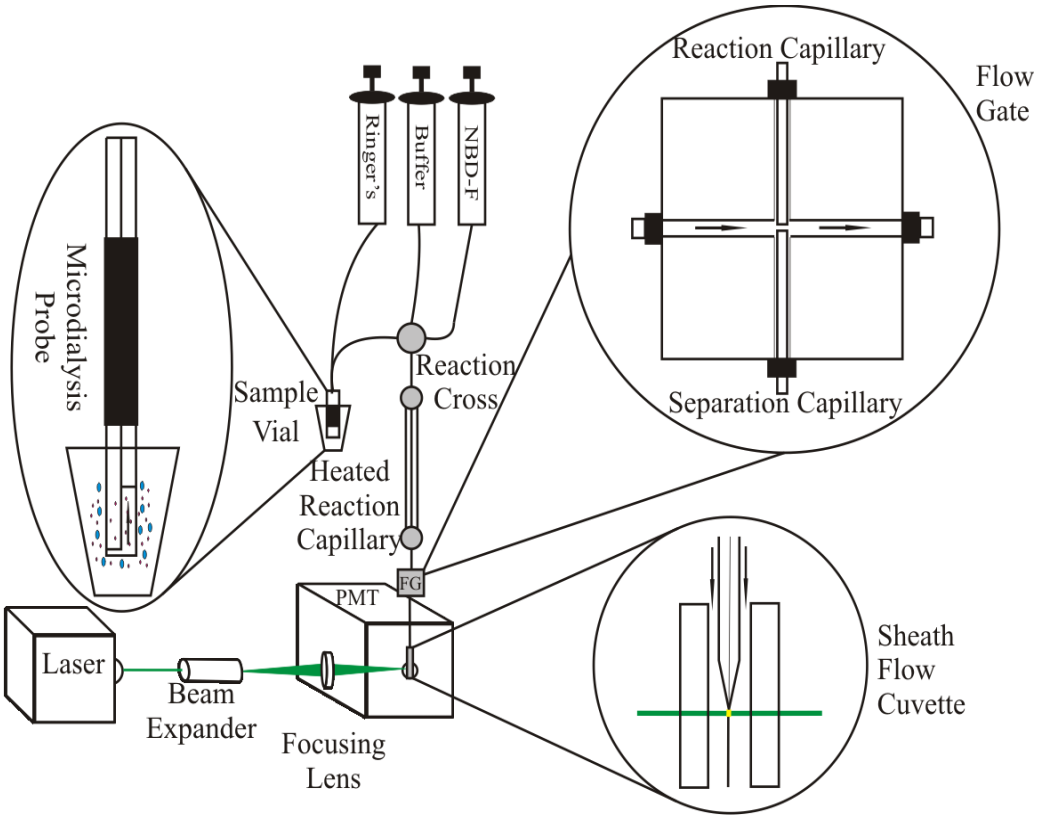

Figure 2.2. Schematic of the online MD-CE system. The microdialysis probe is placed into a microcentrifuge tube containing the amino acids sample. Ringer's solution is perfused through the microdialysis probe, where small molecules diffuse across the membrane and are carried to the reaction cross. Primary and secondary amines are fluorescently labeled using NBD-F as they travel through the reaction capillary to the flow gate interface for injection. Labeled amines are injected, separated using CE, and detected using LIF in a sheath flow cuvette every ~30 seconds.

2.3.8 **LIF Detection**

LIF detection was performed at the exit of the CE separation capillary in a fused-silica sheath flow cuvette (2 mm square with a 400 µm × 400 µm square inner bore).[82,135] The 488 nm line of an argon ion laser (150 mW, Melles Griot, Carlsbad, CA) was passed through a 10× beam expander (Edmond Optics, Barrington, NJ), and focused using a 1× lens to a point just below the exit of the CE separation capillary in the sheath flow cuvette. Fluorescence emission was collected at 90° with a 60×, 0.7 NA long working

distance objective (Universe Kogaku, Oyster Bay, NJ), filtered through spatial (~1 mm diameter) and bandpass filters (543.5 ± 10 nm) (Melles Griot, Irvine, CA) and measured using a photomultiplier tube (PMT, R1477, Hamamatsu Corp., Bridgewater, NJ). Current from the PMT was converted to a potential (Keithley 428 Current Amplifier, Keithley Instruments Inc., Cleveland, OH), filtered with a 10 ms rise time, and recorded using a data acquisition card (National Instruments Corp., Austin, TX). Data analysis was performed using Cutter Analysis 7.0.[136]

2.3.9 **Measuring BCAA Uptake**

3T3-L1 cells were cultured and maintained in T25 flasks as described above until a confluent monolayer was established. The differentiation process proceeded for 96 h. Cells were washed four times with 1.00 mL Ringer's solution containing 200 µM of isoleucine, leucine, and valine and 5 mM glucose (incubation medium). After four washes, 1.00 mL of incubation medium was added to the flask. Flasks were placed in the incubator and allowed to incubate for various lengths of time (5, 15, 30, 45 or 60 min). After the incubation period, 500 µL was withdrawn from the flask, spiked with 25 µL of 1 mM D-2-amino-adipic acid, which is used as an internal standard, and used for CE analysis. To remove the 3T3-L1 cells from the flask for protein analysis, 1.00 mL of mammalian protein extraction reagent supplemented with Halt Protease Inhibitor Cocktail, EDTA free, and Halt™ Phosphatase Inhibitor Cocktail was added to the flask and allowed to incubate at room temperature for 5-30 min until all cells were detached from flask walls. This 1.00 mL aliquot was collected for protein quantification using a bicinchoninic acid (BCA) assay.

2.3.10 **Bicinchoninic Acid (BCA) Assay**

All measured amino acid concentrations were normalized according to cell protein content using a BCA assay. In order to measure cell protein content, a Pierce™ BCA Protein Assay Kit was purchased and utilized according to included instructions. Briefly, working reagent was prepared by combining "Reagent A" and "Reagent B" in a ratio of 50:1 (A: B). 25 µL of each sample or standard was pipetted into individual wells of a 96 well plate; 200 µL of working reagent was then added to each well. All samples were measured in triplicate. The plate was gently shaken for 30 s to ensure mixing of the working reagent and samples. The plate was then incubated at 37°C for 30 min. The plate was removed from the incubator and the absorbance at 562 nm was recorded using a plate reader (Spectromax Plus; Molecular Devices). A calibration curve was generated from standards. Using this standard curve, protein content from each flask was determined and used for normalizing amino acid signals obtained from CE separation.

2.4 **Results and Discussion**

2.4.1 **CE Separation Optimization**

Previous studies have demonstrated online MD-CE assays able to separate and detect 20 biological amines in 20 sec.[90,115] These studies were optimized for the analysis of neurochemicals including glutamate, aspartate, GABA, glycine, and taurine Notably, the BCAAs are not resolved under these conditions (see Figure 2.3A). Isoleucine and leucine are particularly difficult to separate under physiological conditions due to their identical molecular weights and similar chemical structures. We initially made minor changes to our previously reported MD-CE conditions[90] in an

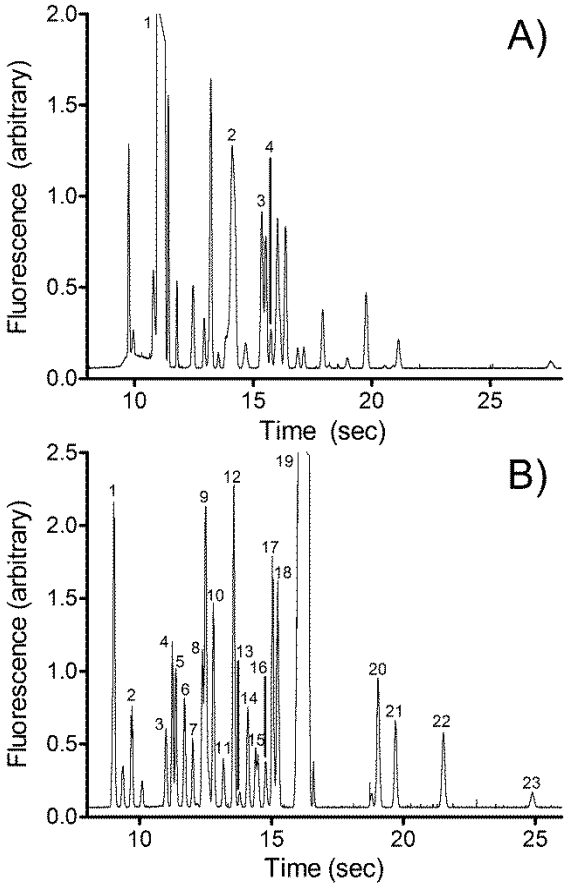

Figure 2.3. Electropherograms from online MD—CE analyses of a 20 µM standard amino acid solution. (A) Separation Buffer: 100 mM borate/20 mM HP-β-CD, pH=10.5; Peaks Identified: (1) NBD-OH, (2) leucine, isoleucine, (3) valine, (4) citrulline. (B) Separation Buffer, 90 mM borate/35 mM α-CD, pH=9.8; Peaks Identified: (1) PEA, arginine, (2) threonine, (3) lysine, (4) isoleucine, (5) leucine, (6) ornithine, (7) methionine, (8) phenylalanine, (9) valine, citrulline, (10) α-ABA, (11) histidine, (12) GABA, (13) glutamine, (14) alanine, (15) β-ABA, (16) threonine, (17) β-alanine, (18) glycine, (19) NBD-OH, (20) taurine, (21) internal standard, (22) glutamate, and (23) aspartate.

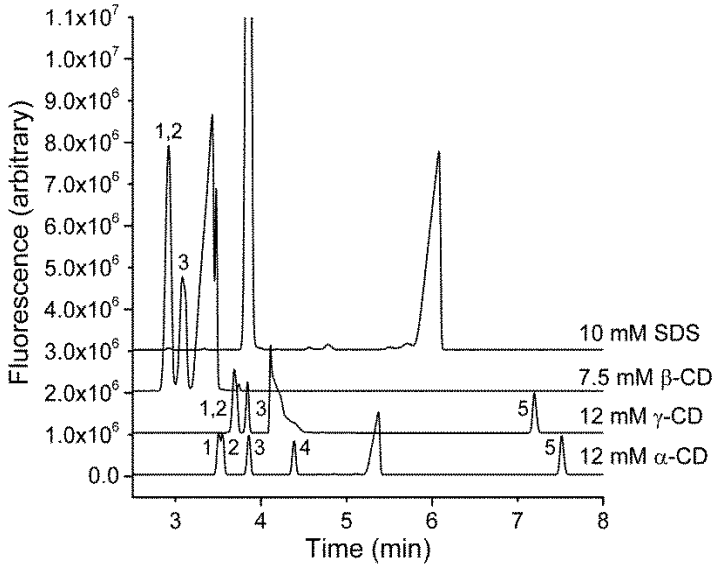

Figure 2.4. Effect of buffer additives on CE separation of NBD labeled BCAA's and related metabolites (20 μM). Separation Buffer: 90 mM borate at pH = 9.8 with 20 mM SDS, 7.5 mM β-CD, 12 mM γ-CD or 2 mM α-CD. Peak Identification: 1) isoleucine, 2) leucine, 3) valine, 4) alanine and 5) glutamate.

attempt to separate isoleucine and leucine without losing separation of previously resolved analytes. Unfortunately, we were unable to resolve isoleucine and leucine through modifications to the separation buffer pH or HP-β-CD concentration. Lorenzo *et al.* previously demonstrated near baseline resolution of NBD labeled isoleucine and leucine using CE with a borate/β-CD separation buffer.[129] Unfortunately, this protocol did not provide sufficient resolution under conditions necessary for our online MD-CE assay. This forced us to re-evaluate the separation more thoroughly.

Optimization of the separation was performed using an automated, commercial CE system. Although the separations take longer using the commercial system, separation conditions are more easily changed allowing a wide range of separation buffers to be assessed efficiently. Our initial strategy was to assess a range of separation buffers and complexation additives to determine which had the potential to resolve the NBD labeled BCAA's. Various aqueous and methanol based buffers were assessed

including: 7.5 mM β-CD in 90 mM borate (pH= 10.0), 12 mM α-CD in 90 mM borate (pH = 10.0), 12 mM γ-CD in 90 mM borate (pH= 10.0), 10 mM SDS in 100 mM borate (pH = 10.5), MeOH with 50 mM borate, MeOH With Triton X-100/50 mM borate, and MeOH with CAPS/50 mM borate. As shown in Figure 2.4, addition of α-CD and γ-CD to the separation buffer provided the most promising leads for the resolution of isoleucine and leucine.

Our next step was to assess the separation of the NBD labeled BCAA's across a range of α-CD and γ-CD concentrations to identify the window of conditions where adequate resolution of isoleucine and leucine was achieved. As shown in Figure 2.5, both α-CD and γ-CD are able to partially resolve NBD labeled isoleucine and leucine across a range of concentrations. Better resolution was observed across a wider range of concentrations using α-CD so this buffer additive was used going forward.

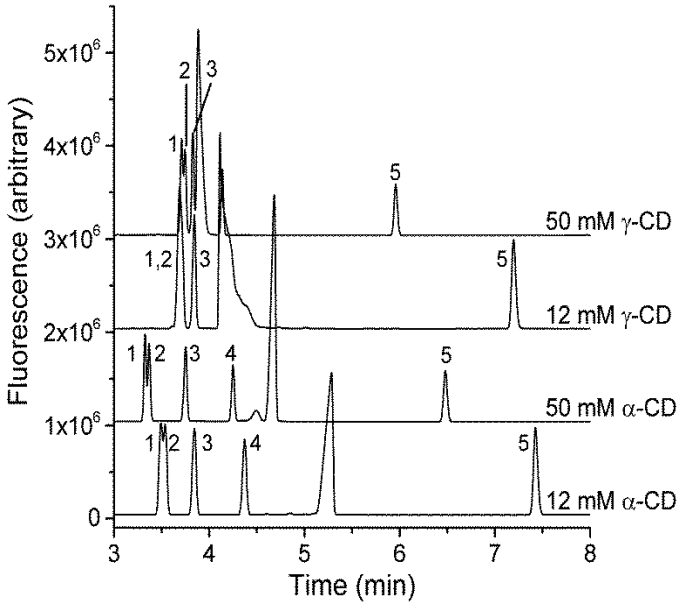

Figure 2.5. Effect of α-CD and γ-CD concentration on CE separation of NBD labeled BCAA's and related metabolites (20 μM). Separation Buffer: 90 mM borate at pH = 9.8 with 50 γ-CD, 12 mM γ-CD, 50 mM α-CD or 12 mM α-CD. Peak Identification: 1) isoleucine, 2) leucine, 3) valine, 4) alanine and 5) glutamate.

After the separation window of α-CD concentrations was identified, it remained necessary to find conditions where the NBD labeled BCAA's were resolved from other amines commonly encountered in biological samples. Figure 2.6 demonstrates CE separations of a mixture of 20 NBD labeled amines across a range of α-CD concentrations. Addition of α-CD had a pronounced effect on the position of the NBD-OH peak in the separation. NBD-OH is a hydrolysis byproduct of the fluorogenic labeling reaction, which often obscures nearby analyte peaks. Increased α-CD concentration selectively pulls many analytes well ahead of the NBD-OH peak, improving resolution in the region of the electropherogram where the peak density is highest.

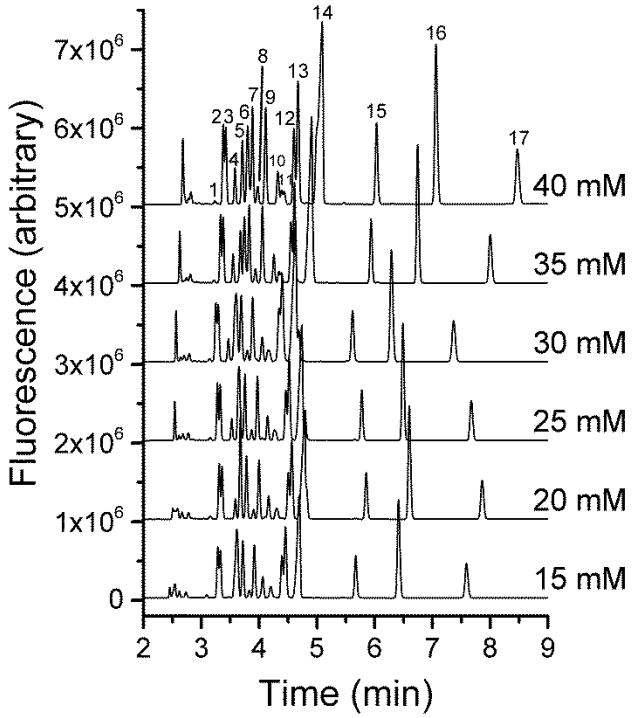

Figure 2.6. Effect of α-CD concentration on CE separation of NBD labeled amines (20 μM). Separation Buffer: 90 mM borate at pH = 9.8 with 15-40 mM α-CD. Peak Identification: 1) lysine, 2) isoleucine, 3) leucine, 4) methionine, 5) phenylalanine, 6) valine, 7) lysine/α-aminobutyric acid, 8) histidine, 9) GABA, 10) alanine, 11) β-aminobutyric acid, 12) β-alanine, 13) glycine, 14) NBD-OH, 15) taurine, 16) glutamate, 17) aspartate.

From these separations 35 mM α-CD was chosen as the optimum separation buffer that balanced resolution of isoleucine/leucine pair with resolution of valine from phenylalanine, lysine and α-aminobutyric acid. α-CD concentrations higher than 35 mM increased separation time without further improving resolution. It should be noted that

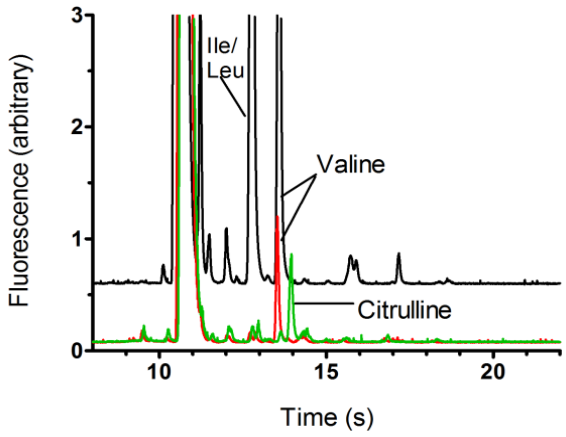

Figure 2.7. Electropherogram from an online MD-CE analysis of supernatant and standard solutions after 3T3-L1 cells were incubated with Ringer's Solution + 5 mM glucose and 200 µM isoleucine, leucine, and valine. Separation Buffer: 100 mM borate/20 mM HP-β-CD, pH=10.5. The cell sample (black) has been offset for clarity from individual 20 µM standard solutions of valine (red) and citrulline (green). Valine and citrulline are clearly resolved under these separation conditions. No citrulline is observed in the cell supernatant.

the peak density of early migrating analytes is approaching the peak capacity of the separation requiring careful control of the separation conditions. Once optimized there is little opportunity for further adjustments to squeeze out additional resolution between individual analyte pairs without losing resolution elsewhere in the electropherogram.

Figure 2.3B shows the separation of a similar amine mixture analyzed using the online MD-CE instrument, demonstrating that the separation conditions optimized using the commercial instrument are directly transferable to our high-speed assay.. Twenty-one amino acids were resolved in <30 sec. Isoleucine and leucine were separated while maintaining resolution from the other amines expected to be present. Alanine, glutamine, and glutamate, all downstream BCAA metabolites and potential biomarkers of lipogenesis, were also well resolved. Unfortunately, valine co-migrates with citrulline under the newly optimized conditions. We confirmed that no measureable citrulline is effluxed from 3T3-L1 cells using the original separation conditions shown in Figure 2.3A (see Figure 2.7). Efficiencies of 216,000 (isoleucine),

170,000 (leucine), and 100,000 (valine) theoretical plates were observed with average peak widths of ~220 ms. The % relative standard deviation (%RSD) of peak heights in replicate measurements ranged from 23-26% for the BCAA's. Normalization with the internal standard improved reproducibility dramatically, reducing %RSD in replicate peak height measurements to 5-7%.

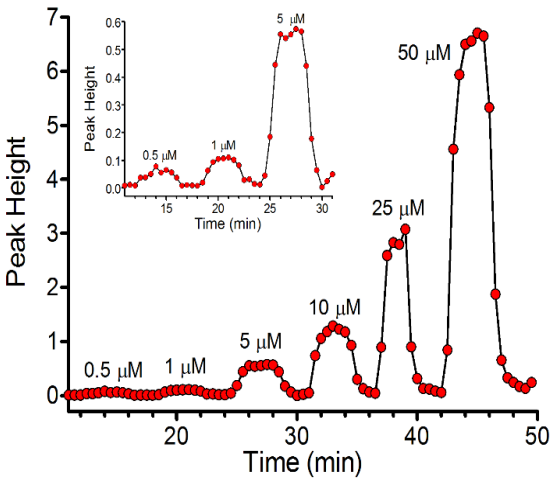

Figure 2.8. MD-CE analysis for valine as the microdialysis probe is moved between Ringer's and amino acid standard solutions of increasing concentrations. Electropherograms were recorded every 30 s. Maximum peak height is achieved within 2-3 separations, demonstrating 60-90 s temporal resolution. Inset is an expanded view of the 0.5 µM – 5 µM analyses.

2.4.2 Temporal Resolution and Limits of Detection (LOD)

To measure the temporal resolution of the MD-CE assay, a microdialysis probe was transferred from Ringer's solution to a 20 µM standard of 24 amino acids for three min and then returned to Ringer's solution. Electropherograms were recorded every 30 s. As shown in Figure 2.8, peak height reached a plateau within 2-3 separations, indicating that the MD-CE assay is able to respond to changes in concentration at the probe surface with 60-90 second temporal resolution. The temporal response of the assay is limited by diffusion that occurs as analytes travel through the connecting capillary from the microdialysis probe to the flow gate interface. The high temporal resolution of the MD-CE instrument allows a high-throughput analysis of a series of samples to be performed. The microdialysis probe

can simply be transferred between a sample or standard and Ringer's solution, then back to another sample for continuous sampling. Ten replicates can be obtained in as little as 5 min (30 s/separation) with only 1-2 min between samples.

A similar analysis using offline CE would typically take >100 min to perform 10 replicate separations. Manual labeling reactions for individual samples would also be necessary, further reducing throughput. As shown in Figure 2.8, concentrations as low as 500 nM can reliably be analyzed using the online MD-CE assay. Limits of detection of the assay for the BCAAs were estimated to be 400, 200, and 100 nM for isoleucine, leucine, and valine, respectively.

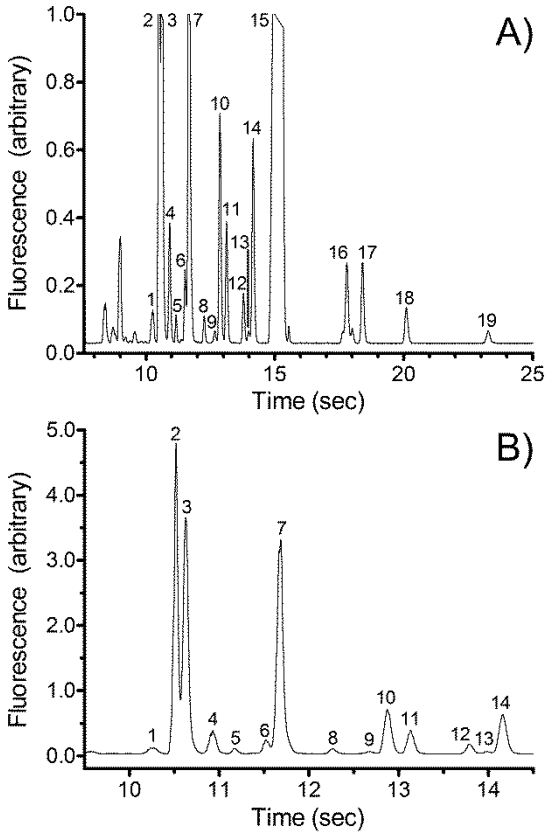

Figure 2.9. Electropherogram from an online MD-CE analysis of supernatant after 3T3-L1 cells were incubated with Ringer's solution + 5 mM glucose and 200 µM isoleucine, leucine and valine for 30 min. A) depicts the full electropherogram. The scale is expanded in B) to demonstrate the BCAA separation more clearly. Peaks identities are: (1) lysine, (2) isoleucine, (3) leucine, (4) ornithine, (5) methionine, (6) phenylalanine, (7) valine, (8) ornithine, (9) GABA, (10) glutamine, (11) alanine, (12) threonine, (13) β-alanine, (14) glycine, (15) NBD-OH, (16) taurine, (17) internal standard, (18) glutamate, (19) aspartate.

These are LODs for the BCAA concentration outside the probe and therefore account for microdialysis recovery and labeling efficiency in the online reaction.

2.4.3 **BCAA Uptake and Amino Acid Efflux and in 3T3-L1 Cells**

3T3-L1 cells were grown to confluency in T-25 flasks and differentiation was induced. Experiments were performed 96 h into the induction protocol. This time point was chosen because 3T3-L1 cells are not yet fully differentiated into mature adipocytes and are rapidly accumulating lipids through lipogenesis. Cells were incubated with 1.00 mL of 5 mM glucose containing 200 μM isoleucine, leucine, and valine for a set time period after which the supernatant was removed for MD-CE analysis. A typical electropherogram after 30 min of incubation is shown in Figure 2.9. Peaks for the BCAAs isoleucine, leucine and valine are clearly observed. During the incubation period 3T3-L1 cells effluxed many biogenic amines not present in the

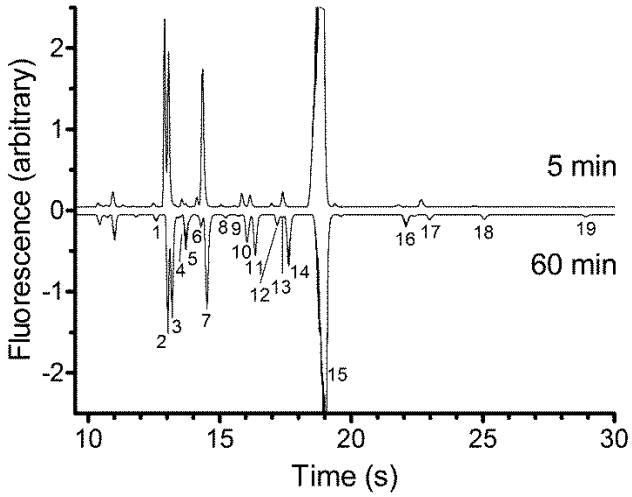

Figure 2.10. Butterfly plot of electropherograms comparing biogenic amine concentrations in the supernatant of 3T3-L1 cells incubated with Ringer's solution + 5 mM glucose and 200 μM isoleucine, leucine and valine for 5 min (top) and 60 min (bottom). Peak intensities of the BCAAs decreased with longer incubation indicating net uptake consistent with lipogenesis. Other biogenic amines were effluxed over the incubation period. Peaks identities are: (1) lysine, (2) isoleucine, (3) leucine, (4) ornithine, (5) methionine, (6) phenylalanine, (7) valine, (8) ornithine, (9) GABA, (10) glutamine, (11) alanine, (12) threonine, (13) β-alanine, (14) glycine, (15) NBD-OH, (16) taurine, (17) internal standard, (18) glutamate, (19) aspartate.

incubation medium giving rise to clear peaks, well above the LOD. Effluxed amines that were detected include lysine, ornithine, alanine, glutamine, glutamate, taurine, and glycine. Peak identities were confirmed by transferring the microdialysis probe from an aliquot of the cell supernatant to a vial containing individual amines and then returning to the original sample to clearly identify which peaks co-migrated with the standards.

Figure 2.10 compares electropherograms recorded after different incubation times. The peak intensities of effluxed biogenic amines increased with longer incubation periods. It should be noted that the rate of increase varied for different amines. Differing rates of release, combined with a gradual release over time, confirms that the cells did not lyse prematurely and that the observed changes in concentration are due to a cellular response. The intensities of the peaks for the isoleucine, leucine and valine decreased over time, consistent with the BCAA uptake necessary for lipogenesis. This is an important confirmation that the MD-CE assay is able to detect net BCAA uptake into 3T3-L1 cells at the concentrations and incubation times assessed.

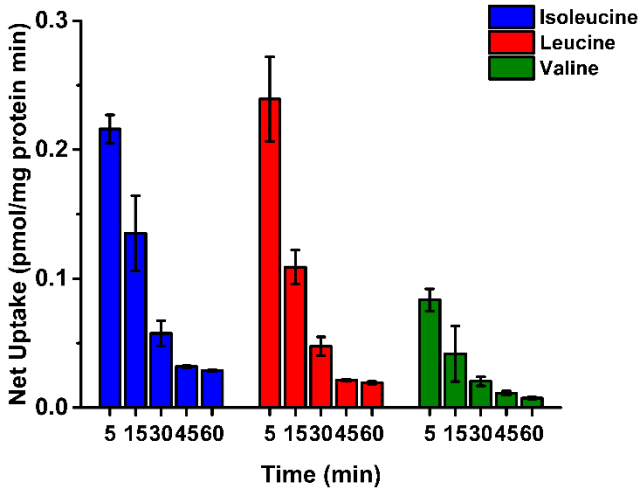

Figure 2.11. Net BCAA uptake by 3T3-L1 cells incubated with Ringer's solution + 5 mM glucose and 200 µM isoleucine, leucine and valine for time periods ranging from 5 to 60 minutes. Rates were normalized to cell protein content as determined by BCA assay. Error bars are SE for n=3 samples.

Figure 2.11 shows the net rate of isoleucine, leucine and valine uptake observed over incubation times ranging from 5 to 60 min. Rates were normalized to the protein content of the 3T3-L1 cells (BCA assay) to account for differences in cell number or size between incubation flasks. The net rate of uptake was highest within the first 5 min of incubation with sustained uptake occurring over periods as long as 60 min. The high initial rate of uptake indicates that 3T3-L1 cells respond quickly to glucose and BCAA exposure. Assays with fast sampling rates will therefore be necessary to accurately observe the response of 3T3-L1 cells to stimuli that induce lipogenesis.

Figure 2.12 shows the net rate of efflux for glutamine, alanine, and glutamate over incubation times

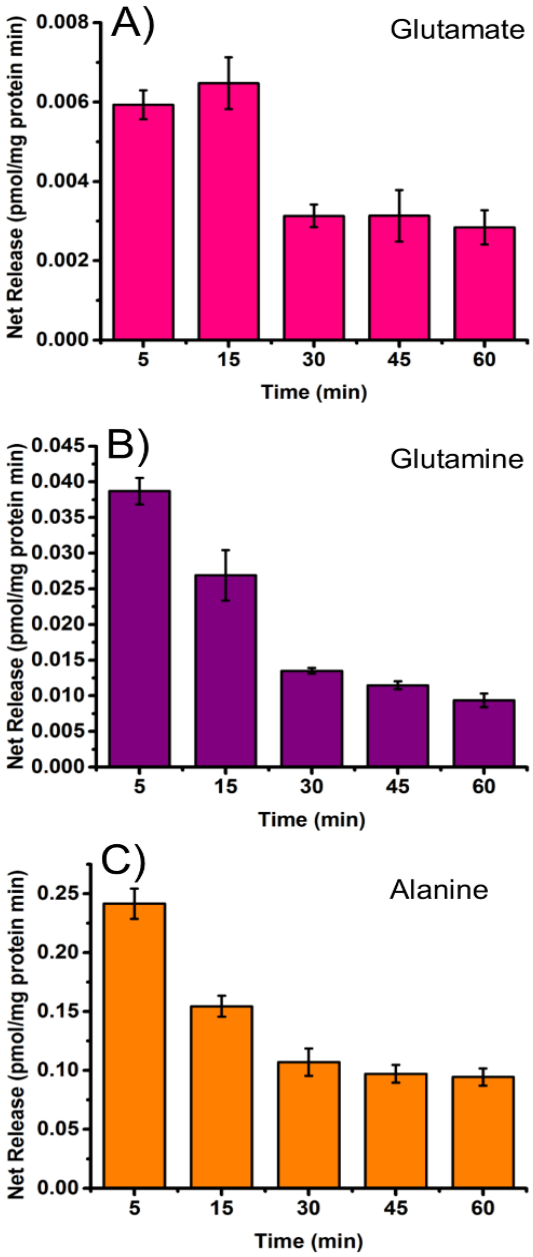

Figure 2.12. Net rate of glutamine, alanine and glutamate efflux by 3T3-L1 cells incubated with Ringer's solution + 5 mM glucose and 200 µM isoleucine, leucine and valine for time periods ranging from 5 to 60 minutes. Rates were normalized to cell protein content as determined by BCA assay. Error bars are SE for n=3 samples.

ranging from 5 to 60 min. Glutamine, alanine, and glutamate are downstream metabolites of lipogenesis. Increased efflux of these amino acids may therefore be able to be used as biomarkers of increased lipogenesis. The observed trends in glutamine, alanine, and glutamate efflux track those observed for BCAA uptake, supporting this hypothesis. Again, the rate of efflux is highest within the first 5 min of incubation, reinforcing the need for high temporal resolution assays to monitor changes in adipocyte metabolism.

2.5 **Conclusions**

We have demonstrated an online MD-CE assay for BCAAs and their downstream metabolites. Separation conditions were optimized to resolve isoleucine, leucine, valine, glutamine, alanine, glutamate and many other biogenic amines in <30 sec. Peak widths were ~220 ms with theoretical plates reaching >150,000. The combination of simple microdialysis sample introduction with high-speed CE separation allowed us to perform a high-throughput analysis of a series of biological samples. In this study, we were able to analyze 15 samples with 8 replicates/sample in 2 h. A similar analysis using traditional offline CE would have taken >20 h.

The BCAAs and their downstream metabolites play key roles in the TCA cycle and lipogenesis in adipocytes.[30] Monitoring BCAA uptake and downstream metabolite efflux may therefore allow us to gain insight into how adipocyte metabolism responds to various stimuli including food ingredients/additives or environmental toxins. This information is sorely lacking in our attempts to better understand what is driving the obesity epidemic facing modern society. The MD-CE assay described here provides a

high-throughput assay that can be used to perform these studies in traditional adipocyte cell models. The assay is also compatible with *in vivo* or *in vitro* MD-CE approaches, which would allow higher temporal resolution studies to be performed in a wider range of obesity models.

Chapter 3: Utilization of Branched Chain Amino Acids by 3T3-L1 Adipocytes throughout Differentiation

3.1 **Summary**

Net release and uptake of the branched chain amino acids (BCAAs), isoleucine, leucine, and valine, as well as the downstream metabolites of lipogenesis, alanine, glutamine, and glutamate, was monitored using online microdialysis-capillary electrophoresis with laser induced fluorescence detection (CE-LIF). Changes were monitored in order to see how utilization of BCAAs changed throughout differentiation as lipogenic needs changed. Differences in net release and uptake profiles were observed at various stages in the 3T3-L1 differentiation process into mature adipocytes. BCAA release is lowest during periods of increased lipogenesis and uptake of BCAAs is highest during this same time period. It was also observed that BCAA release and uptake is slowed once the cells have reached a fully differentiated state. Downstream metabolites supported these trends with increased release during later stages of development when lipogenesis occurs most rapidly. The presence of physiological concentrations of BCAAs appears to stimulate lipogenesis, as indicated by an increase in downstream lipogenic markers.

3.2 **Introduction**

Branched chain amino acids play an important role in signaling throughout the body and evidence suggests that adipocytes regulate BCAA concentrations through uptake, providing signals to the rest of the body about the state of energy balance in adipose.[26-29,137-139] BCAA receptors can be found throughout the body, and are known to regulate insulin secretion, protein synthesis in muscle, and appetite control in the brain.[14-16] After consuming a high protein meal, systemic BCAA levels increase, sending a signal that there is a surplus of energy.[6,7,24] Protein turnover is closely regulated by leucine through its ability to stimulate protein synthesis and inhibit protein degradation.[140,141]

The catabolism of BCAAs in adipose tissue supports lipogenesis and the generation of tricarboxylic acid (TCA) cycle intermediates (Figure 1.2).[30,116,117,142-145] Green et al. demonstrated that proliferating 3T3-L1 cells use glutamine and glucose in order to generate acetyl coenzyme A (CoA) to be used in the TCA cycle in order to produce energy for the cells. They also showed that differentiating cells used isoleucine and leucine in order to generate nearly 1/3 of acetyl-CoA used in the TCA cycle, rather than glucose and glutamine alone.[30]

Rapid accumulation of lipids occurs in late stages of 3T3-L1 differentiation, usually 5-7 days after the initiation of differentiation. Cells use BCAAs in order to rapidly produce TCA cycle intermediates for storage of energy as triglycerides. Excess energy is stored in adipocytes as triglycerides, for later use when energy stores are low. Through lipid accumulation, cells are able to regulate whole body BCAA levels. In order to assess how physiological concentrations of BCAAs modulate amino acid release and

uptake, we use the immortalized 3T3-L1 mouse model cell line. 3T3-L1 cells were isolated from parent 3T3 cultures after identification of colonies with a lipid accumulating phenotype once cells reached confluency.[39] These cells are simple to culture compared to primary cell lines and have well established protocol for differentiation. Other cell lines commonly used for adipocyte research include 3T3-F422A, TA1, and OB1771.[17] Various differentiation procedures were tested until a protocol with nearly 100% differentiation was achieved.[40,146,147]

Microdialysis sampling is used to create a high-throughput sampling method, and has been used in combination with CE for the sampling of various biological amines including glutamate, aspartate, GABA, glycine, taurine, glutamine, D-serine, and many others.[74,78,79,90,130-132] Using microdialysis sampling coupled with an online reaction and high-speed CE has been shown to dramatically improve temporal resolution; temporal resolutions as low as 3 s have been achieved for amine neurotransmitters.[74] We used a previously developed high-speed CE separation scheme to measure BCAAs and related amines.[148] This method allows for the detection of BCAAs and the downstream markers of lipogenesis, alanine, glutamine, and glutamate, among other amino acids. In total, 22 amino acids can be separated in less than 30 s using this method. Limits of detection for amino acids of interest are as low as 100 nM for valine, 400 nM for isoleucine, and 300 nM for leucine.[148]

In this work, we used a high-speed CE-LIF method for the separation, detection, and analysis of amino acids released from 3T3-L1 cells. This allows us to study the effect of BCAAs on lipogenesis at different stages throughout differentiation.

3.3 Materials and Methods

3.3.1 Chemicals and Reagents

α-Cyclodextrin was purchased from CTD Holdings, Inc. (technical grade, Alachua, FL). 3-Isobutyl-1-methylxanthine (IBMX), dexamethasone, insulin, and all amino acids were purchased from Sigma-Aldrich (St. Louis, MO). Dulbecco's Modified Eagle's Medium (DMEM), newborn calf serum (NCS), fetal bovine serum (FBS), and penicillin-streptomycin (5,000U/mL) were purchased from Invitrogen Molecular Probes (Eugene, OR). Trypsin solution (.25% Trypsin/0.53mM EDTA in Hank's Balanced Salt Solution) was purchased from ATCC (Manassas, VA). Phosphate-buffered saline (PBS, 10X) was purchased from Bio-Rad Laboratories (Hercules, CA). Ciglitazone was purchased from VWR International (Radnor, Pennsylvania). Mammalian Protein Extraction Reagent (M-PER®), Halt Protease Inhibitor Cocktail, EDTA free, Halt™ Phosphatase Inhibitor Cocktail, a Pierce™ BCA Protein Assay Kit (product 23225), and sodium borate tetrahydrate were purchased from Fisher Scientific (Pittsburgh, PA). 4-Fluoro-7-Nitro-2, 1, 3-Benzoxadiazole (NBD-F) was purchased from TCI America (Portland, OR).

3.3.2 Buffers and Solutions

All solutions were prepared in deionized water (Milli-Q, 18.2 MΩ; Millipore, Bedford, MA) and filtered (0.22μm) unless otherwise described. CE separation buffer contained 90 mM borate/35 mM α-cyclodextrin and was adjusted to pH 9.8. Sheath flow buffer contained 90 mM borate and was also adjusted to pH 9.8. Ringer's solution was prepared with NaCl (123 mM), $CaCl_2$ (1.5 mM), and KCl (5 mM), pH 7.5, and then

autoclaved for sterilization. Derivatization solution was prepared daily by dissolving 40 mM NBD-F in methanol and diluting in equal parts with 500 µM HCl, giving a final solution of 20 mM NBD-F/250 µM HCl in 50% methanol which was degassed under vacuum for 2 min. Stock standard solutions (1 mM) of amino acids were prepared individually in Ringer's solution.

3.3.3 **Cell Culture**

3T3-L1 fibroblasts (ATCC® CL-173™) were maintained in 25 cm^2 tissue culture flasks (T-25 flasks) containing 8 mL of high glucose DMEM supplemented with 10% NCS and 1% penicillin/streptomycin. Cultures were maintained in a 37° C incubator (5% CO_2). 3T3-L1 cells were differentiated using methods previously described [146]. Briefly, differentiation was induced by adding high glucose DMEM containing 10% FBS, 0.5 mM IBMX, 0.25 µM dexamethasone, 2 µM ciglitazone, and 170 µM insulin. IBMX, ciglitazone, and dexamethasone were removed after 48 h, and insulin was removed after 4 days. Maintenance media (high glucose DMEM, 10% FBS, and 1% penicillin/streptomycin) was used after 4 days. Experiments were conducted at 4 different time points—"Day 0" is prior to any differentiation, but confluent; "Day 2" is after 48 h of incubation with DMEM, FBS, IBMX, dexamethasone, ciglitazone, and insulin; "Day 4" is 96 h after differentiation induction, when media contains DMEM, FBS, and insulin; and finally, "Day14" is 14-16 days after time point "Day 0." Images were taken using a SPOT Insight QE camera (Model 4.1, Diagnostic Instruments, Inc., SPOT Imaging, Sterling Heights, MI) mounted on a LaboMED TCM400 microscope (Labo America Inc., Fremont, CA) at 20×.

3.3.4 **Measuring Bulk Branched Chain Amino Acid Uptake/Release**

3T3-L1 cells were cultured and maintained in T25 flasks, as described above. Once a confluent monolayer of cells was established, differentiation was initiated. At each experimental time point, cells were rinsed four times with 1.00 mL Ringer's solution containing 5 mM glucose with or without 200 µM isoleucine, leucine, and valine (incubation medium). Cells were incubated with 1.00 mL of the corresponding incubation medium, for 30 min. After 30 min, the 1.00 mL of incubation medium was removed and 500 µL of this sample was spiked with 25 µL of 1 mM D-2-amino-adipic-acid (internal standard), and used for CE analysis. Cells were removed from the flask walls for protein analysis using 1.00 mL of mammalian protein extraction reagent, supplemented with Halt Protease Inhibitor Cocktail, EDTA free, and Halt™ Phosphatase Inhibitor Cocktail. Flasks incubated with this solution at room temperature until all cells were detached from flask walls (5-25 min). This 1.00 mL aliquot was collected for protein quantification using a bicinchoninic acid (BCA) assay.

3.3.5 **Microdialysis Probes**

Microdialysis probes were constructed in-house using a side-by-side geometry, as described previously.[131] Briefly, two 40 µm i.d. x 105 µm o.d. fused silica capillaries (Polymicro Technologies, Phoenix, AZ) were inserted into a 200 µm i.d. piece of hollow fiber dialysis tubing made from regenerated cellulose (13 kD MWCO, Spectrum Laboratories, Inc., Rancho Dominguez, CA). A sampling region was created by offsetting the capillaries by 1 cm, which was sealed using polyimide resin (Alltech, Deerfield, IL). Probes were conditioned prior to use by flushing with ethanol (45µL/h) for five min,

followed by ten min of Ringer's solution (25µL/h). Small molecules diffuse across the probe membrane according to a concentration gradient, making microdialysis a useful sampling method for biological samples.[54]

3.3.6 **Online Derivatization**

Probes were perfused with Ringer's solution at 25 µL/h throughout experiments. Small molecules diffuse across the probe membrane according to a concentration gradient, making microdialysis a useful sampling method for biological samples.[54] Dialysate was carried in a 30-40 cm long × 40 µm i.d. × 360 µm o.d. fused silica capillary to a 250 µm i.d. stainless steel cross (Valco Instruments Co. Inc, Houston, TX) where it was mixed with a 5 µL/h stream of borate buffer and a 5 µL/h stream of derivatization solution in order to be fluorescently labeled. Labeling the primary and secondary amines with NBD-F allows for LIF detection, giving high sensitivity from small concentrations of analytes.[83,91]The derivatization of primary and secondary amines took place as the dialysate mixture traveled through a 90 cm long, 75 µm i.d. × 360 µm o.d. fused silica capillary from the reaction cross to the flow gate interface; 66 cm of this capillary was heated to accelerate the reaction by passing through flexible tubing that was circulating water from a water bath at 80°C (NESLAB EX-7 Digital One heating bath circulator, Thermo, Newington, NH). The length of the reaction capillary and flow rates used resulted in a 5 min reaction time, allowing the labeling reaction to go to completion.[90] Labeling the primary and secondary amines with NBD-F allows for LIF detection, giving high sensitivity from small concentrations of analytes.[83,91]

3.3.7 **High-Speed Capillary Electrophoresis (CE)**

An 8-8.5 cm long, 10 µm i.d. × 360 µm o.d. fused silica capillary (separation capillary) was aligned coaxially (~50 µm apart) with the reaction capillary in a polycarbonate flow gate interface block.[73] A syringe pump (Pump 22 syringe pump, Harvard Apparatus, Holliston, MA) pumped separation buffer at 40 mL/h through this gap. Separation buffer flow was stopped using a pneumatically actuated valve (C2-300A 10 port valve, Valco Instruments Co. Inc., Houston, TX) for 500 ms allowing sample to fill the gap. An injection voltage of -13 kV was applied to the exit of the separation capillary for 200 ms. After this time, flow through the flow gate is resumed and a separation voltage of -19 kV was applied. Injections were controlled by an in-house LabView program. Separations were performed every 30 sec.

3.3.8 **LIF Detection**

488 nm argon ion laser was used for LIF detection (150 mW, Melles Griot, Carlsbad, CA). The laser beam was passed through a 10× beam expander (Edmond Optics, Barrington, NJ), and focused using a 1× lens to a point just past the exit of the CE separation capillary in a fused-silica sheath flow cuvette(2 mm square with a 400 µm × 400 µm square inner bore).[82,135] Fluorescence emission is collected at 90° with a 60×, 0.7 NA long working distance objective (Universe Kogaku, Oyster Bay, NJ), filtered through spatial (~1 mm diameter) and bandpass filters (543.5 ± 10 nm) (Melles Griot, Irvine, CA), and recorded using a photomultiplier tube (PMT R1477, Hamamatsu Corp., Bridgewater, NJ). Current from the PMT was amplified (Keithley 428 Current Amplifier, Keithley Instruments Inc., Cleveland, OH), filtered with a 10 ms rise time, and recorded

using a data acquisition card (National Instruments Corp., Austin, TX). Data analysis was performed using Cutter Analysis 7.0.[149]

3.3.9 **Bicinchoninic Acid (BCA) Assay**

Amino acid concentrations were normalized according to cell protein content, as measured using a BCA assay. A Pierce™ BCA Protein Assay Kit was used according to the included instructions. Briefly, working reagent was prepared by combining "Reagent A" and "Reagent B" in a ratio of 50:1 (A: B). 25 µL of each sample or standard was pipetted into individual wells of a 96 well plate followed by 200 µL of working reagent; all samples were analyzed in triplicate. The plate was gently shaken for 30 s to ensure mixing of the working reagent and samples. After shaking, the plate was incubated at 37°C for 30 min. After incubation, the plate was removed from the incubator and absorbance at 562 nm was measured using a plate reader (Spectromax Plus; Molecular Devices, LLC, Sunnyvale, CA). A calibration curve was generated from bovine serum albumin (BSA) standards. Using this standard curve, protein content for each flask was determined and used for normalizing amino acid signals obtained from CE separation.

3.3.10 **Statistical Analysis**

All Figures show mean ±S.E. Differences between groups were assessed using Student's two-tailed *t* test or two-way ANOVA unless otherwise indicated. *,#, or & indicates p-value between 0.01 and 0.05; **, ##, or && indicates p-value <0.01.

3.4 **Results & Discussion**

3T3-L1 cells were used as a model of adipocytes allowing changes in BCAA utilization throughout differentiation to be monitored.

3.4.1 **3T3-L1 Differentiation**

Images were recorded to confirm successful differentiation of 3T3-L1 cells

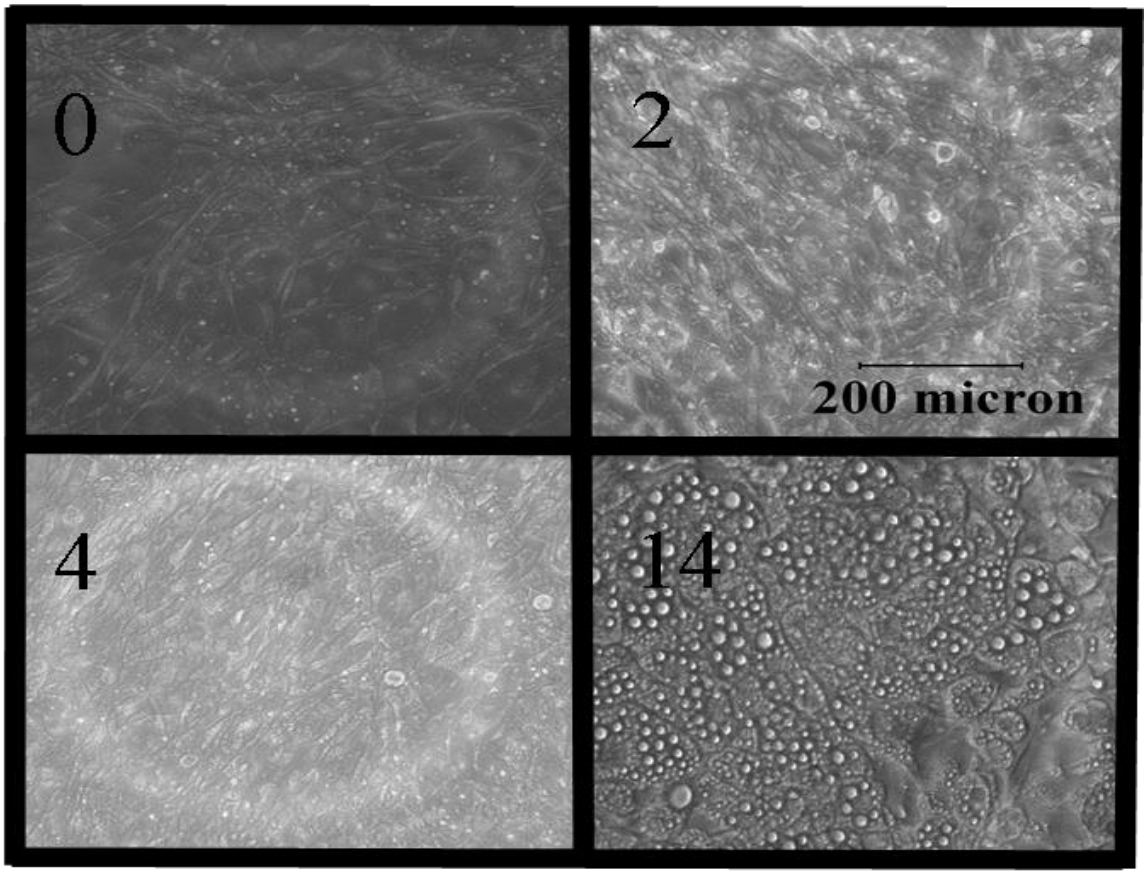

Figure 3.1. Microscopic images of 3T3-L1 cells at various time points throughout the differentiation process. Cell monolayers were imaged using an inverted phase contrast microscope, magnification 20×. "Day 0" (upper left) is prior to any differentiation, but confluent; "Day 2" (upper right) is after 48 hour of incubation with DMEM, FBS, IBMX, dexamethasone, ciglitazone, and insulin; "Day 4" (lower left) is 48 hour after "Day 2" when media contains DMEM, FBS, and insulin; and finally, "Day 14" (lower right) is 14-16 days after the start of differentiation.

(Figure 3.1). 3T3-L1 cells were cultured in T-25 flasks until confluency was reached. Differentiation of 3T3-L1 cells is induced by the addition of ciglitazone, insulin, IBMX, and dexamethasone after cells achieved confluency. Cells were imaged at four stages throughout differentiation, as described previously. Figure 3.1-0 (upper left) shows a confluent monolayer of cells with a normal, pre-differentiation fibroblast-like appearance. Figure 3.1-2 (upper right) shows the cells 2 days after the induction of differentiation. At this point, the cells still have a fibroblast-like appearance, with little change in confluency. Figure 3.1-4 (lower left) shows the cells 4 days after the induction of differentiation, and 2 days after the removal of IBMX, ciglitazone, and dexamethasone from the cell culture medium. At this point, the cells continue to have a fibroblast-like appearance, with a few flasks showing signs of lipid accumulation. After 14-16 days, the cells show accumulation of lipids. Lipid accumulation is fast at the beginning, and slows over the final 8-10 days. Figure 3.1-14 (lower right) shows successful differentiation with approximately 95% of cells showing lipid accumulation.

3.4.2 **BCAA Efflux**

Utilization of BCAAs changes throughout the course of differentiation, as previously demonstrated.[30] As 3T3-L1 cells differentiate, the need for lipogenic amines increases as cells being to accumulate lipids. Figure 3.2 shows example electropherograms collected from 3T3-L1 cells that have been incubated in Ringer's solution with 5 mM glucose for 30 min on Day 0 and Day 14. The cells released many amines above the high-speed CE instrument's limits of detection. Utilization of BCAAs was modified as the cells released fewer BCAAs on Day 14 (red) compared to Day 0

(black). Peaks were identified by transferring the microdialysis probe between a vial containing the cell sample, to a vial containing individual standards, then returning the probe back to the cell sample vial. In total, 17 amino acids can be identified in a ~20 second separation window. Peaks identified include: lysine, isoleucine, leucine, ornithine, methionine, phenylalanine, valine, ornithine, GABA, glutamine, alanine, threonine, β-alanine, glycine, taurine, glutamate, and aspartate.

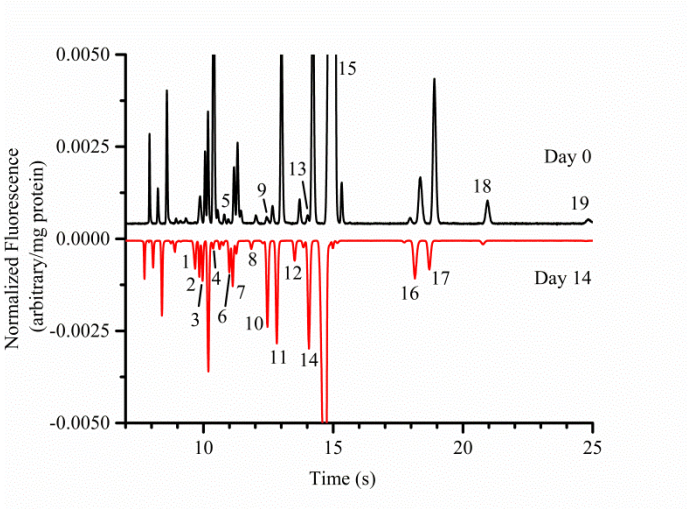

Figure 3.2. Butterfly plot of electropherograms comparing NBD-F labeled amino acids released from 3T3-L1 cells incubated with Ringer's solution containing 5 mM glucose at Day 0 (top) and Day 14 (bottom) of the differentiation process. Peak intensities and relative ratios of amines show changes in release profiles. Peak identities are: (1) lysine, (2) isoleucine, (3) leucine, (4) ornithine, (5) methionine, (6) phenylalanine, (7) valine, (8) ornithine, (9) GABA, (10) glutamine, (11) alanine, (12) threonine, (13) β-alanine, (14) glycine, (15) hydrolysis product, (16) taurine, (17) internal standard, (18) glutamate, (19) aspartate.

Figure 3.3 shows the release of the BCAAs at each stage of differentiation. Less release of all three BCAAs during periods of high lipogenesis is observed. Lipogenesis is expected to occur most rapidly 4 days after the induction of differentiation. Statistical differences in release of BCAAs is observed between Day 0 and Day 14 for isoleucine and leucine, while statistical differences in release of leucine and valine show differences between Day 0 and Day 4. All three BCAAs show statistical differences in release

between Days 2 and 4. In agreement with the BCAAs, the downstream lipogenesis marker glutamine, as shown in Figure 3.4A (red), has increased release during periods of increased lipogenesis, 2 days after differentiation was started, and continuing until at least 4 days after differentiation induction. However, the release profile of alanine contradicts these findings. 3T3-L1 adipocytes release less alanine throughout differentiation, including 4 days after differentiation was induced, as shown in Figure 3.4B, in red. Glutamate (Figure 3.4C, red) shows a similar pattern to alanine over the course of differentiation. These observations could be due to a shift in equilibrium of BCAA catabolism byproducts to generate tricarboxylic acid (TCA) cycle and fatty acid synthesis precursor molecules in order to make acetyl CoA products (Figure 1.2), and a lack of available pyruvate. When lipid accumulation has stabilized, as on Day 14, increased release of glutamine, alanine, and glutamate is observed, compared to Day 4. The changes in

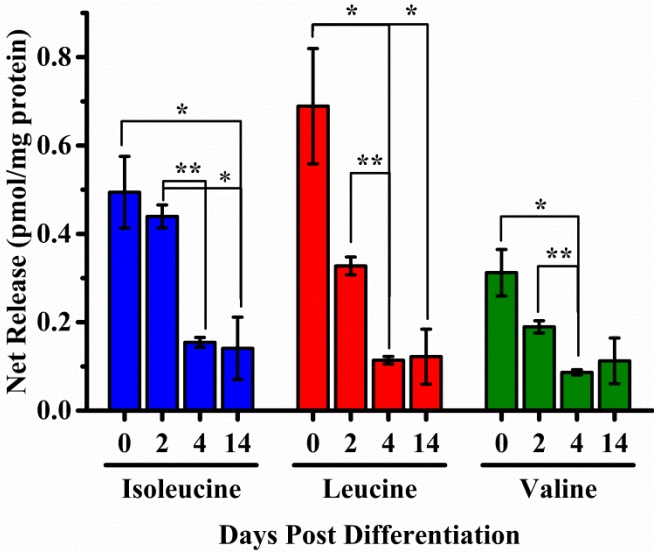

Figure 3.3. Release of BCAAs at each stage of differentiation when incubated with Ringer's solution containing 5 mM glucose for 30 minutes at different points during differentiation. Error bars are SEM; n=3. *, p-value < 0.05, **, p-value < 0.01.

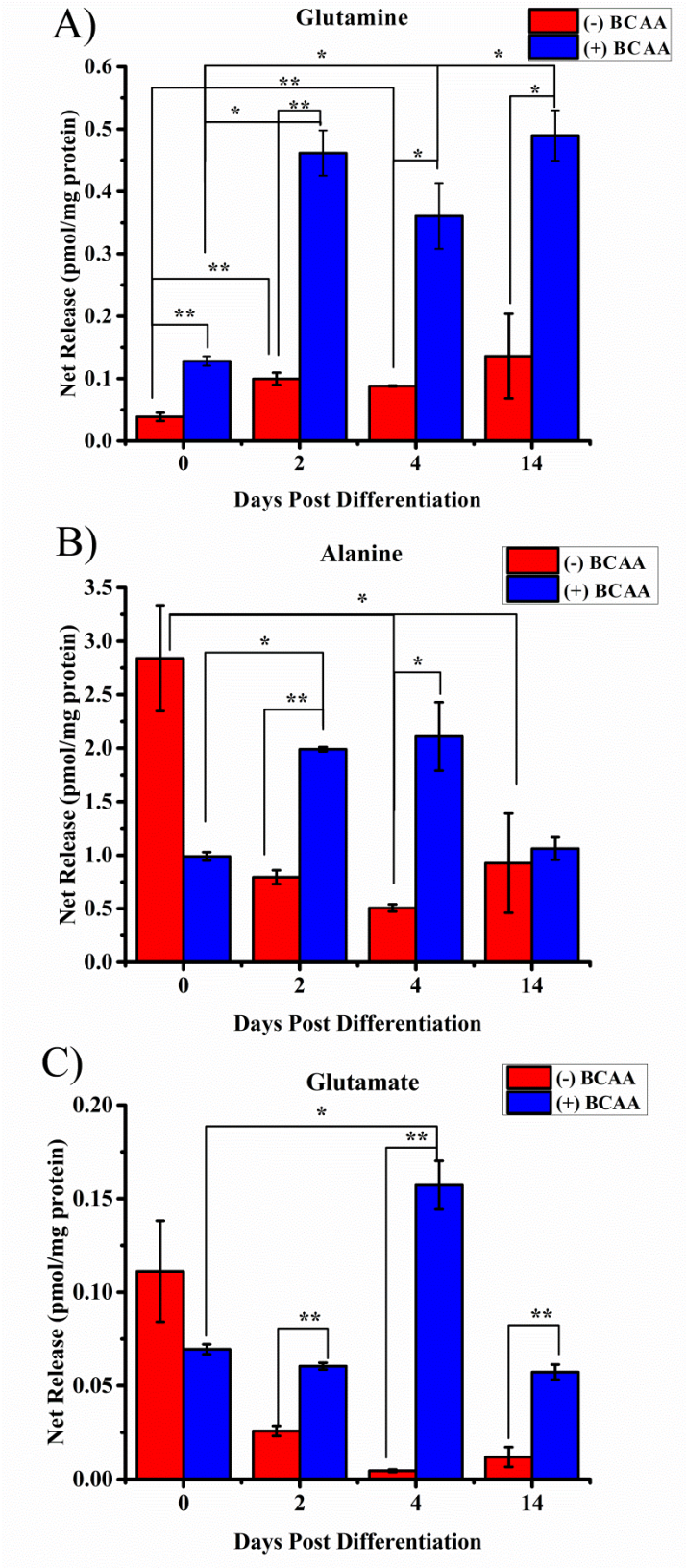

Figure 3.4. Rate of glutamine (A), alanine (B), and glutamate (C) release by 3T3-L1 cells incubated with Ringer's solution + 5 mM glucose without (Red) and with (Blue) 200 µM isoleucine, leucine, and valine, throughout the differentiation process. Concentrations were normalized using an IS and to cell protein content as determined by the BCA assay. *, p-value < 0.05, **, p-value < 0.01.

utilization of BCAAs and downstream metabolites reflect changes in energy needs of the cells throughout the course of differentiation.

3.4.3 **BCAA Uptake throughout Differentiation**

Although BCAA efflux followed expected patterns; release of downstream markers of lipogenesis did not follow expected patterns. In an effort to assess required substrates for lipid accumulation, a follow-up experiment was conducted. Cells were incubated in Ringer's solution contacting 5 mM glucose with 200 µM of each BCAA, in order to assess the patterns of lipogenesis in 3T3-L1 adipocytes as a function of BCAA presence, as the cells differentiate from pre-adipocytes to fully mature adipocytes. Figure 3.5 shows electropherograms collected from 3T3-L1 cells that have been incubated in this solution; peak intensities have

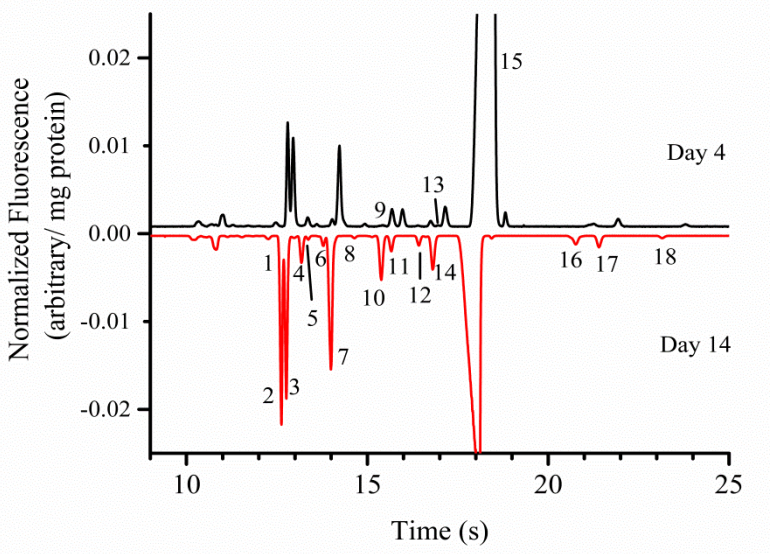

Figure 3.5. Butterfly plot of electropherograms comparing NBD-F labeled amino acids released from 3T3-L1 cells incubated with Ringer's solution containing 5 mM glucose and 200 µM isoleucine, leucine, and valine at Day 2 (top) and Day 14 (bottom) of the differentiation process. Peak intensities and relative ratios of amines show changes in release profiles. Peak identities are: (1) lysine, (2) isoleucine, (3) leucine, (4) ornithine, (5) methionine, (6) phenylalanine, (7) valine, (8) ornithine, (9) GABA, (10) glutamine, (11) alanine, (12) threonine, (13) β-alanine, (14) glycine, (15) hydrolysis product, (16) taurine, (17) internal standard, (18) glutamate.

changed throughout the course of differentiation. Relative peak heights are changed when comparing the net flux at Day 2 (top) and Day 14 (bottom). As shown in Figure 3.6, the uptake of BCAAs into the cells did not change statistically over the course of 3T3-L1 cell differentiation. Downstream

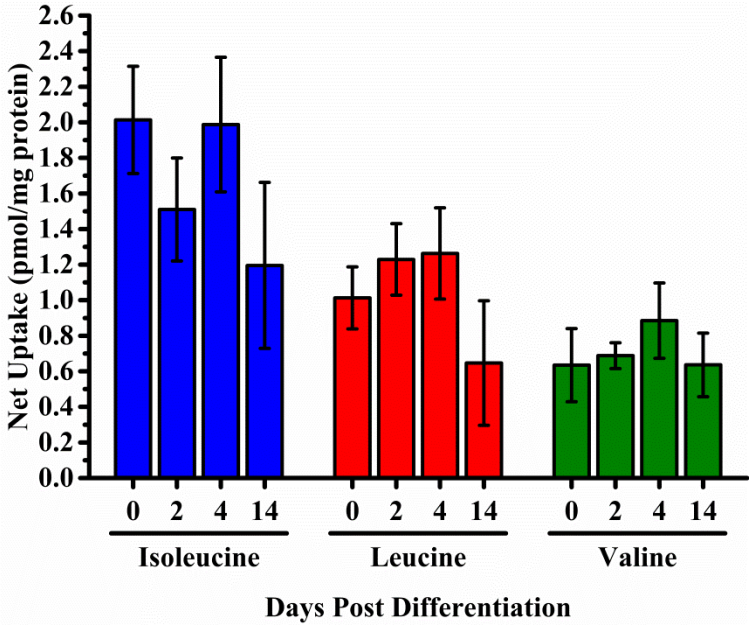

Figure 3.6. Uptake of BCAAs at each stage of differentiation when incubated with Ringer's solution containing 5 mM glucose and 200 µM BCAAs for 30 minutes, at different points during differentiation. Error bars are SEM; n=3. No statistical differences were observed.

metabolites, alanine, glutamine, and glutamate, however, did show statistical differences in release as the cells progress through differentiation, shown in blue in Figure 3.4. Previous studies have shown that differentiated adipocytes have increased catabolism of BCAAs, as compared to undifferentiated cells.[30] Our results agree with this and are evidenced by the accumulation of lipid vesicles (Figure 3.1-14). These experimental results suggest that BCAA flux (Figure 3.6) slows once cells are fully differentiated, as the need for energy storage decreases. The BCAA flux and downstream markers alanine and glutamate are in agreement with this observation (Figure 3.4A and Figure 3.4B, blue).

3.4.4 **Differences in Release of Dowstream Metabolites**

When comparing the relative amounts released between experiments, there is a 150% increase in released alanine, 2 days after the induction of differentiation, and 300%+ increase in released alanine 4 days after differentiation is initiated. Similar trends are seen in Figure 3.4A and Figure 3.4C, for glutamine and glutamate. Glutamine had statistically more release throughout all stages when comparing flasks that did or did not contain BCAAs in the incubation medium. All stages had over 225% relative increase for glutamine. Glutamate saw similar trends, except at the first stage, Day 0, which was not statistically different between the two experiments. These relative increases in downstream metabolites between experiments suggest that the presence of BCAAs promotes lipogenesis in 3T3-L1 adipocytes.

3.5 **Conclusions**

BCAA flux and BCAA effects on 3T3-L1 lipogenesis has been measured using online high-speed CE-LIF. Using this assay, in conjunction with microdialysis sampling, allows for high-throughput measurements of many small molecule amines from cell samples. This assay has shown its ability to measure lipogenesis in 3T3-L1 cells, by monitoring lipogenesis markers (alanine, glutamine, and glutamate), as well as monitor adipocyte signaling through the release of amino acids. Using this assay, we have been able to see that the rate of lipogenesis is fastest ~4 days after differentiation is initiated and slows once cells have fully accumulated lipids, about 14-16 days after differentiation is started. The effect of excess BCAAs on lipogenesis can be seen by changes in the release of the downstream metabolites, as there is more release as the cells progress

through the stages of differentiation. The techniques used here can be used to measure many other small molecule analytes from various cell types, *in vitro*, as well as *in vivo*, including changes under whole body or local stimulation.

Chapter 4: Effect of Glucose and Branched Chain Amino Acids on Lipogenesis throughout Differentiation of 3T3-L1 Adipocytes

4.1 **Summary**

Lipogenesis was monitored in 3T3-L1 adipocytes over the course of differentiation when cells were incubated with varying concentrations of glucose. Alanine, glutamine, and glutamate, downstream metabolites of lipogenesis were monitored, as well as isoleucine, leucine, and valine uptake and release. Amino acids were monitored using online microdialysis-capillary electrophoresis with laser induced fluorescence detection (CE-LIF). The effect of various glucose concentrations (0-20 mM) was assessed at various stages in the 3T3-L1 differentiation process. BCAA release is lowest on Day 4 of differentiation, as expected, when lipid accumulation is most rapid. BCAA uptake is highest, under most conditions, on Day 2 or Day 4, when lipid accumulation is most rapid. Efflux of downstream metabolites are in agreement with this observation, with alanine, glutamine, and glutamate having the most release on Day 2 or Day 4. No significant trends were observed when examining how incubation with glucose affects lipogenesis at each step in the differentiation process.

4.2 **Introduction**

BCAAs are known to play a role in signaling throughout the body.[29,137-139] Circulating BCAA concentrations relay information about energy balance from adipose tissue to other organs. As a result, energy related functions are regulated, including appetite control, glucose metabolism, and insulin secretion.[14-16,150] Previous studies have shown that adipose tissue regulates circulating BCAA concentrations through uptake and lipogenesis. BCAAs may be involved in many other cellular processes as BCAA receptors can be found throughout the body. Individuals who are overweight or obese have increased circulating BCAA levels.[26,116,151] Dysregulation of BCAA metabolism has been seen in many diseased states and is oftentimes associated with impaired glucose metabolism and type 2 diabetes.[152,153]

Under normal conditions, glucose metabolism is a highly regulated process and is the primary energy source for many biological processes. Glucose metabolism is regulated by many factors, including insulin,[154-157] glucagon,[157,158] and glucagon-like peptide-1[157,159]. Nishitani, et al. found that BCAAs regulated and improved the metabolism of glucose in rats with liver cirrhosis by promoting glucose uptake in skeletal muscle.[160]

A high speed capillary electrophoresis (CE) assay was previously developed in order to monitor changes in the uptake and release of branched chain amino acids (BCAAs). This assay has also proven to be useful for measuring the release of downstream markers of lipogenesis, including alanine, glutamine, and glutamate. Using this assay, we can measure how biologically relevant stimuli, such as glucose, influence

the uptake and release of BCAAs, as well as the release of the downstream metabolites, thus providing a good assay for measuring lipogenesis in 3T3-L1 adipocytes.

We wanted to investigate how local glucose concentrations affect the metabolism of BCAAs, over the course of differentiation of the 3T3-L1 model cell line. In order to do so, we first looked at glucose's effect on 3T3-L1 cells and lipogenesis. Glucose concentrations were varied (0-20 mM) to see if lipogenesis changed as a function of local glucose concentration, at varying stages of maturation. BCAA and downstream metabolite efflux was measured at each stage of differentiation. A follow-up experiment monitored changes in the uptake of BCAAs after incubation with varying glucose concentrations (0-20 mM) and 200 μM BCAAs. By monitoring changes in downstream metabolites, alanine, glutamine, and glutamate, we can provide insight into how local BCAA and glucose concentrations affect lipogenesis.

4.3 **Experimental**

4.3.1 **Chemicals and Reagents**

Ciglitazone was purchased from VWR International (Radnor, Pennsylvania). α-cyclodextrin (α-CD) was purchased from CTD Holdings, Inc. (technical grade, Alachua, FL). Dulbecco's Modified Eagle's Medium (DMEM), newborn calf serum (NCS), fetal bovine serum (FBS), and penicillin-streptomycin (5,000U/mL) were purchased from Invitrogen Molecular Probes (Eugene, OR). D-glucose, Mammalian Protein Extraction Reagent (M-PER®), Halt Protease Inhibitor Cocktail, EDTA free, Halt™ Phosphatase Inhibitor Cocktail, and sodium borate tetrahydrate were purchased from Fisher Scientific (Waltham, MA). 3-Isobutyl-1-methylxanthine (IBMX), dexamethasone, insulin (human), and all amino acids were purchased from Sigma-Aldrich (St. Louis, MO).Trypsin

solution (0.25% Trypsin/0.53mM EDTA in Hank's Balanced Salt Solution) was purchased from ATCC (Manassas, VA). Phosphate-buffered saline (PBS, 10×) was purchased from Bio-Rad Laboratories (Hercules, CA). 4-Fluoro-7-Nitro-2, 1, 3-Benzoxadiazole (NBD-F) was purchased from TCI America (Portland, OR).

4.3.2 **Buffers and Solutions**

All solutions were prepared in deionized water (Milli-Q, 18.2 MΩ; Millipore, Bedford, MA) and filtered (0.22μm) unless otherwise noted. Stock standard solutions (1 mM) of amino acids were prepared in Ringer's solution. Ringer's solution was prepared with 123 mM NaCl, 1.5 mM $CaCl_2$, and 5 mM KCl, adjusted to pH 7.5; and autoclaved for sterilization. Ringer's solution containing glucose (0, 5, 10, 15, and 20 mM) was prepared with 123 mM NaCl, 1.5 mM $CaCl_2$, and 5 mM KCl, adjusted to pH 7.5; and autoclaved for sterilization. Sheath flow buffer contained 90 mM borate adjusted to pH 9.8. CE separation buffer contained 90 mM borate/35 mM α-cyclodextrin adjusted to pH 9.8. Derivatization solution was prepared daily by dissolving NBD-F (4-fluoro-7-nitro-2,1,3-benzoxadiazole; TCI America, Portland, OR) in methanol and diluting with equal parts 500 μM HCl and degassing under vacuum, giving a final solution of 20 mM NBD-F/250 μM HCl in 1:1 methanol: water.

4.3.3 **Cell Culture**

3T3-L1 fibroblasts (ATCC® CL-173™) were maintained in 25 cm^2 tissue culture flasks containing 8 mL of high glucose DMEM supplemented with 10% NCS and 1% penicillin/streptomycin. Cultures were maintained in a 37° C incubator (5% CO2). 3T3-L1 cells were differentiated using methods previously described.[44] Briefly, differentiation

was induced by adding high glucose DMEM containing 10% FBS, 0.5 mM IBMX, 0.25 µM dexamethasone, 2 µM ciglitazone, and 170 µM insulin. IBMX, ciglitazone, and dexamethasone were removed after 2 days; insulin was removed after 4 days. Maintenance media (high glucose DMEM, 10% FBS, and 1% penicillin/streptomycin) was used after 4 days. Experiments were conducted at 4 different time points—"Day 0" is prior to any differentiation, but confluent; "Day 2" is after 48 h of incubation with DMEM, FBS, IBMX, dexamethasone, ciglitazone, and insulin; "Day 4" is 96 h after differentiation induction, when media contains DMEM, FBS, and insulin; and finally, "Day14" is 14-16 days after the induction of differentiation.

4.3.4 **Measuring Bulk Amino Acid Release/Uptake**

3T3-L1 cells were cultured and maintained in T25 flasks, as described above. Once a confluent monolayer of cells was established, differentiation was initiated.. At each corresponding time point, cells were rinsed four times with Ringer's solution containing 5 mM glucose with or without 200 µM isoleucine, leucine, and valine (incubation medium). Cells were incubated with 1.00 mL of the corresponding incubation medium, for 30 min. After 30 min, the 1.00 mL of incubation medium was removed and 500µL of this sample was spiked with 25 µL of 1 mM D-2-amino-adipic-acid (internal standard), and was used for online microdialysis- CE analysis. Cells were removed from the flask walls for protein analysis using 1.00 mL of mammalian protein extraction reagent, supplemented with Halt Protease Inhibitor Cocktail, EDTA free, and Halt™ Phosphatase Inhibitor Cocktail. Flasks incubated with this solution at room temperature,

until all cells were detached from flask walls (5-25 min). This 1.00 mL aliquot was collected for protein quantification using a bicinchoninic acid (BCA) assay.

4.3.5 **Microdialysis probes**

Microdialysis probes were constructed in-house using a side-by-side geometry, as described previously[131]. Briefly, two 40 µm i.d. x 105 µm o.d. fused silica capillaries (Polymicro Technologies, Phoenix, AZ) were inserted into a 200 µm i.d. piece of hollow fiber dialysis tubing made from regenerated cellulose (13 kD MWCO, Spectrum Laboratories, Inc., Rancho Dominguez, CA). A sampling region was created by offsetting the capillaries by 1 cm, and sealing using polyimide resin (Alltech, Deerfield, IL). Probes were conditioned prior to use by flushing with ethanol (45µL/h) for five min, followed by ten min of Ringer's solution (25µL/h). Probes were perfused with Ringer's solution at 25 µL/h throughout experiments.

4.3.6 **Online Derivatization**

Dialysate was carried in a 30-40 cm long × 40 µm i.d. × 360 µm o.d. fused silica capillary to a 250 µm i.d. stainless steel cross (Valco Instruments Co. Inc, Houston, TX) where it was mixed with a 5 µL/h stream of borate buffer and a 5 µL/h stream of derivatization solution. The derivatization of primary and secondary amines took place as the dialysate mixture traveled through a 90 cm long, 75 µm i.d. × 360 µm o.d. fused silica capillary from the reaction cross to the flow gate interface; 66 cm of this capillary was heated to accelerate the reaction by passing through flexible tubing that was circulating water from a water bath at 80°C (NESLAB EX-7 Digital One heating bath circulator,

Thermo, Newington, NH). The length of the reaction capillary and flow rates used resulted in a 5 min reaction time, allowing the labeling reaction to go to completion.[90]

4.3.7 **High Speed Capillary Electrophoresis**

An 8-8.5 cm long, 10 µm i.d. × 360 µm o.d. fused silica capillary (separation capillary) was aligned coaxially, with a 50 µm gap, with the reaction capillary in a polycarbonate flow gate interface block.[73] A syringe pump (Pump 22 syringe pump, Harvard Apparatus, Holliston, MA) pumped separation buffer at 40 mL/hthrough this gap. Separation buffer flow was controlled by a pneumatically actuated valve (C2-300A 10 port valve, Valco Instruments Co. Inc., Houston, TX); crossflow of the separation buffer was stopped to for 500 ms allowing a sample plug to build up in the gap. An injection voltage of -13 kV was applied to the exit of the separation capillary for 200 ms. The flow stream though the flow gate was resumed and a separation voltage of -19 kV was applied. Separations were performed every 30 s. Injections were controlled by an in-house LabVIEW program.

4.3.8 **LIF Detection**

A 488 nm argon ion laser was used for LIF detection (150 mW, Melles Griot, Carlsbad, CA). The laser beam was passed through a 10× beam expander (Edmond Optics, Barrington, NJ), and focused using a 1× lens to a point just past the exit of the CE separation capillary in a fused-silica sheath flow cuvette(2 mm square with a 400 µm × 400 µm square inner bore).[82,135] Fluorescence emission is collected at 90° with a 60×, 0.7 NA long working distance objective (Universe Kogaku, Oyster Bay, NJ) and filtered through spatial (~1 mm diameter) and bandpass filters (543.5 ± 10 nm) (Melles Griot,

Irvine, CA), and recorded using a photomultiplier tube (PMT R1477, Hamamatsu Corp., Bridgewater, NJ). Current from the PMT was amplified (Keithley 428 Current Amplifier, Keithley Instruments Inc., Cleveland, OH), filtered with a 10 ms rise time, and recorded using a data acquisition card (National Instruments Corp., Austin, TX). Data analysis was performed using Cutter Analysis 7.0.[149]

4.3.9 **Bicinchoninic Acid (BCA) Assay**

Amino acid concentrations were normalized according to cell protein content, as measured using a BCA assay. A Pierce™ BCA Protein Assay Kit was used according to included instructions. Briefly, working reagent was prepared by combining "Reagent A" and "Reagent B" in a ratio of 50:1 (A: B). 25 µL of each sample or standard was pipetted into individual wells of a 96 well plate followed by 200 µL of working reagent; all samples were analyzed in triplicate. The plate was gently shaken for 30 s to ensure mixing of the working reagent and samples. After shaking, the plate was incubated at 37°C for 30 min. After incubation, the plate was removed from the incubator and absorbance at 562 nm was measured using a plate reader (Spectromax Plus; Molecular Devices, LLC, Sunnyvale, CA). A calibration curve was generated from BSA standards. Using this standard curve, protein content for each flask was determined and used for normalizing amino acid signals obtained from CE separation.

4.3.10 **Statistical Analysis**

All Figures show mean ±S.E. Differences between groups were assessed using Student's two-tailed *t* test.

4.4 Results & Discussion

4.4.1 Amino Acid Efflux in the Presence of Glucose

4.4.1.1 BCAA Efflux

Through catabolism of BCAAs, acetyl-CoA products are generated (Figure 1.2). During periods of low energy, these products are directed and used in the TCA cycle for generation of ATP. During periods of high energy, the acetyl-CoA products are used in fatty acid synthesis and are then stored as triglycerides in lipid vesicles in the cytoplasm of adipocytes. As the cells progress through differentiation, cellular needs change, and at later stages, the cells rapidly accumulate lipids. This rapid accumulation of lipids leads to increased utilization of BCAAs, compared to earlier stages. BCAA release was monitored over the course of 3T3-L1 cell differentiation into mature adipocytes to monitor these changes in energy usage, when incubated with various concentrations of glucose for 30 min. As shown in Figure 4.1, 3T3-L1 cells released the most isoleucine at early stages in the maturation process (Day 0 & 2) and released the least isoleucine during times of rapid lipid accumulation (Day 4). The same trend was seen at all glucose concentrations administered (0-20 mM; Figure 4.1A-E). For all glucose concentrations, the release of isoleucine on Day 4 was statistically different ($p<0.05$) from earlier developmental stages (Day 0 & 2), however, was not statistically different than the fully differentiated state, Day 14, as shown in Figure 4.1A-E.

Utilization of leucine and valine showed similar patterns. The least efflux of leucine and valine from 3T3-L1 cells occurred on Days 4 & 14, regardless of local glucose concentration (Figure 4.2A). The observed results support previous research by Green, et al. suggesting that consumption of BCAAs increases as the cells progress

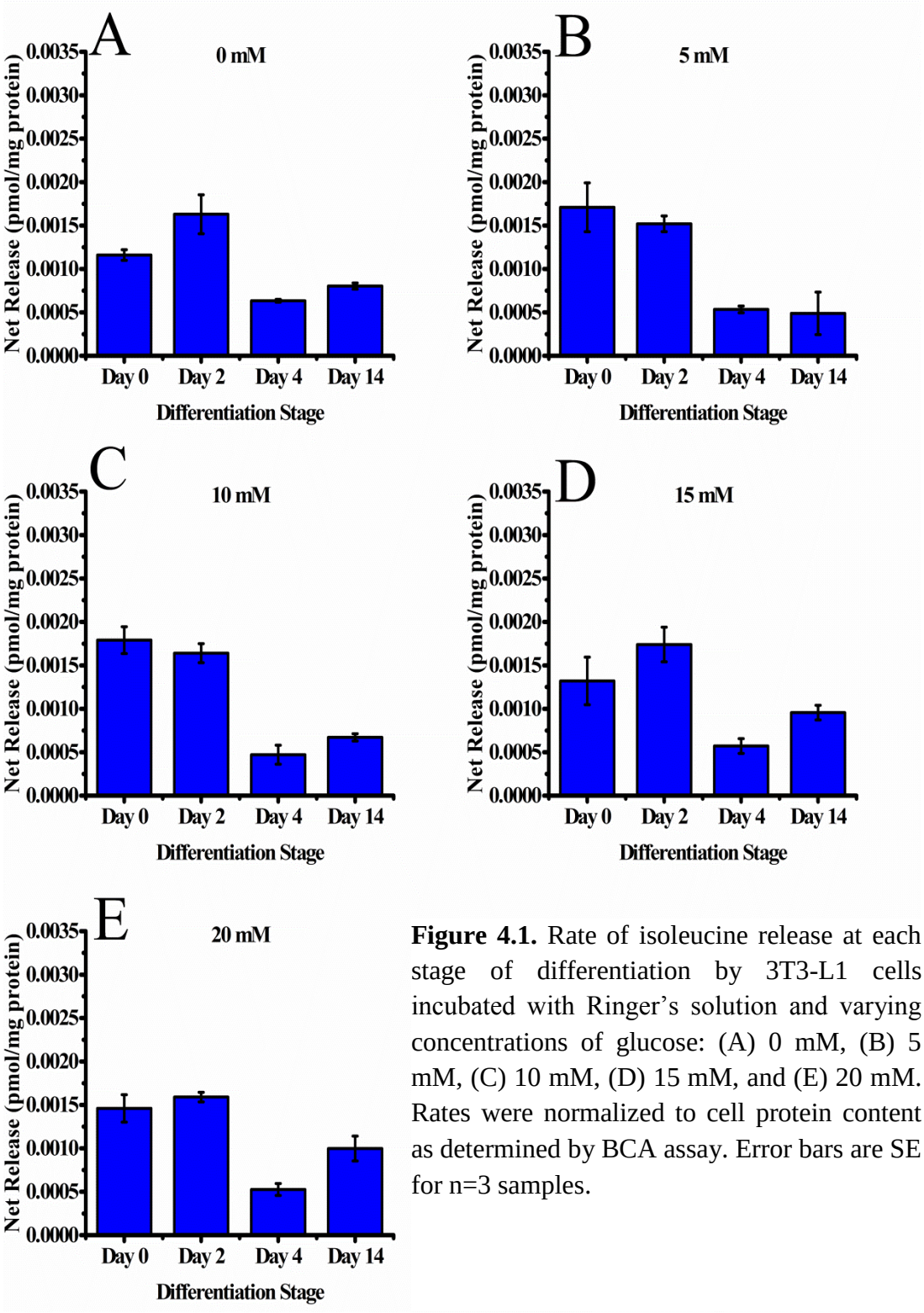

Figure 4.1. Rate of isoleucine release at each stage of differentiation by 3T3-L1 cells incubated with Ringer's solution and varying concentrations of glucose: (A) 0 mM, (B) 5 mM, (C) 10 mM, (D) 15 mM, and (E) 20 mM. Rates were normalized to cell protein content as determined by BCA assay. Error bars are SE for n=3 samples.

through differentiation, as is shown in Figure 4.1. [30] BCAAs can be catabolized to generate fatty acid synthesis and TCA cycle precursor molecules.

When looking at the release of BCAAs based on developmental stage, we see very little changed in released isoleucine (Figure 4.3), regardless of the local glucose concentration. When the cells are in the pre-adipocyte stage (Day 0; A in Figure 4.3), the most isoleucine release occurs at 5 & 10 mM glucose; however, this is not the case once the cells have progressed further into the differentiated state. Once the 3T3-L1 cells are more committed to the differentiated state, the least amount of isoleucine release occurs at 5 & 10 mM glucose (Figure 4.3B,C, & D). This trend holds true from Day 2

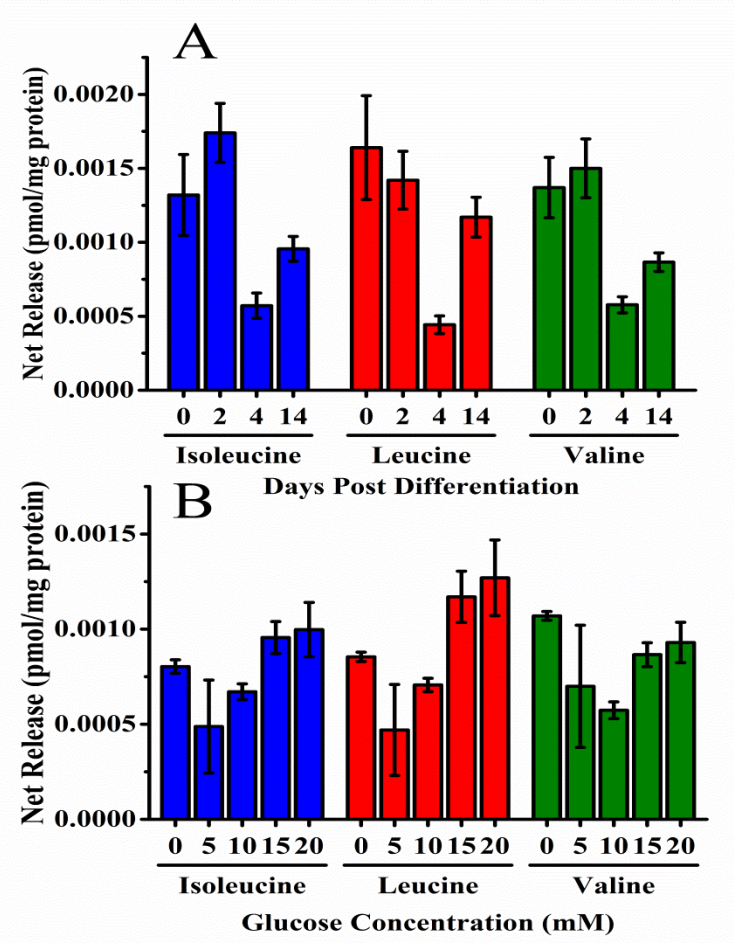

Figure 4.2. (A) Rate of BCAA release from 3T3-L1 after incubation with 15 mM glucose, at each stage of differentiation. Amounts were normalized to cell protein content as determined by BCA assay. Error bars are SE for n=3 samples. (B) Rate of BCAA release from 3T3-L1 cells after incubation with varying concentrations of glucose, on Day 14. Rates were normalized to cell protein content as determined by BCA assay. Error bars are SE for n=3 samples.

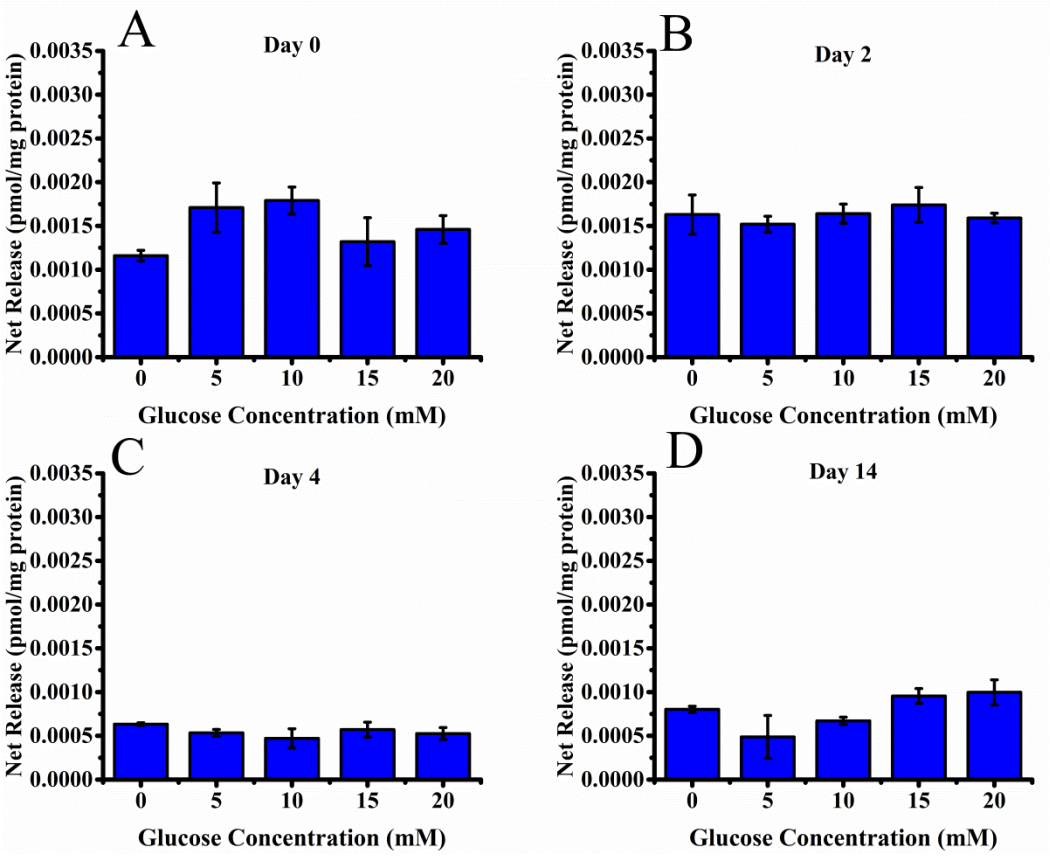

Figure 4.3. Rate of isoleucine release from 3T3-L1 cells after incubation with Ringer's solution and varying concentrations of glucose (0-20 mM) at each stage of differentiation: (A) Day 0, (B) Day 2, (C) Day 4, (D) Day 14. Amounts were normalized to cell protein content as determined by BCA assay. Error bars are SE for n=3 samples**.**

through Day 14, as depicted in Figure 4.3B-D. The trends seen in isoleucine are the same as what is seen when analyzing the release patterns of leucine and valine as well. Figure 4.2B shows the release of all 3 BCAAs on Day 14, showing that at biologically relevant concentrations of glucose, 3T3-L1 cells release the least amount of BCAAs. Higher local concentrations of glucose appear to promote glycolysis rather than BCAA catabolism, as utilization of BCAAs is decreased at these concentrations.

4.4.1.2 **Downstream Metabolite Efflux**

In order to see if changes in BCAA release correspond to increases in catabolism of BCAAs and thus, increases in lipogenesis, we tracked the release of downstream metabolites, alanine, glutamate, and glutamine. 3T3-L1 cells released the most alanine at Day 0, when the cells are in the earliest stages of maturation (Figure 4.4, black). This contradicts what we would expect, as we would expect very little lipid accumulation to be occurring at this time point, as cells have just begun differentiation. At stages when lipogenesis is expected to be highest (i.e. Day 4), alanine release is lowest, which is again, the opposite of what is expected. This could be attributed to a lack of upstream BCAAs to catabolize, or a lack of available pyruvate to convert glutamate to alanine. Pyruvate is generated through the metabolism of glucose through the process of glycolysis. The same trend is seen at all glucose concentrations assessed, indicating that extracellular glucose alone does not promote BCAA catabolism (Figure 4.4A-E, black).

Glutamine and glutamate have similar trends (Figure 4.5B & 4.5C), however, once cells have fully matured, the glutamate/glutamine pathway seems to be affected by the glucose concentration. At 15 mM glucose, glutamine release at Day 14 drops to nearly 0 net release, while glutamate release increases dramatically, as shown in black in Figure 4.5B & 4.5C. This trend is also seen at 10 mM and 20 mM glucose concentrations. When looking at the release trends as a function of glucose concentration, alanine has the most release at Day 0, when the cells were incubated with 5 or 10 mM glucose. Day 2 has the most release when incubated with 0 mM glucose, with the least release at 5 mM;

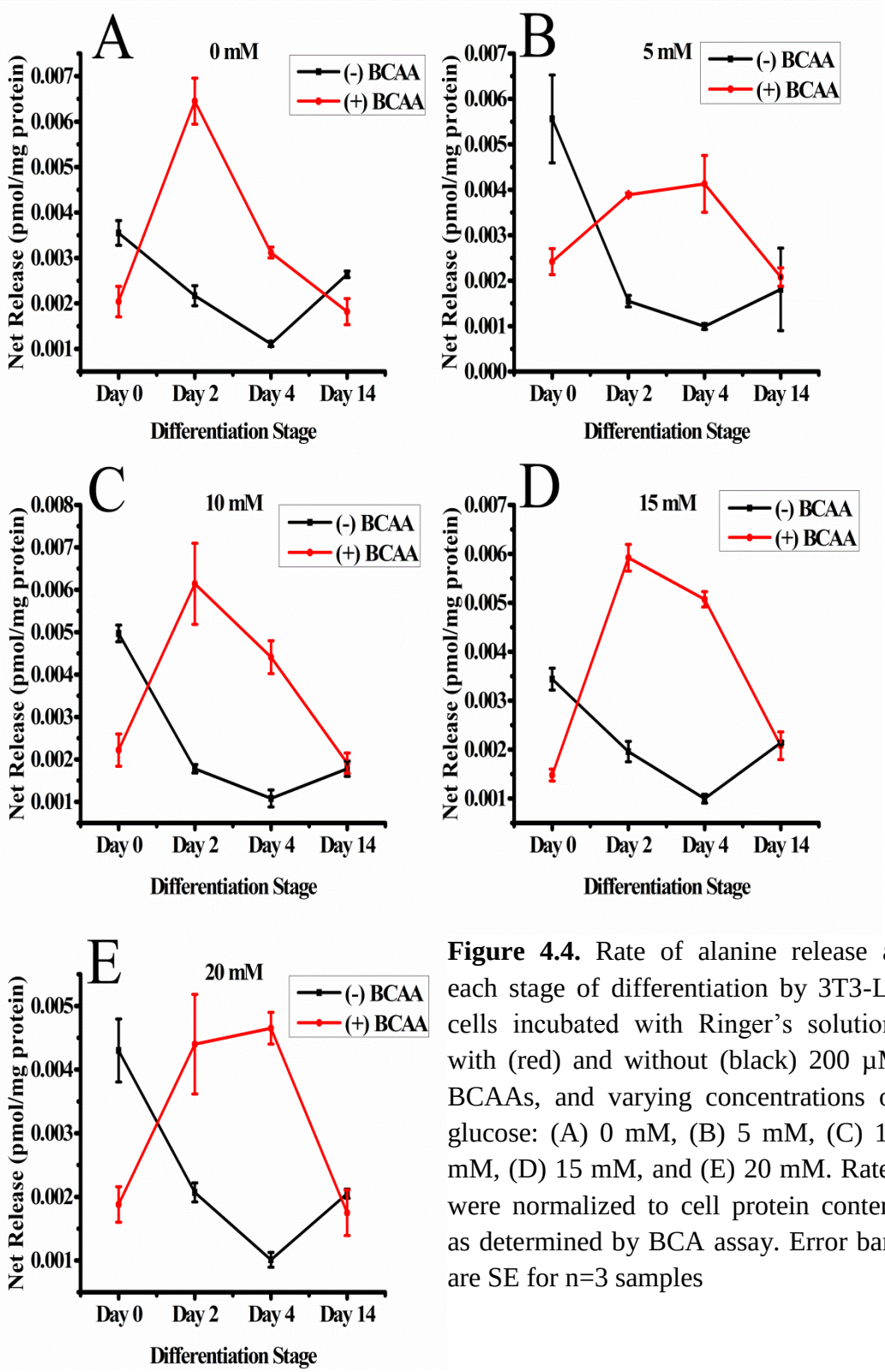

Figure 4.4. Rate of alanine release at each stage of differentiation by 3T3-L1 cells incubated with Ringer's solution, with (red) and without (black) 200 µM BCAAs, and varying concentrations of glucose: (A) 0 mM, (B) 5 mM, (C) 10 mM, (D) 15 mM, and (E) 20 mM. Rates were normalized to cell protein content as determined by BCA assay. Error bars are SE for n=3 samples

there appears to be an upward trend in the release, with all higher glucose concentrations having more release the previous concentration (from 5 mM), as shown in Figure 4.6 (black). On Day 4, there is no trend in the release of alanine over the range of glucose concentrations. Once the cells have fully matured, Day 14, alanine is released the most when incubated without glucose, indicating that catabolism of BCAAs may be occurring.

Similar trends are seen when looking at glutamine and glutamate release at Day 0. Glutamate has the same trend on Day 2 as alanine, but glutamine does not; glutamine has the most release when incubated with 20 mM glucose. Day 4 has similar trends when looking at all three downstream metabolites, while Day 14 has unusual trends in glutamine and glutamate as discussed previously.

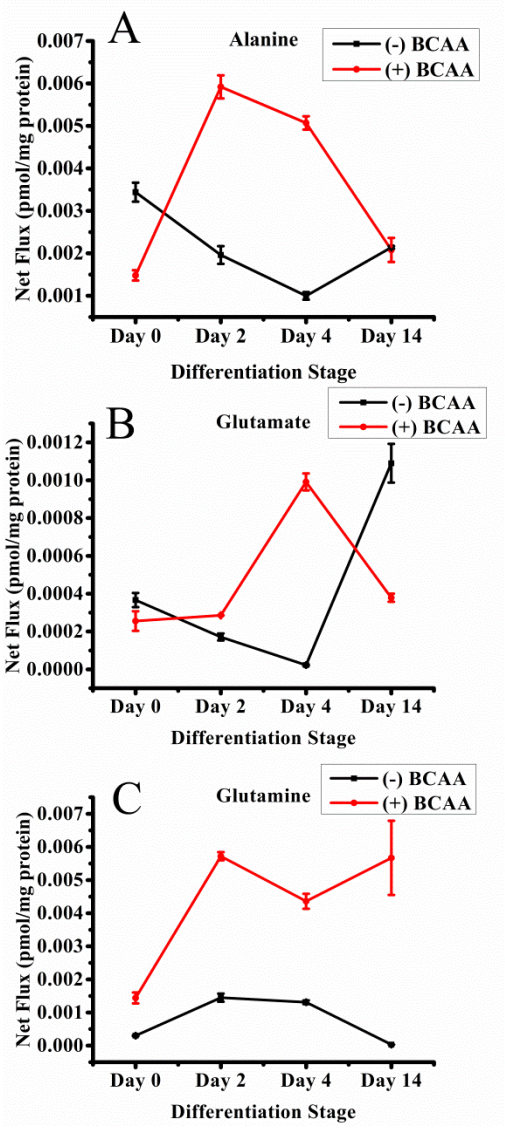

Figure 4.5. Release of downstream metabolites, alanine, glutamate, and glutamine at each stage of differentiation when 3T3-L1 cells are incubated with Ringer's solution containing 15 mM glucose with (red) or without (black) 200 µM BCAAs for 30 minutes. Error bars are SEM; n=3.

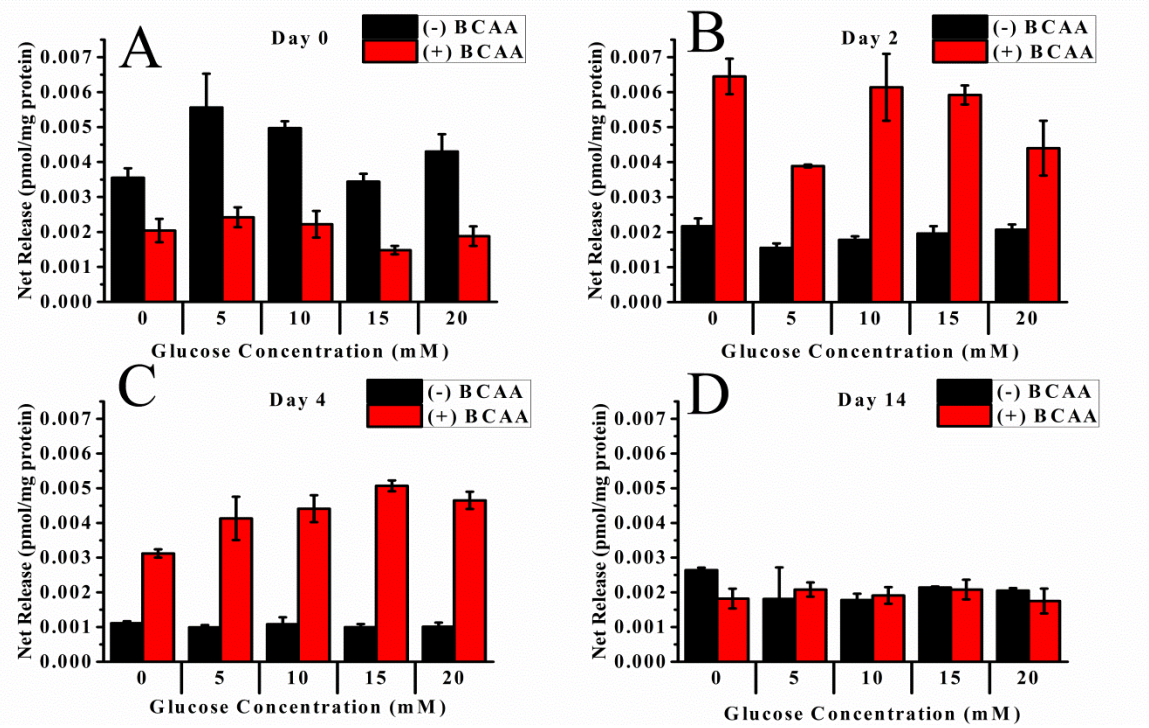

Figure 4.6. Rate of alanine release after incubation with varying concentrations of glucose, at each stage of differentiation, by 3T3-L1 cells incubated with Ringer's solution, with (red) and without (black) 200 µM BCAAs, and varying concentrations of glucose (0-20 mM): (A) Day 0, (B) Day 2, (C) Day 4, (D) Day 14. Amounts were normalized to cell protein content as determined by BCA assay. Error bars are SE for n=3 samples.

4.4.2 Amino Acid Efflux in the Presence of Glucose and 200 µM BCAAs

4.4.2.1 BCAA Uptake

In order to determine if local BCAA concentrations influence glucose and its effect on 3T3-L1 lipogenesis, 3T3-L1 cells were incubated with 200 µM BCAAs for 30 min. Amino acid release from those 3T3-L1 cells was monitored throughout

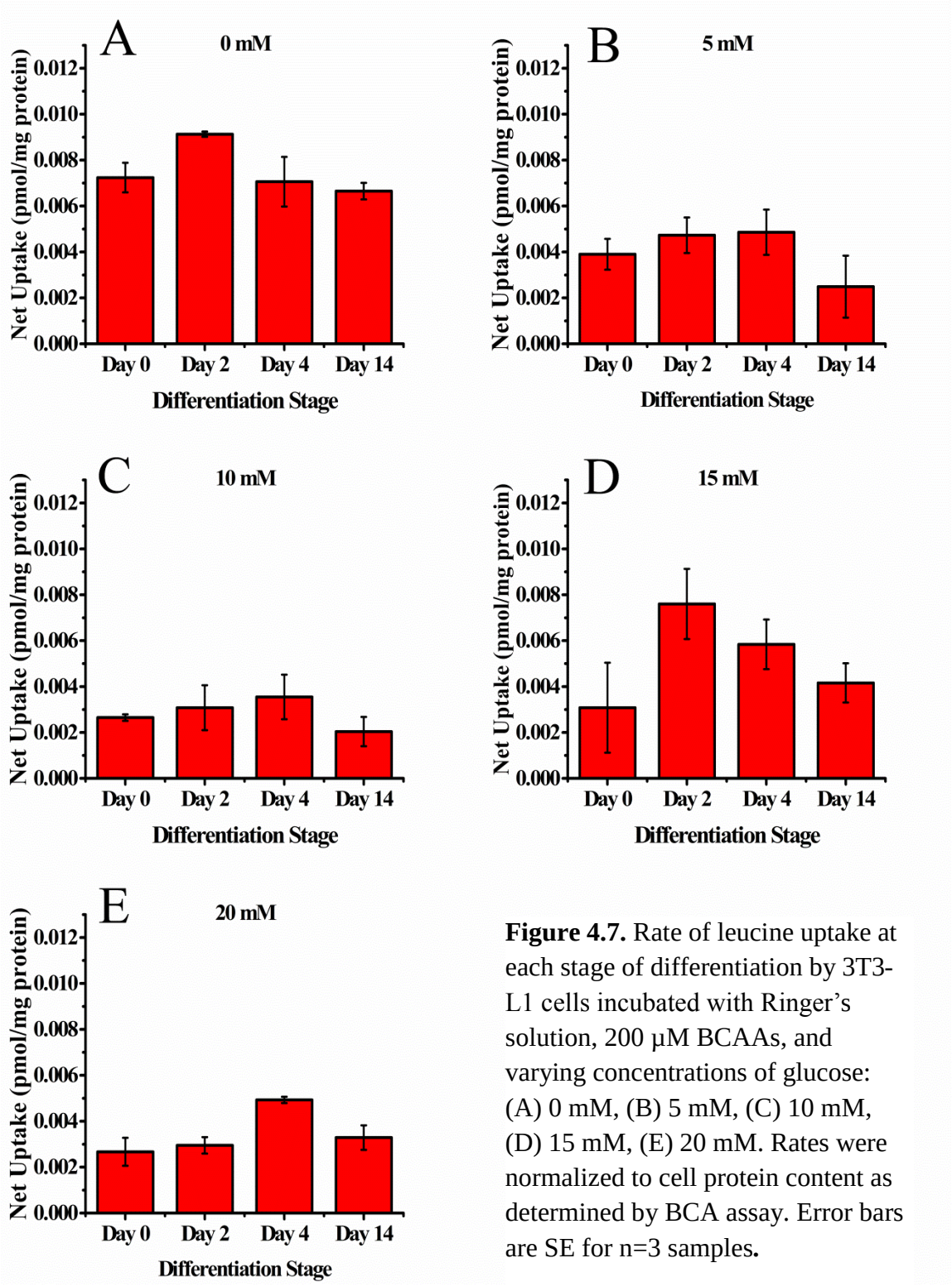

Figure 4.7. Rate of leucine uptake at each stage of differentiation by 3T3-L1 cells incubated with Ringer's solution, 200 µM BCAAs, and varying concentrations of glucose: (A) 0 mM, (B) 5 mM, (C) 10 mM, (D) 15 mM, (E) 20 mM. Rates were normalized to cell protein content as determined by BCA assay. Error bars are SE for n=3 samples.

differentiation with varying doses of glucose. Figure 4.7 shows changes and trends observed for leucine after incubation with various glucose concentrations (0-20 mM) and 200 µM BCAAs for 30 min. When 3T3-L1 cells are incubated with 0 mM glucose and 200 µM BCAAs, the most uptake occurs on Day 2 (Figure 4.7C). The same trend is observed at 5, 10, and 15 mM glucose concentrations as well. At 20 mM glucose, however, the most uptake of leucine occurs on Day 4, during the peak of lipogenesis (Figure 4.7E). Overall patterns and trends are similar for isoleucine and valine, with most uptake occurring on either Day 2 or Day 4, regardless of the glucose concentration present during incubation. Figure 4.8 shows the uptake of all three BCAAs over the course of development after incubation with 10 mM glucose and 200 µM BCAAs.

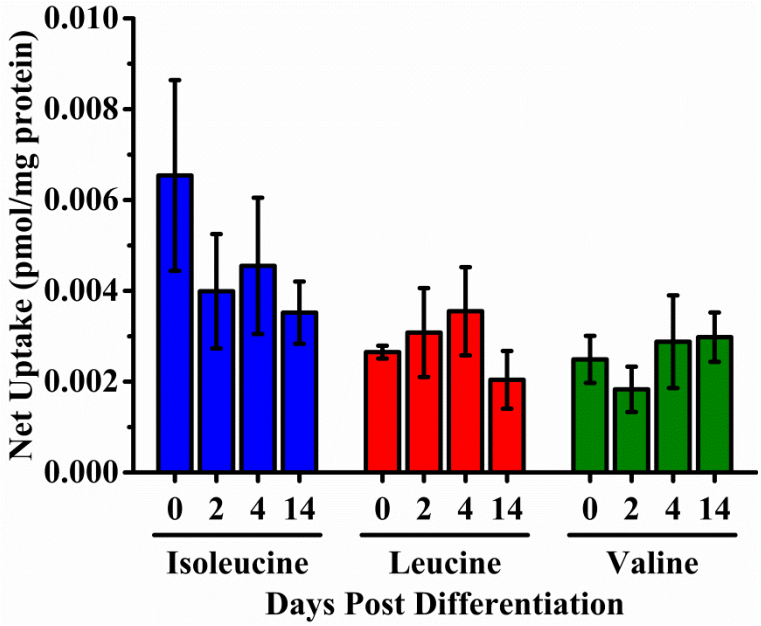

Figure 4.8. Uptake of BCAAs at each stage of differentiation when 3T3-L1 cells are incubated with Ringer's solution containing 200 µM BCAAs and 10 mM glucose for 30 minutes. Error bars are SEM; n=3.

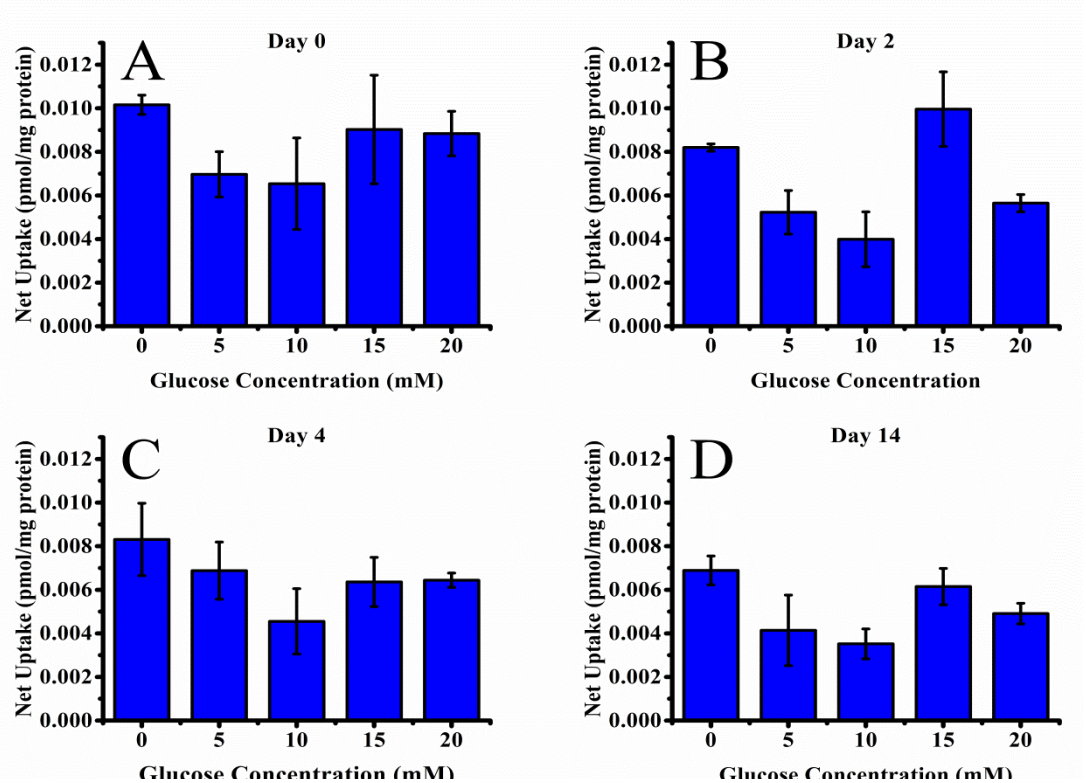

Figure 4.9 Rate of isoleucine uptake from 3T3-L1 cells after incubation in Ringer's solution with varying concentrations of glucose (0-20 mM) and 200 µM isoleucine, leucine, and valine, at each stage of differentiation: (A) Day 0, (B) Day 2, (C) Day 4, (D) Day 14. Amounts were normalized to cell protein content as determined by BCA assay. Error bars are SE for n=3 samples.

The effects of glucose and BCAA concentrations on 3T3-L1 adipocytes can be monitored as a function of differentiation state (Figure 4.9). At the earliest stage of differentiation, Day 0 (Figure 4.9A), 3T3-L1 cells had the most uptake of isoleucine at 0 mM, with the least amount of uptake at 10 mM. Day 2 (Figure 4.9B) had the most uptake of isoleucine at 15 mM, while Day 4 (Figure 4.9C) & 14 (Figure 4.9D) had the most isoleucine uptake at 0 mM, similar to Day 0. All four time points had the least release when incubated with 10 mM glucose. Leucine and valine have similar trends, except on Day 2, with 20 mM glucose, as valine had net release, rather than uptake. Uptake of

BCAAs on Day 4, when cells are undergoing lipogenesis most rapidly, looking at trends in glucose concentration is shown in Figure 4.10.These data suggest that glucose concentration affects 3T3-L1 cells differently at different maturation stages.

4.4.2.2 **Alanine, Glutamate & Glutamine Release**

Monitoring alanine, glutamate, and glutamine allows us to monitor lipogenesis as a function of BCAA presence. As shown in Figure 4.5A, alanine release is highest on Day 2 after incubation with 15 mM glucose and BCAAs; the same is true after incubation with 20 mM glucose and BCAAs as well. The release of glutamine and glutamate follow similar trends to alanine at each glucose concentration, however, there appears to be equilibrium between glutamine and glutamate that is maintained. As shown in Figure 4.5C, when glutamine concentrations decrease on Day 4, glutamate concentrations increase (Figure 4.5B), at all glucose concentrations assessed. Alanine has the most release on Day 2, glutamine has the most release at Day 2 & 4,

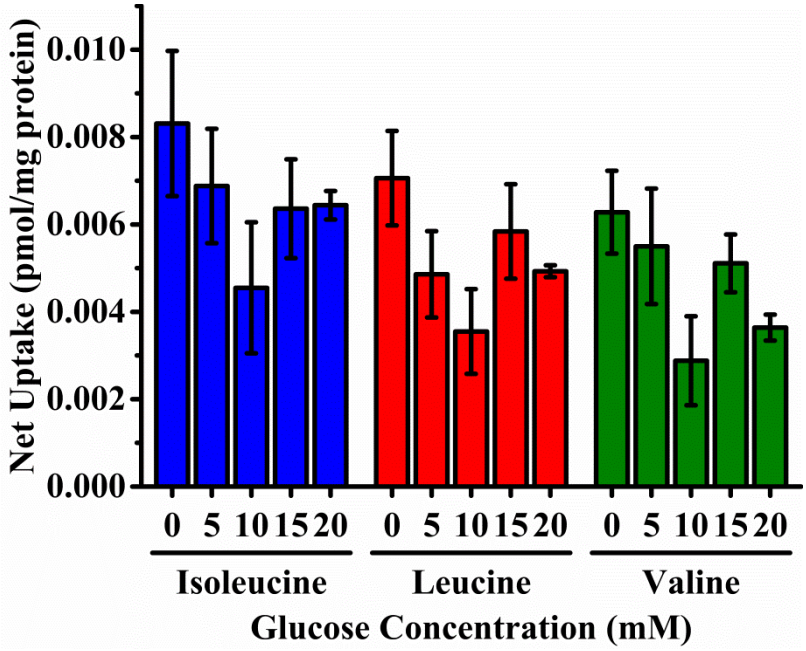

Figure 4.10. Uptake of BCAAs on Day 4 when incubated with Ringer's solution containing 200 μM BCAAs and varying concentrations of glucose (0-20 mM) for 30 minutes. Error bars are SEM; n=3.

while glutamate has the most release on Day 4, when incubated with 0 mM glucose and 200 µM BCAAs. 5 mM glucose gives the most release of alanine and glutamate at Day 4, Day 2 & 14 have the most release of glutamine. When 3T3-L1 cells are incubated in 10 mM glucose and 200 µM BCAAs, alanine and glutamine have the most release on Day 2 of the differentiation process, while glutamate is released the most on Day 4. The trends seen in the downstream metabolites correspond closely with the patterns observed in the uptake of BCAAs at similar glucose concentrations. No significant trends can be deciphered when analyzing the downstream metabolites based on cells' maturation stage. Fluctuations in release of downstream metabolites are observed, however, the observations do not follow expected results. This could be due to interactions with glucose and its effects on lipogenesis in 3T3-L1 cells.

4.4.3 **Comparing incubation with and without BCAAs**

Comparing the results between the experiments performed when cells were incubated with circulating levels of BCAAs to those when cells were not, allows use to determine the effects of the BCAAs on lipogenesis. Examining these results also allows us to assess their influence on lipogenesis throughout the differentiation process, while monitoring changes in lipogenesis markers, as a function of local glucose concentration.

When comparing the two experiments, looking at the development of the cells, throughout the differentiation process, at each glucose concentration, we see that alanine has the opposite trend when the BCAAs are present, as shown in Figure 4.4A-E. We can see that no matter what the local glucose concentration was, the cells released the most alanine during the intermediate stages of development, Days 2 & 4, when incubated with

200 μM BCAAs (red), and the least amount of alanine is released on Day 4 when the cells are incubated in Ringers solution without BCAAs (black). Between experiments, there is a 180% increase, on average, in the total alanine released on Day 2, and a 300%+ increase on Day 4. Increases in glutamine and glutamate are even larger, but trends hold true for both of those amino acids (see Appendix, Figure A.8). When looking at the experiments and how the glucose concentration affects the release, as a function of differentiation stage, we see that there are no statistically significant trends for any of the downstream lipogenesis markers (See Figure 4.6A-D). It could be argued that on Days 2 & 4, the cells release more alanine, glutamine, and glutamate, regardless of local glucose concentration, solely due to the nature of the stage of differentiation that the cells are in. These intermediate stages are when cells are accumulating lipids and catabolize BCAAs most rapidly.

4.5 **Conclusion**

Changes in BCAA uptake and release as a function of local glucose and BCAA concentration was monitored using an online high-speed CE-LIF assay. This assay allows the BCAAs, as well as downstream metabolites, alanine, glutamine, and glutamate, to be monitored to assess changes in release patterns based on local glucose and BCAA concentrations. Using this assay, we were able to observe different lipogenic processes as cells progress through differentiation. Downstream metabolites suggest that 3T3-L1 cells are accumulating lipids and doing so by catabolism of BCAAs. When cells were incubated with Ringer's solution containing only glucose (0-20 mM), BCAA release diminished as the cells accumulated more lipids, while alanine, glutamine, and glutamate

release did not follow expected increasing trends. This gives evidence that BCAA catabolism was not the only mechanism behind lipid accumulation. When cells were incubated in Ringer's solution containing glucose and BCAAs, uptake occurred most rapidly during periods of expected high lipogenesis. Released alanine closely followed these patterns, suggesting BCAA catabolism. Glucose concentration did not appear to affect the release or uptake of BCAAs, regardless of concentration. Uptake patterns suggest that at increased glucose concentrations, the primary energy source for the cells is glucose, rather than BCAAs, even in a high-energy state.

Chapter 5: Applications of Online High-Speed CE

5.1 **Summary**

Lipogenesis was monitored using the previously developed high-speed CE assay, after differentiated 3T3-L1 cells were incubated with various biologically relevant stimuli. Two stimulants that we are particularly interested in investigating are insulin and artificial sweeteners. BCAA uptake was influenced by incubation with insulin or artificial sweeteners, while downstream metabolites were largely unaffected. Insulin's effect on BCAA uptake changes based on local BCAA concentration, with increased uptake with larger localized BCAA concentrations. Of the artificial sweeteners assessed, acesulfame K+ had an amino acid release profile similar to glucose. Saccharine, aspartame, and fructose had less BCAA uptake than glucose, but did not generate corresponding decreases in downstream metabolites, as would be expected from less catabolism of BCAAs. Additional experiments are needed in order to clarify the impacts of insulin or artificial sweeteners on lipogenesis in 3T3-L1 cells.

5.2 Introduction

5.2.1 Effect of Insulin on Lipogenesis

It has been well established that BCAAs act as signaling molecules throughout the body and whole body BCAA concentrations are highly regulated by adipose tissue. [29,137-139] Many studies have investigated the role of insulin and its relationship with obesity, however, the mechanism underlying the connection is still unknown. Previously, Cammisotto, et al. investigated the effect of insulin on the release of leptin, a prominent hormone related to obesity, at various glucose concentrations.[32]In their study, it was found that glucose was required in incubation media in order for insulin to affect leptin release from cells, however, the concentration of glucose (5 mM – 25 mM) did not affect the amount of released leptin. Throughout all of the experiments performed, it was obvious that insulin is a potent stimulator of leptin secretion from isolated adipocytes.[32] We hypothesized that other signaling molecules may be increased when adipocytes are incubated with insulin due to the fact that marked increases are observed in leptin secretion under similar conditions. Increases in leptin, operate in a negative feedback loop, signaling that energy is high, and it is hypothesized that this would promote lipogenesis. If such is the case, incubation with insulin should stimulate the uptake and catabolism of BCAAs and increases in downstream metabolites should be observed. Using the previously developed assay, we are able to measure both uptake and secretion of downstream metabolites as a measure of lipogenesis.

5.2.2 **Effect of Sweeteners on Lipogenesis**

In an effort to curb obesity, many artificial sweeteners have become low-calorie replacements for glucose in our diets. While, at first glance, these sweeteners seemingly provide all of the desired benefits, sweet taste without the calories, the anti-obesity benefits seem to be lacking. Obesity rates have continued to increase dramatically since the incorporation of these artificial sweeteners in our diets.[161] Adding artificial sweeteners is likely one of many factors playing an important role in the development of obesity, according to initial studies. [161] These artificial sweeteners trigger the "sweet" carbohydrate receptors found throughout the body and signal for anabolism to occur, but don't provide the necessary calories to do so.[162] As such, energy is stored and metabolism is reduced, thus causing weight gain, even when calorie intake is limited.[163] Because the artificial sweeteners are more potent than glucose itself,[164,165] they could lead to desensitization of carbohydrate receptors.[163] In one study, saccharine was shown to be effective in initiating the formation of new adipocytes and promoting lipogenesis in mature adipocytes.[166]

We hypothesize that if artificial sweeteners are acting on the same receptors as glucose and other carbohydrates, we would see a marked increase in the release of lipogenic markers, alanine, glutamine, and glutamate, after increased uptake of the BCAAs. Using our microdialysis-CE assay, we can easily detect any changes in uptake and secretion of metabolites to assess 3T3-L1 adipocyte response to fructose, saccharine, acesulfame K+ (AceK), and stevioside.

5.3 Materials and Methods

5.3.1 Chemicals and Reagents

Ciglitazone was purchased from VWR International (Radnor, Pennsylvania). α-cyclodextrin (α-CD) was purchased from CTD Holdings, Inc. (technical grade, Alachua, FL). Dulbecco's Modified Eagle's Medium (DMEM), newborn calf serum (NCS), fetal bovine serum (FBS), and penicillin-streptomycin (5,000U/mL) were purchased from Invitrogen Molecular Probes (Eugene, OR). D-glucose, Mammalian Protein Extraction Reagent (M-PER®), Halt Protease Inhibitor Cocktail, EDTA free, Halt™ Phosphatase Inhibitor Cocktail, and sodium borate tetrahydrate were purchased from Fisher Scientific (Waltham, MA). 3-Isobutyl-1-methylxanthine (IBMX), dexamethasone, insulin (human), and all amino acids were purchased from Sigma-Aldrich (St. Louis, MO).Trypsin solution (0.25% Trypsin/0.53mM EDTA in Hank's Balanced Salt Solution) was purchased from ATCC (Manassas, VA). Phosphate-buffered saline (PBS, 10×) was purchased from Bio-Rad Laboratories (Hercules, CA). 4-Fluoro-7-Nitro-2, 1, 3-Benzoxadiazole (NBD-F) was purchased from TCI America (Portland, OR).

5.3.2 Buffers and Solutions

All solutions were prepared in deionized water (Milli-Q, 18.2 MΩ; Millipore, Bedford, MA) and filtered (0.22μm) unless otherwise noted. Stock standard solutions (1 mM) of amino acids were prepared in Ringer's solution. Ringer's solution was prepared with 123 mM NaCl, 1.5 mM $CaCl_2$, and 5 mM KCl, adjusted to pH 7.5; and autoclaved for sterilization. Ringer's solution containing glucose (0, 5, 10, 15, and 20 mM) was prepared with 123 mM NaCl, 1.5 mM $CaCl_2$, and 5 mM KCl, adjusted to pH 7.5; and

autoclaved for sterilization. Sheath flow buffer contained 90 mM borate adjusted to pH 9.8. CE separation buffer contained 90 mM borate/35 mM α-cyclodextrin adjusted to pH 9.8. Derivatization solution was prepared daily by dissolving NBD-F (4-fluoro-7-nitro-2,1,3-benzoxadiazole; TCI America, Portland, OR) in methanol and diluting with equal parts 500 µM HCl and degassing under vacuum, giving a final solution of 20 mM NBD-F/250 µM HCl in 1:1 methanol: water.

5.3.3 **Cell Culture**

3T3-L1 fibroblasts (ATCC® CL-173™) were maintained in 25 cm^2 tissue culture flasks containing 8 mL of high glucose DMEM supplemented with 10% NCS and 1% penicillin/streptomycin. Cultures were maintained in a 37° C incubator (5% CO2). 3T3-L1 cells were differentiated using methods previously described.[44] Briefly, differentiation was induced by adding high glucose DMEM containing 10% FBS, 0.5 mM IBMX, 0.25 µM dexamethasone, 2 µM ciglitazone, and 170 µM insulin. IBMX, ciglitazone, and dexamethasone were removed after 2 days; insulin was removed after 4 days. Maintenance media (high glucose DMEM, 10% FBS, and 1% penicillin/streptomycin) was used after 4 days. Experiments were conducted at 4 different time points—"Day 0" is prior to any differentiation, but confluent; "Day 2" is after 48 h of incubation with DMEM, FBS, IBMX, dexamethasone, ciglitazone, and insulin; "Day 4" is 96 h after differentiation induction, when media contains DMEM, FBS, and insulin; and finally, "Day14" is 14-16 days after the induction of differentiation.

5.3.4 **Measuring Bulk Amino Acid Release/Uptake**

5.3.4.1 **Insulin Experiments**

3T3-L1 cells were cultured and maintained in T25 flasks, as described above. Once a confluent monolayer of cells was established, differentiation was initiated. Experiments took place at two time points throughout the differentiation cycle, as defined previously. “Day 4” is 96 h after differentiation induction, when media contains DMEM, FBS, and insulin; “Day 14” is 14-16 days after the induction of differentiation. At each corresponding time point, cells were rinsed four times with Ringer’s solution containing 5 mM glucose, 200 µM isoleucine, leucine, and valine, with or without 10 nM insulin (incubation medium). Cells were incubated with 1.00 mL of the corresponding incubation medium, for 30 min. After 30 min, the 1.00 mL of incubation medium was removed and 500 µL of this sample was spiked with 25 µL of 1 mM D-2-amino-adipic-acid (internal standard), and was used for microdialysis—CE analysis. Cells were removed from the flask walls for protein analysis using 1.00 mL of mammalian protein extraction reagent, supplemented with Halt Protease Inhibitor Cocktail, EDTA free, and Halt™ Phosphatase Inhibitor Cocktail. Flasks incubated with this solution for 5-25 min at room temperature, until all cells were detached from flask walls. This 1.00 mL aliquot was collected for protein quantification using a bicinchoninic acid (BCA) assay.

5.3.4.2 **Sweetener Experiments**

3T3-L1 cells were cultured and maintained in T25 flasks, as described above. Once a confluent monolayer of cells was established, differentiation was initiated. Experiments were performed at “Day 4” 96 h after differentiation induction, when media contained DMEM, FBS, and insulin. At this time point, cells were rinsed four times with

Ringer's solution containing 5 mM glucose, 200 µM isoleucine, leucine, and valine. Cells were then incubated with 1.00 mL of one of five sweetener solutions, as described above, for 30 min. After 30 min, the 1.00 mL of the sweetener solution was removed and 500 µL of this sample was spiked with 25 µL of 1 mM D-2-amino-adipic-acid (internal standard), and was used for microdialysis—CE analysis. Cells were removed from the flask walls for protein analysis using 1.00 mL of mammalian protein extraction reagent, supplemented with Halt Protease Inhibitor Cocktail, EDTA free, and Halt™ Phosphatase Inhibitor Cocktail for 5-25 min at room temperature. This 1.00 mL aliquot was collected for protein quantification using a bicinchoninic acid (BCA) assay.

5.3.5 **Microdialysis probes**

Microdialysis probes were constructed in-house using a side-by-side geometry, as described previously[131]. Briefly, two 40 µm i.d. x 105 µm o.d. fused silica capillaries (Polymicro Technologies, Phoenix, AZ) were inserted into a 200 µm i.d. piece of hollow fiber dialysis tubing made from regenerated cellulose (13 kD MWCO, Spectrum Laboratories, Inc., Rancho Dominguez, CA). A sampling region was created by offsetting the capillaries by 1 cm, and sealing using polyimide resin (Alltech, Deerfield, IL). Probes were conditioned prior to use by flushing with ethanol (45µL/h) for five min, followed by ten min of Ringer's solution (25µL/h). Probes were perfused with Ringer's solution at 25 µL/h throughout experiments.

5.3.6 **Online Derivatization**

Dialysate was carried in a 30-40 cm long × 40 µm i.d. × 360 µm o.d. fused silica capillary to a 250 µm i.d. stainless steel cross (Valco Instruments Co. Inc, Houston, TX)

where it was mixed with a 5 µL/h stream of borate buffer and a 5 µL/h stream of derivatization solution. The derivatization of primary and secondary amines took place as the dialysate mixture traveled through a 90 cm long, 75 µm i.d. × 360 µm o.d. fused silica capillary from the reaction cross to the flow gate interface; 66 cm of this capillary was heated to accelerate the reaction by passing through flexible tubing that was circulating water from a water bath at 80°C (NESLAB EX-7 Digital One heating bath circulator, Thermo, Newington, NH). The length of the reaction capillary and flow rates used resulted in a 5 min reaction time, allowing the labeling reaction to go to completion.[90]

5.3.7 **High Speed Capillary Electrophoresis**

An 8-8.5 cm long, 10 µm i.d. × 360 µm o.d. fused silica capillary (separation capillary) was aligned coaxially, with a 50 µm gap, with the reaction capillary in a polycarbonate flow gate interface block.[73] A syringe pump (Pump 22 syringe pump, Harvard Apparatus, Holliston, MA) pumped separation buffer at 40 mL/hthrough this gap. Separation buffer flow was controlled by a pneumatically actuated valve (C2-300A 10 port valve, Valco Instruments Co. Inc., Houston, TX); crossflow of the separation buffer was stopped to for 500 ms allowing a sample plug to build up in the gap. An injection voltage of -13 kV was applied to the exit of the separation capillary for 200 ms. The flow stream though the flow gate was resumed and a separation voltage of -19 kV was applied. Separations were performed every 30 s. Injections were controlled by an in-house LabVIEW program.

5.3.8 **LIF Detection**

A 488 nm argon ion laser was used for LIF detection (150 mW, Melles Griot, Carlsbad, CA). The laser beam was passed through a 10× beam expander (Edmond Optics, Barrington, NJ), and focused using a 1× lens to a point just past the exit of the CE separation capillary in a fused-silica sheath flow cuvette(2 mm square with a 400 µm × 400 µm square inner bore).[82,135] Fluorescence emission is collected at 90° with a 60×, 0.7 NA long working distance objective (Universe Kogaku, Oyster Bay, NJ) and filtered through spatial (~1 mm diameter) and bandpass filters (543.5 ± 10 nm) (Melles Griot, Irvine, CA), and recorded using a photomultiplier tube (PMT R1477, Hamamatsu Corp., Bridgewater, NJ). Current from the PMT was amplified (Keithley 428 Current Amplifier, Keithley Instruments Inc., Cleveland, OH), filtered with a 10 ms rise time, and recorded using a data acquisition card (National Instruments Corp., Austin, TX). Data analysis was performed using Cutter Analysis 7.0.[149]

5.3.9 **Bicinchoninic Acid (BCA) Assay**

Amino acid concentrations were normalized according to cell protein content, as measured using a BCA assay. A Pierce™ BCA Protein Assay Kit was used according to included instructions. Briefly, working reagent was prepared by combining "Reagent A" and "Reagent B" in a ratio of 50:1 (A: B). 25 µL of each sample or standard was pipetted into individual wells of a 96 well plate followed by 200 µL of working reagent; all samples were analyzed in triplicate. The plate was gently shaken for 30 s to ensure mixing of the working reagent and samples. After shaking, the plate was incubated at 37°C for 30 min. After incubation, the plate was removed from the incubator and

absorbance at 562 nm was measured using a plate reader (Spectromax Plus; Molecular Devices, LLC, Sunnyvale, CA). A calibration curve was generated from BSA standards. Using this standard curve, protein content for each flask was determined and used for normalizing amino acid signals obtained from CE separation.

5.3.10 **Bicinchoninic Acid (BCA) Assay**

Amino acid concentrations were normalized according to cell protein content, as measured using a BCA assay. A Pierce™ BCA Protein Assay Kit was used according to included instructions. Briefly, working reagent was prepared by combining "Reagent A" and "Reagent B" in a ratio of 50:1 (A: B). 25 µL of each sample or standard was pipetted into individual wells of a 96 well plate followed by 200 µL of working reagent; all samples were analyzed in triplicate. The plate was gently shaken for 30 s to ensure mixing of the working reagent and samples. After shaking, the plate was incubated at 37°C for 30 min. After incubation, the plate was removed from the incubator and absorbance at 562 nm was measured using a plate reader (Spectromax Plus; Molecular Devices, LLC, Sunnyvale, CA). A calibration curve was generated from BSA standards. Using this standard curve, protein content for each flask was determined and used for normalizing amino acid signals obtained from CE separation.

5.4 Results and Discussion

5.4.1 Effect of Insulin on Lipogenesis

Previous studies have shown that insulin influences the release of leptin and other important chemicals found in 3T3-L1 cells. We hypothesized that insulin would also influence the rate of uptake of BCAAs, promoting lipogenesis in 3T3-L1 adipocytes. Using the techniques presented here, one could imagine culturing the cells and incubating them with various concentrations of insulin, to see how the presence of insulin affects lipogenesis.

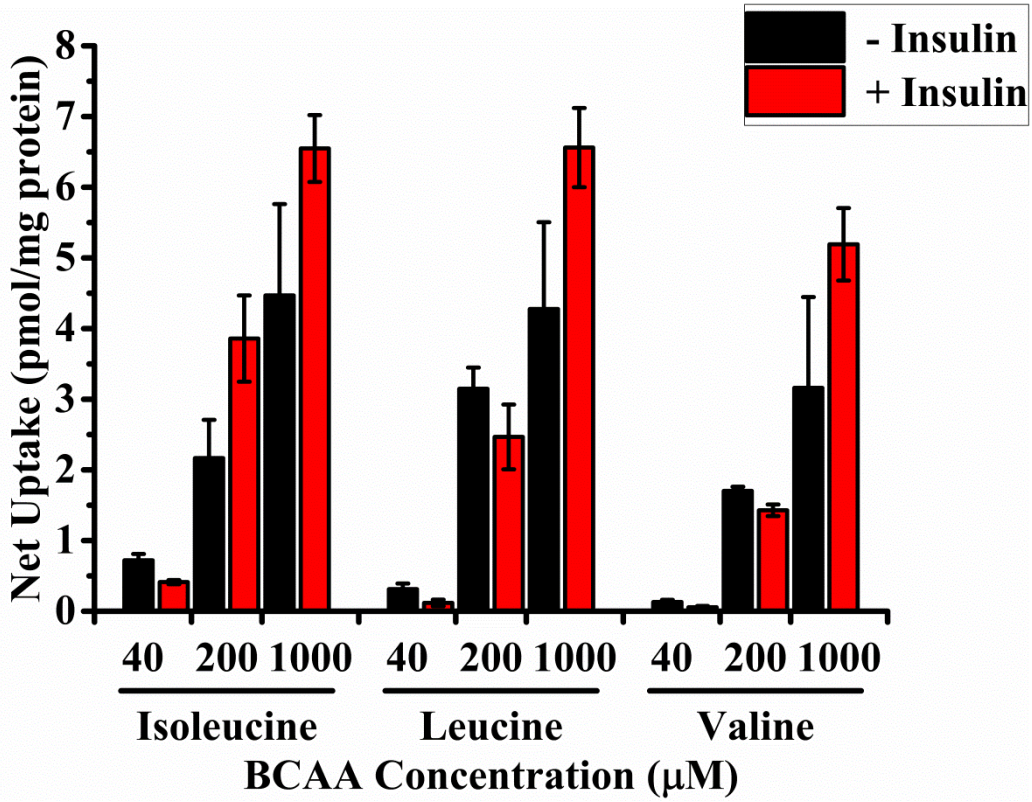

Figure 5.1. Uptake of BCAAs on Day 4 when incubated in Ringer's solution with (red) and without (black) 10 nM insulin, 5 mM glucose, and either 40, 200, or 1000 μM BCAAs for 30 minutes. Error bars are SEM; n=3.

As shown in Figure 5.1, a range of BCAA concentrations were investigated, along with incubation with or without 10 nM insulin. 10 nM insulin was chose as the incubation concentration as it correlates with normal circulating concentrations found in mice plasma. The effect of influence of insulin on the uptake of BCAAs, depends on local BCAA concentration, as shown in Figure 5.1 Isoleucine uptake changes as a function of both incubated BCAA concentration and insulin presence. At lower concentrations of BCAAs (40µm), 3T3-L1 cells had less uptake when insulin is present (red). This trend is observed for all 3 BCAAs. However, when BCAA concentrations are increased to a biological concentration (200 µM), isoleucine has more uptake when insulin is present (red), while leucine and valine do not. At high concentrations (1 mM), all three BCAAs show increased uptake of BCAAs when incubated with insulin (red), compared to without insulin (black). This could be due to

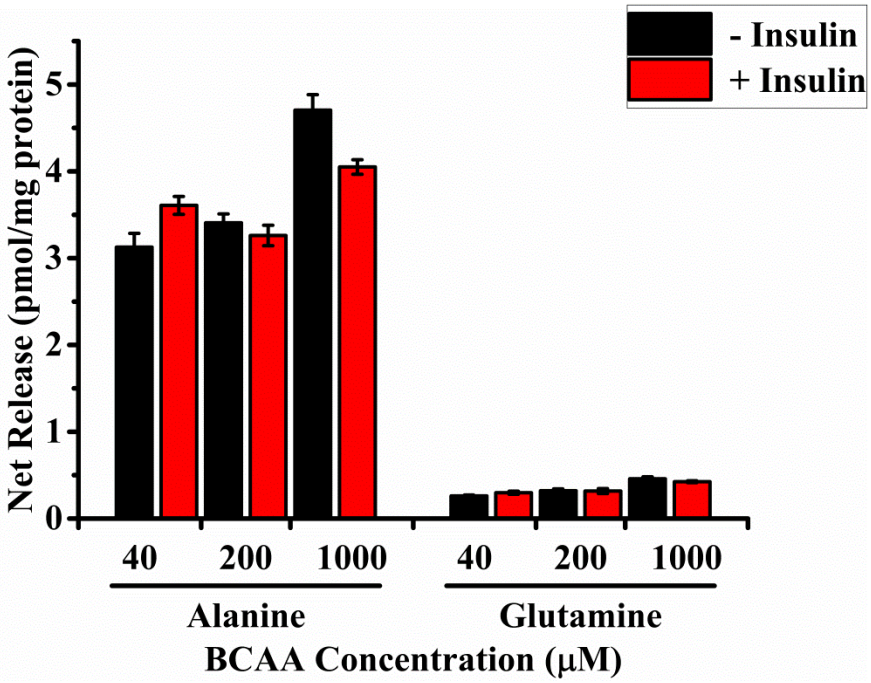

Figure 5.2. Release of alanine and glutamine on Day 4 when incubated in Ringer's solution with (red) and without (black) 10 nM insulin, 5 mM glucose, and either 40, 200, or 1000 µM BCAAs for 30 minutes. Error bars are SEM; n=3.

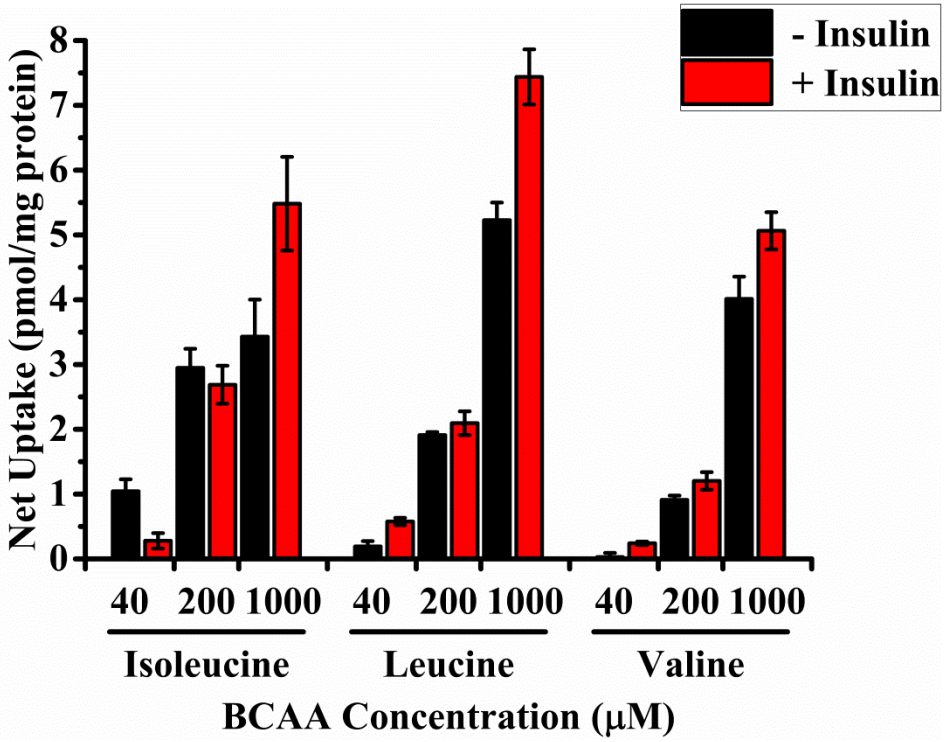

Figure 5.3. Uptake of BCAAs on Day 14 when incubated in Ringer's solution with (red) and without (black) 10 nM insulin, 5 mM glucose, and either 40, 200, or 1000 μM BCAAs for 30 minutes. Error bars are SEM; n=3

localization of insulin receptors on the outer cell membrane to promote the uptake of glucose into the cells, rather than BCAAs.

Downstream release of alanine and glutamine remains largely unchanged when comparing the release profiles in the presence of insulin, no matter the BCAA concentration, as shown in Figure 5.2. In fact, the trend at 1000 μM shows less release of lipogenic marker alanine, in the presence of 10 nM insulin. Because this trend was unexpected, the experiment was repeated once the cells reached the fully mature state, on Day 14. This was done to investigate whether insulin's effect on 3T3-L1 cells is the same, no matter what maturation stage the cells are in. Figure 5.3**Error! Reference source not found.**shows the uptake of BCAAs when incubated with Ringer's solution, 5

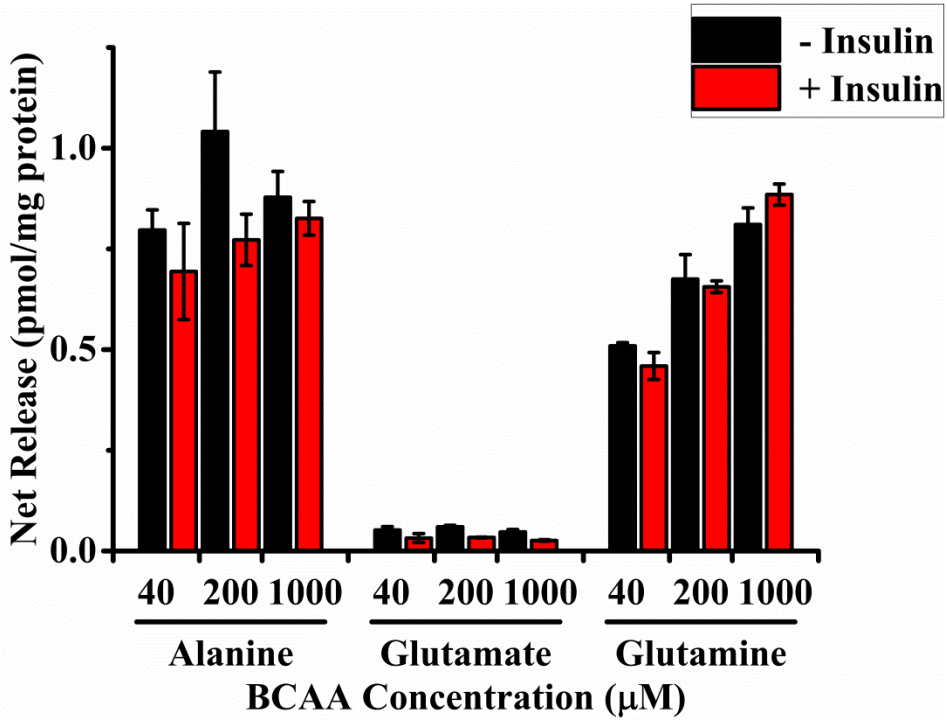

Figure 5.4. Release of alanine, glutamine on Day 4 when incubated in Ringer's solution with (red) and without (black) 10 nM insulin, 5 mM glucose, and either 40, 200, or 1000 μM BCAAs for 30 minutes. Error bars are SEM; n=3

mM glucose, BCAAS (40, 200, o4 1000 μM), with or without insulin. Similar trends to those seen on Day 4 are observed for both the BCAAs (Figure 5.3) and downstream lipogenic markers (Figure 5.4).Figure 5.4 shows that as BCAA concentration is increased, release of alanine, and glutamine increases, regardless of insulin presence. Using the developed assay, additional exploration about insulin's role in lipogenesis in 3T3-L1 adipocytes can be conducted. The high-throughput nature of the assay allows for multiple conditions to be analyzed quickly when analyzing information from bulk cell culture.

5.4.2 **Effect of Artificial Sweeteners on Lipogenesis**

As shown in Figure 5.5(orange), when 3T3-L1 cells are incubated on Day 4with the maximum daily allowance of fructose and 5 mM glucose, uptake of the BCAAs is diminished, compared to the uptake when incubated with only 5 mM glucose (Figure 5.5, black). The downstream metabolites, however, have no significant change in release, as shown in Figure 5.6. This suggests that BCAAs are not participating in lipogenesis and may suggest that fructose is a more preferred energy source for differentiating adipocytes over BCAAs. The maximum daily allowance was converted to a concentration for each sweetener, using average blood volume and weight of a mouse. The presence of AceK, in

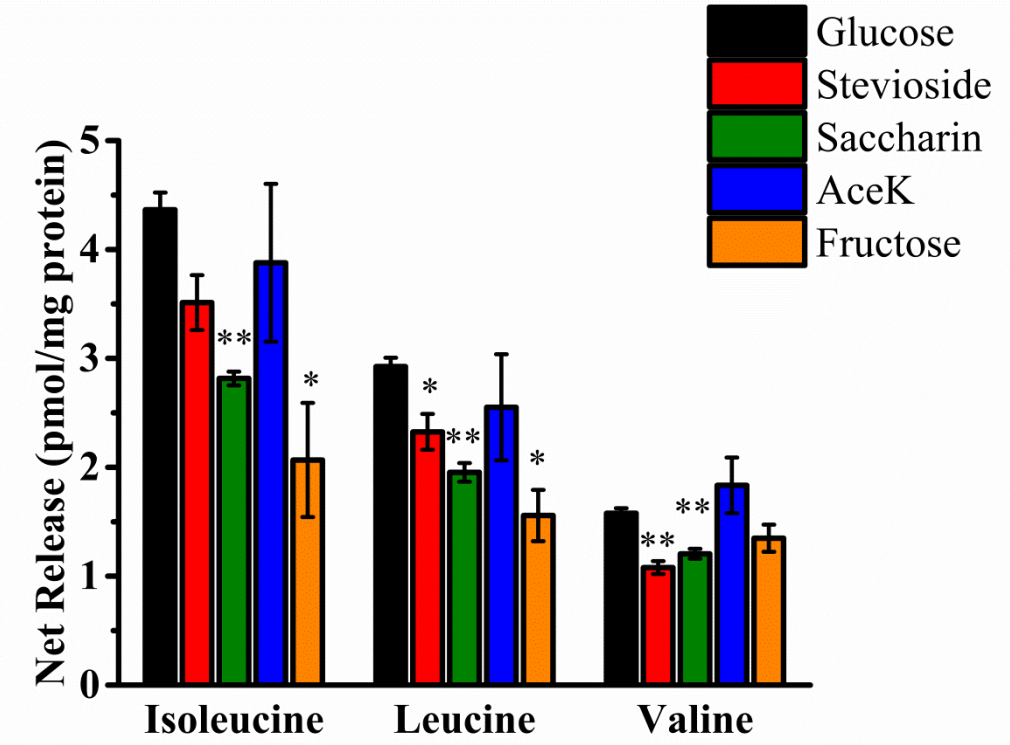

Figure 5.5. Uptake of BCAAs on Day 4 when incubated in Ringer's solution, 200 µM BCAAs, and and either glucose (5 mM, black), or 5 mM glucose plus one of the following: stevioside (64.5µM, red), saccharin (350 µM, green), AceK (968 µM, blue), or fructose (30 mM, orange). Error bars are SEM; n = 3 samples. . *, p-value < 0.05, **, p-value < 0.01 compared to incubation with 5 mM glucose only.

addition to 5 mM glucose, however, does not change, statistically, the amount of BCAAs that are taken into the cells (Figure 5.5, blue). Isoleucine and leucine see the highest uptake of BCAAs when incubated with 5 mM glucose only (Figure 5.5, black), while valine is taken into the cells the most when incubated with AceK and 5 mM glucose. Interestingly, the downstream metabolites, alanine, glutamine, and glutamate, as shown in Figure 5.6, do not have increased release with corresponding BCAA uptake. Another interesting discovery is that incubation with stevioside and 5 mM glucose did not

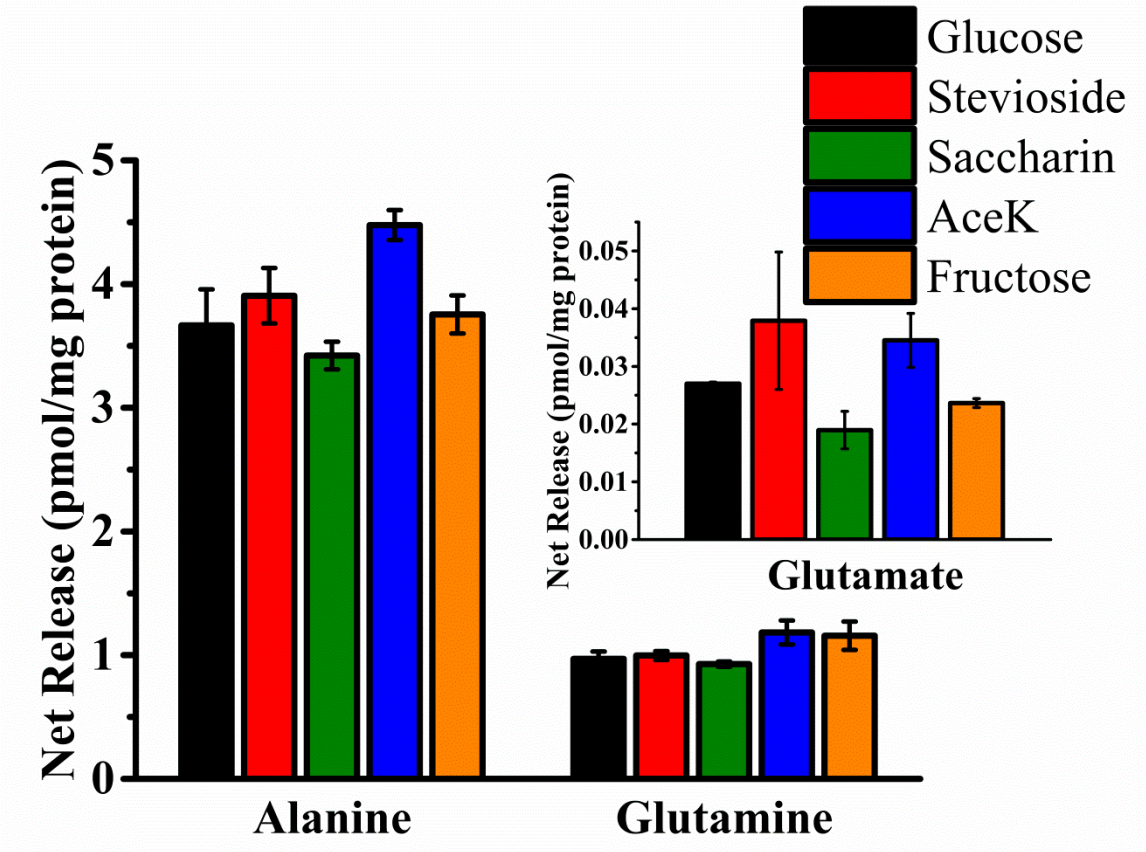

Figure 5.6. Release of alanine, glutamine, and glutamate on Day 4 when incubated in Ringer's solution, 200 µM BCAAs, and either glucose (5 mM, black), or 5 mM glucose plus one of the following: stevioside (64.5µM, red), saccharin (350 µM, green), AceK (968 µM, blue), or fructose (30 mM, orange) for 30 minutes. Error bars are SEM; n = 3 samples. *, p-value < 0.05, **, p-value < 0.01 compared to incubation with 5 mM glucose only.

promote uptake of BCAAs (Figure 5.5, red), but did however, promote the release of glutamate (Figure 5.6, red) compared to control.

5.5 **Conclusions**

The previously developed assay was used for monitoring changes in lipogenesis due to the presence of insulin or artificial sweeteners. As demonstrated, local BCAA concentration appears to have more influence on lipogenesis than presence of insulin, especially at circulating concentrations of BCAAs. At high concentrations of BCAAs, insulin may have an effect on uptake and lipogenesis in 3T3-L1 cells. Further investigation into this observation is necessary as trends vary depending on BCAA concentration.

Additional examination of the trends observed through incubation of 3T3-L1 cells with 5 mM glucose, 200 µM BCAAs, and the maximum daily allowed intake for each the four sweeteners is needed in order to make concrete conclusions about how the sweeteners affect lipogenesis. This data suggests that both AceK and fructose may be affecting the uptake of BCAAs in 3T3-L1 adipocytes. While AceK shows BCAA levels similar to 5 mM glucose control groups, fructose diminishes the uptake of BCAAs. Investigation into the lipogenic markers indicates that there could possibly be an increase in lipogenesis when AceK is present, due to increased release of alanine, glutamine. Although fructose diminishes BCAA uptake, downstream lipogenic metabolites remain at levels similar to control. This result suggests that fructose may interfere with BCAA receptor, blocking their uptake. In either study, it may be useful for the development of sampling method that allows for faster temporal information. Many cellular responses are

fast, so trends may not be observable when experiments are performed every 30 min. Thus, development of a way to sample 3T3-L1 cells on a faster time-scale is needed.

Chapter 6: Summary and Future Applications

6.1 **Summary**

In Chapter 2, we described the development of a high-speed CE assay coupled with microdialysis for the separation and detection of BCAAs. Assay optimization was achieved through careful manipulation of buffer components in order to obtain the best separation of the analytes of interest. LODs of 100-400 nM were achieved for the BCAAs, with 100,000-215,000 theoretical plates easily obtained. As a proof of concept experiment, release and uptake profiles of 3T3-L1 cells were monitored. Cells were incubated with 200 μM BCAAs and 5 mM glucose in Ringer's solution for varying amounts of time, in order to see changes in the rate of uptake of BCAAs and release of downstream metabolites, alanine, glutamine, and glutamate. The rate of release of downstream metabolites stabilized after ~30 min, while BCAA uptake continued to slow over the course of an h. Because downstream release stabilized after 30 min, all future experiments would be based off of this time, a balance between experimental time and detectable signal. This result was exciting and important because it provided information about the speed of uptake catabolism of BCAAs in 3T3-L1 cells and corresponding downstream metabolite release. The development of this high-throughput assay allows for rapid sample throughput, providing large amounts of data that was unknown previously.

In Chapter 3, further investigation into how local concentrations of BCAAs affect cells throughout the differentiation process. 3T3-L1 cells are differentiated into mature adipocytes over the course of ~14 days. Experiments were conducted when a media formulation change induced a physiological change in the cells throughout this process:

on Day 0, Day 2, Day 4, and Day 14. At each of these days, flasks were incubated with or without circulating concentrations of BCAAs, in order to see if there was a change in the metabolism of BCAAs, monitored through the downstream release of alanine, glutamine, and glutamate, at each time point. It was found that BCAA release was lowest during periods of presumed increased lipogenesis, Days 2 and 4, and uptake of BCAAS was highest during those same time periods. Once cells reached a fully mature state, both release and uptake slowed. Alanine, glutamine, and glutamate release profiles supported these trends, with increased release during later stages of maturation. These trends demonstrate that the presence of BCAAs stimulates lipogenesis in 3T3-L1 cells. Understanding the effects of BCAAs on lipogenesis throughout development of cells provides insight into the development of dysregulation of metabolic diseases.

In Chapter 4, we probed the effects of glucose and BCAAs on lipogenesis throughout the development of 3T3-L1 cells even further. In order to do so, 3T3-L1 cells were incubated with or without 200 μM BCAAS, with varying concentrations of glucose (0 mM – 20 mM), in Ringer's solution. The goal of these experiments was to see if different trends were observed in BCAA catabolism, based on local concentrations of glucose or BCAAs, as both are known to be energy sources for cells. 3T3-L1 cells undergo lipogenesis most rapidly on Day 4 of differentiation, and trends observed at all glucose concentrations supported these trends. There were no statistical differences in BCAA uptake or release based on local glucose concentration. There were also no observed statistical differences in downstream lipogenesis markers based on local glucose trends. There were, however, changes in the release of downstream lipogenesis markers,

based on the presence of BCAAs. These trends could be due to the fact that 3T3-L1 cells have few glucose receptors located on the cellular membrane, until they are localized there by insulin. It could also be due to the ease of uptake of BCAAs to generate TCA cycle intermediates, rather than taking in glucose for glycolysis. The breakdown of BCAAs may be more energetically favorable than to glycolysis.

In Chapter 5, preliminary analysis of biological stimuli and their effects on lipogenesis in 3T3-L1 cells was assessed. Using the developed assay, we observed trends that are inconclusive as to the role that insulin plays in relation to BCAA uptake and lipogenesis. Trends observed when 3T3-L1 cells were incubated with varying artificial and natural sweeteners were also inconclusive. Changes in BCAA uptake were not reflected in downstream lipogenesis markers. Further investigations into both of these phenomena through optimization of incubation media as well as expanded concentrations of stimuli provide the opportunity to learn and understand how they affect lipogenesis in cells.

6.2 **Future Applications**

Microdialysis coupled to high-speed CE is an analytical tool that can be used to study many different biological systems and provide answers to many unanswered biological questions. The work presented in this thesis has demonstrated the ability to generate vast amounts of data, using a high-throughput assay. While obesity is a disease that has been around for many decades, many basic questions still remain about the development of the disease. Many experiments to assess the development of disease are

tedious and data collection is slow; using the assay developed in this work can help speed up the data collection process.

6.2.1 **Modifying the sampling platform**

In Chapter 2, we demonstrated the high-speed CE assay and its usefulness as a high-throughput sampling method. Rather than using the assay for high-throughput sampling of fractions collected from bulk culture, the assay could be used online, in conjunction with the profusion chamber, in order to obtain temporal information, approximately every 30 s about any *in vitro* cell model of interest. In particular, obtaining information about 3T3-L1 cells on this time scale will provide insight into the mechanisms of lipogenesis that are otherwise unattainable.

Previously, microdialysis sampling was using in combination with a perfusion

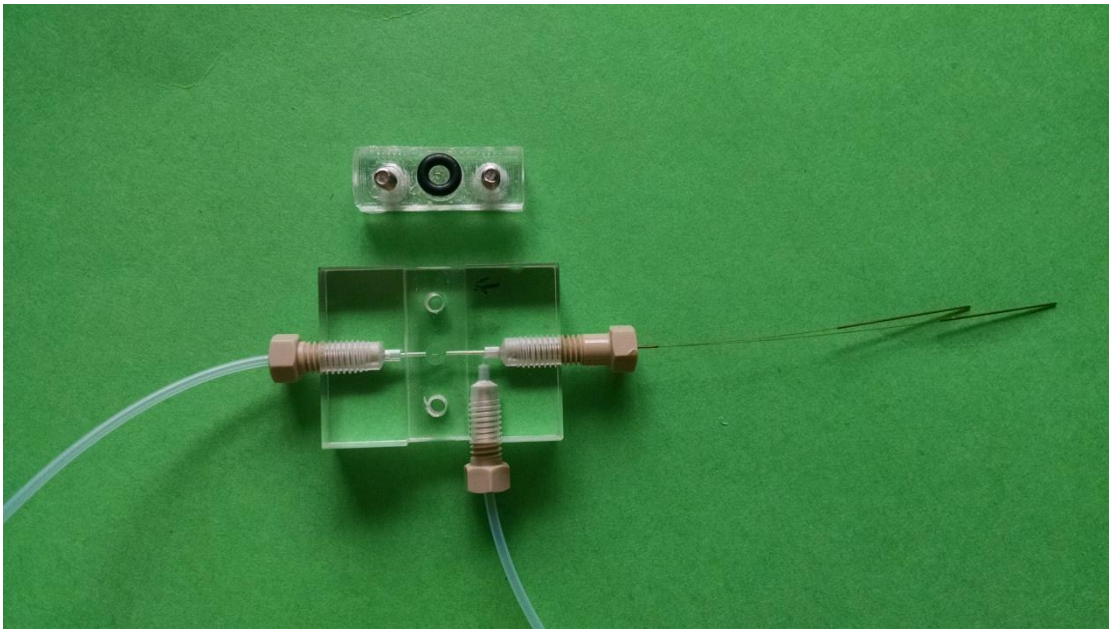

Figure 6.1. Image of profusion chamber device. The top part was 3D printed in order to fit well into the bottom polycarbonate device. A microdialysis probe is inserted into a channel (right) with inlet (left) and outlet (bottom) tubing connecting the device to the online high-speed CE system.

chamber in order to analyze amines released from salamander retinas.[134] Using this device, isolated larval salamander retinas were mounted in the perfusion chamber and perfused with Ringer's solution. Potassium stimulations were performed and amines were monitored using high-speed CE after OPA derivatization.

Using this perfusion chamber device, in conjunction with *in vitro* cell models, provides an opportunity to obtain near real-time information about cellular processes. To do so, cells can be grown directly on the top portion of the device, shown in Figure 6.1.

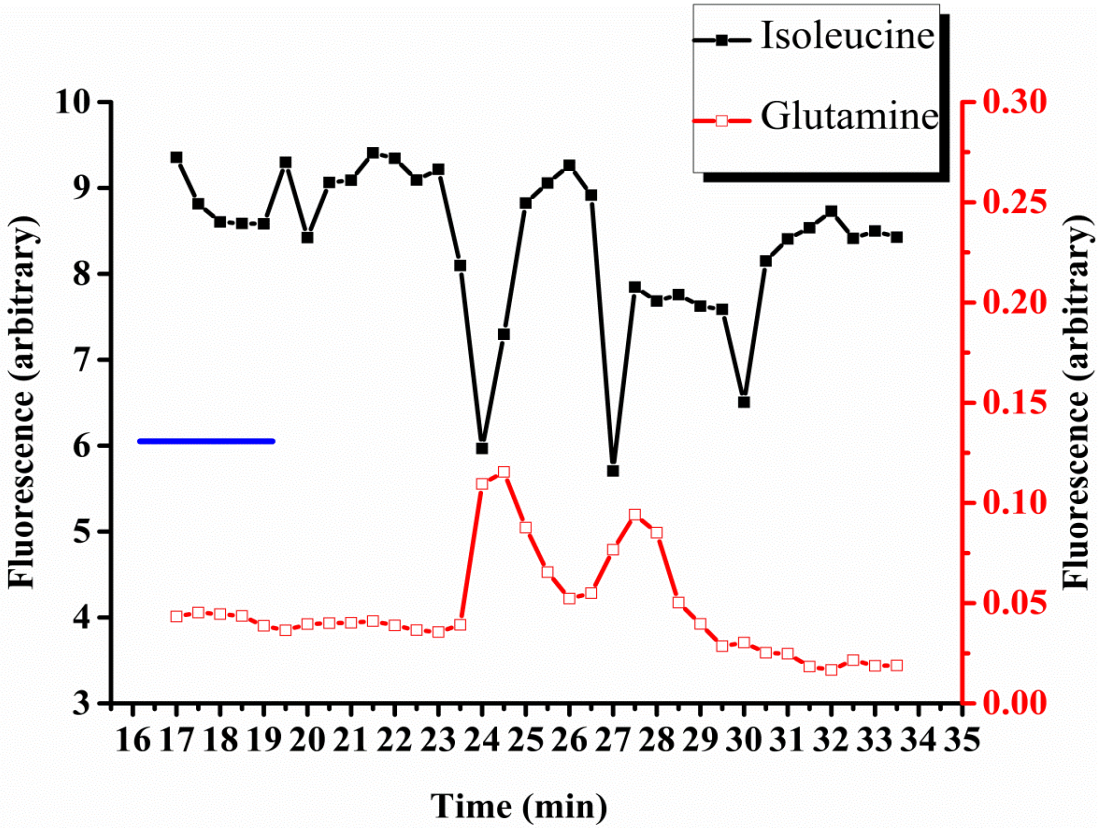

Figure 6.2. Temporal response of the *in vitro* microdialysis CE instrument following a 5 minute stiumatio nof 3T3-L1 adipocyteswith 10 nM insulin. Injections were made every 30 seconds. Top trace is isoleucine (black) and bottom trace is glutamine (red). These two are presented in order to demonstrate the utility of the profusion chamber device and it's ability to monitor fast changes in cellular response.Delay between simulation and increased peak height is due to the time it takes the sample to reach the detector.

As proof of concept, 3T3-L1 cells were cultured and differentiated on the top of the device. The device was assembled and basal levels of released amino acids were monitored. As shown in Figure 6.2, when a stimulation of 10 nM insulin was applied for 5 min, you can see the observed change in peak intensities. Glutamine release (red) increases with corresponding decreases in isoleucine uptake (black, indicated by a decrease in peak intensity). Further optimization of flow rates through the chamber, as well as culturing techniques will provide a useful platform for culturing cells that are unable to be cultured directly onto microdialysis probes. Attempts were made to use this technique,[115] however 3T3-L1 cell bodies are too large to adhere well to the probe's curved surface.

In order to efficiently optimize culturing surface parameters, 3D printing could be employed. 3D printing provides fast turn-around and output for design changes, as well as giving the profusion chamber device a "one-time use" capability, which is often desired when using *in vitro* sampling methods. The top portion of the device can simply be thrown away after use because top pieces can be printed in an efficient, cost effective manner. Ultimately, an entire device (both top and bottom) could be printed, depending on the abilities of the 3D printer involved.

Another useful application of the separation conditions employed throughout this thesis work would be to couple the CE separation mode to a second dimension. Previous work in our group has improved peak capacity by coupling nLC to micro-free flow electrophoresis (μFFE)[167] to separate complex samples. Coupling CE to μFFE would

allow for the separation of amino acids that cannot fully be resolved using the current assay (ex. valine, citrulline), while still maintaining a high-throughput system.

Bibliography

(1) Obesity and Overweight.World Health Organization, 2016.
(2) Trayhurn, P. *Obes. Rev.* **2007**, *8*, 41-44.
(3) Fantuzzi, G. *J. Allergy Clin. Immunol.* **2005**, *115*, 911-919.
(4) Ronti, T.; Lupattelli, G.; Mannarino, E. *Clin. Endocrinol. (Oxf.)* **2006**, *64*.
(5) Greenberg, A. S.; Obin, M. S. *Am. J. Clin. Nutr.* **2006**, *83*, 461S-465S.
(6) Wronska, A.; Kmiec, Z. *Acta Physiol. (Oxf.)* **2012**, *205*, 194-208.
(7) Poulos, S. P.; Hausman, D. B.; Hausman, G. J. *Mol. Cell. Endocrinol.* **2010**, *323*, 20-34.
(8) Mattison, R.; Jensen, M. *Curr. Opin. Endocrinol. Diabetes* **2003**, *10*, 317-321.
(9) Mohamed-Ali, V.; Pinkney, J. H.; Coppack, S. W. *Int. J. Obes.* **1998**, *22*, 1145-1158.
(10) Tam, C. S.; Lecoultre, V.; Ravussin, E. *Circulation* **2012**, *125*, 2782-2791.
(11) Enerback, S. *N. Engl. J. Med.* **2009**, *360*, 2021-2023.
(12) Janský, L. *Biol. Rev. Camb. Philos. Soc.* **1973**, *48*, 85-132.
(13) Carter, E. A.; Bonab, A. A.; Hamrahi, V.; Pitman, J.; Winter, D.; Macintosh, L. J.; Cyr, E. M.; Paul, K.; Yerxa, J.; Jung, W.; Tompkins, R. G.; Fischman, A. J. *Life Sci.* **2011**, *89*, 78-85.
(14) Yang, J. C.; Chi, Y. J.; Burkhardt, B. R.; Guan, Y. F.; Wolf, B. A. *Nutr. Rev.* **2010**, *68*, 270-279.
(15) Howell, J. J.; Manning, B. D. *Trends Endocrinol. Metab.* **2011**, *22*, 94-102.
(16) Dodd, K. M.; Tee, A. R. *Am. J. Physiol. Endocrinol. Metab.* **2012**, *302*, E1329-E1342.
(17) Gregoire, F. M.; Smas, C. M.; Sul, H. S. *Physiol. Rev.* **1998**, *78*, 783-809.
(18) Hausman, D.; DiGirolamo, M.; Bartness, T.; Hausman, G.; Martin, R. *Obes. Rev.* **2001**, *2*, 239-254.
(19) Kershaw, E. E.; Flier, J. S. *J. Clin. Endocrinol. Metab.* **2004**, *89*, 2548-2556.
(20) Margetic, S.; Gazzola, C.; Pegg, G. G.; Hill, R. A. *Int. J. Obes.* **2002**, *26*, 1407-1433.
(21) Ahima, R. S.; Flier, J. S. *Annu. Rev. Physiol.* **2000**, *62*, 413-437.
(22) Blum, W. F. *Horm. Res.* **1997**, *48*, 2-8.
(23) Coppack, S. W. *Proc. Nutr. Soc.* **2001**, *60*, 349-356.
(24) Herman, M. A.; She, P. X.; Peroni, O. D.; Lynch, C. J.; Kahn, B. B. *J. Biol. Chem.* **2010**, *285*, 11348-11356.
(25) Levy, J. R.; Gyarmati, J.; Lesko, J. M.; Adler, R. A.; Stevens, W. *Am. J. Physiol. Endocrinol. Metab.* **2000**, *278*, E892-E901.
(26) Attie, A. D.; Scherer, P. E. *J. Lipid Res.* **2009**, *50*, S395-399.
(27) Calbet, J. A.; MacLean, D. A. *J. Nutr.* **2002**, *132*, 2174-2182.
(28) Maggs, D. G.; Jacob, R.; Rife, F.; Lange, R.; Leone, P.; During, M. J.; Tamborlane, W. V.; Sherwin, R. S. *J. Clin. Invest.* **1995**, *96*, 370-377.
(29) She, P.; Van Horn, C.; Reid, T.; Hutson, S. M.; Cooney, R. N.; Lynch, C. J. *Am. J. Physiol. Endocrinol. Metab.* **2007**, *293*, E1552-E1563.
(30) Green, C. R.; Wallace, M.; Divakaruni, A. S.; Phillips, S. A.; Murphy, A. N.; Ciaraldi, T. P.; Metallo, C. M. *Nat. Chem. Biol.* **2016**, *12*, 15-21.

(31) Li, F.; Yin, Y.; Tan, B.; Kong, X.; Wu, G. *Amino Acids* **2011**, *41*, 1185-1193.
(32) Cammisotto, P. G.; Gelinas, Y.; Deshaies, Y.; Bukowiecki, L. J. *Am. J. Physiol. Endocrinol. Metab.* **2005**, *289*, E166-E171.
(33) Roh, C.; Han, J. R.; Tzatsos, A.; Kandror, K. V. *Am. J. Physiol. Endocrinol. Metab.* **2003**, *284*, E322-E330.
(34) Bonadonna, R. C.; Leif, G.; Kraemer, N.; Ferrannini, E.; Prato, S. D.; DeFronzo, R. A. *Metabolism* **1990**, *39*, 452-459.
(35) Hotamisligil, G. S.; Shargill, N. S.; Spiegelman, B. M. *Science* **1993**, *259*, 87-87.
(36) Speakman, J.; Hambly, C.; Mitchell, S.; Król, E. *Lab. Anim.* **2008**, *42*, 413-432.
(37) Lutz, T. A.; Woods, S. C. In *Current Protocols in Pharmacology*; John Wiley & Sons, Inc., 2001.
(38) Armani, A.; Mammi, C.; Marzolla, V.; Calanchini, M.; Antelmi, A.; Rosano, G.; Fabbri, A.; Caprio, M. *J. Cell. Biochem.* **2010**, *110*, 564-572.
(39) Green, H.; Kehinde, O. *Cell* **1974**, *1*, 113-116.
(40) Thomson, M. J.; Williams, M. G.; Frost, S. C. *J. Biol. Chem.* **1997**, *272*, 7759-7764.
(41) Tremblay, F.; Gagnon, A.; Veilleux, A.; Sorisky, A.; Marette, A. *Endocrinology* **2005**, *146*, 1328-1337.
(42) Crown, S. B.; Marze, N.; Antoniewicz, M. R. *PLoS One* **2015**, *10*.
(43) Zebisch, K.; Voigt, V.; Wabitsch, M.; Brandsch, M. *Anal. Biochem.* **2012**, *425*, 88-90.
(44) Student, A. K.; Hsu, R. Y.; Lane, M. D. *J. Biol. Chem.* **1980**, *255*, 4745-4750.
(45) Chaurasia, C. S. *Biomed. Chromatogr.* **1999**, *13*, 317-332.
(46) Davies, M. I.; Lunte, C. E. *Chem. Soc. Rev.* **1997**, *26*, 215-222.
(47) Hogan, B. L.; Lunte, S. M.; Stobaugh, J. F.; Lunte, C. E. *Anal. Chem.* **1994**, *66*, 596-602.
(48) Lada, M. W.; Kennedy, R. T. *J. Neurosci. Methods* **1995**, *63*, 147-152.
(49) Watson, C. J.; Venton, B. J.; Kennedy, R. T. *Anal. Chem.* **2006**, *78*, 1391-1399.
(50) Ungerstedt, U. In *Measurement of Neurotransmitter Release In Vivo*, Marsden, C. A., Ed.; John Wiley & Sons: New York, 1984, pp 81-105.
(51) Eliasson, A., Microdialysis-Principles of Recovery; 1991.
(52) Lafontan, M.; Arner, P. *Trends Pharmacol. Sci.* **1996**, *17*, 309-313.
(53) Bungay, P. M.; Morrison, P. F.; Dedrick, R. L. *Life Sci.* **1990**, *46*, 105-119.
(54) Nandi, P.; Lunte, S. M. *Anal. Chim. Acta* **2009**, *651*, 1-14.
(55) Stenken, J. A. *Anal. Chim. Acta* **1999**, *379*, 337-358.
(56) Menacherry, S.; Hubert, W.; Justice, J. B. *Anal. Chem.* **1992**, *64*, 577-583.
(57) Hsiao, J. K.; Ball, B. A.; Morrison, P. F.; Mefford, I. N.; Bungay, P. M. *J. Neurochem.* **1990**, *54*, 1449-1452.
(58) Bourne, J. A. *Clin. Exp. Pharmacol. Physiol.* **2003**, *30*, 16-24.
(59) Peters, J. L.; Yang, H.; Michael, A. C. *Anal. Chim. Acta* **2000**, *412*, 1-12.
(60) Song, Y.; Lunte, C. E. *Anal. Chim. Acta* **1999**, *379*, 251-262.
(61) Zhou, S. Y.; Zuo, H.; Stobaugh, J. F.; Lunte, C. E.; Lunte, S. M. *Anal. Chem.* **1995**, *67*, 594-599.
(62) Jensen, S. M.; Hansen, H. S.; Johansen, T.; Malmlof, K. *J. Pharm. Biomed. Anal.* **2007**, *43*, 1751-1756.

(63) Sato, N.; Takeda, S.; Ikimura, K.; Nishino, H.; Rakugi, H.; Morishita, R. *Neuroscience* **2011**, *186*, 110-119.
(64) Song, Y.; Lunte, C. E. *Anal. Chim. Acta* **1999**, *400*, 143-152.
(65) Lada, M. W.; Schaller, G.; Carriger, M. H.; Vickroy, T. W.; Kennedy, R. T. *Anal. Chim. Acta* **1995**, *307*, 217-225.
(66) Cano-Cebrian, M. J.; Zornoza, T.; Polache, A.; Granero, L. *Curr. Drug Metab.* **2005**, *6*, 83-90.
(67) Michael, A. C.; Yang, H.; Peters, J. L.; Allen, C.; Chern, S. S.; Coalson, R. D. *Anal. Chem.* **2000**, *72*, 2042-2049.
(68) Stahle, L. *Adv. Drug Del. Rev.* **2000**, *45*, 149-167.
(69) Lonnroth, P.; Jansson, P. A.; Smith, U. *Am. J. Physiol.* **1987**, *253*, E228-E231.
(70) Lunte, S. M.; Nandi, P. *Anal. Chim. Acta* **2009**, *651*, 1-14.
(71) Skoog, D. A.; Holler, F. J.; Crouch, S. R. *Principles of Instrumental Analysis*; Brooks Cole, 2006.
(72) Jorgenson, J. W.; Lukacs, K. D. *Anal. Chem.* **1981**, *53*, 1298-1302.
(73) Hooker, T. F.; Jorgenson, J. W. *Anal. Chem.* **1997**, *69*, 4134-4142.
(74) Lada, M. W.; Vickroy, T. W.; Kennedy, R. T. *Anal. Chem.* **1997**, *69*, 4560-4565.
(75) Lunte, S. M.; Zhou, J. X.; Heckert, D. M.; Zuo, H.; Lunte, C. E. *Anal. Chim. Acta* **1999**, *379*, 307-317.
(76) Lada, M. W.; Kennedy, R. T. *J. Neurosci. Methods* **1997**, *72*, 153-159.
(77) Schultz, K. N.; Kennedy, R. T. *Annu. Rev. Anal. Chem. (Palo Alto Calif.)* **2008**, *1*, 627-661.
(78) Bowser, M. T.; Kennedy, R. T. *Electrophoresis* **2001**, *22*, 3668-3676.
(79) Zhou, S. Y.; Zuo, H.; Stobaugh, J. F.; Lunte, C. E.; Lunte, S. M. *Anal. Chem.* **1995**, *67*, 594-599.
(80) Lada, M. W.; Kennedy, R. T. *Anal. Chem.* **1996**, *68*, 2790-2797.
(81) Ewing, A. G.; MacTaylor, C. E. *Electrophoresis* **1997**, *18*, 2279-2290.
(82) Zhang, J. Z.; Chen, D. Y.; Wu, S.; Harke, H. R.; Dovichi, N. J.; Zhang, J. Z.; Chen, D. Y.; Wu, S.; Harke, H. R.; Dovichi, N. J. *Clin. Chem.* **1991**, *37*, 1492-1496.
(83) Chen, D. Y.; Dovichi, N. J. *J. Chromatogr. B Biomed. Appl.* **1994**, *657*, 265-269.
(84) Fukushima, T.; Usui, N.; Santa, T.; Imai, K. *J. Pharm. Biomed. Anal.* **2003**, *30*, 1655-1687.
(85) Underberg, W. J. M.; Waterval, J. C. M. *Electrophoresis* **2002**, *23*, 3922-3933.
(86) Szulc, M. E.; Krull, I. S. *J. Chromatogr.* **1994**, *659*, 231-245.
(87) Colyer, C. *Cell Biochem. Biophys.* **2000**, *33*, 323-337.
(88) Lingeman, H.; Bardelmeijer, H. A.; de Ruiter, C.; Underberg, W. J. M. *J. Chromatogr.* **1998**, *807*, 3-26.
(89) Molnar-Perl, I.; Vasanits, A. *J. Chromatogr.* **1999**, *835*, 73-91.
(90) Ciriacks Klinker, C.; Bowser, M. T. *Anal. Chem.* **2007**, *79*, 8747-8754.
(91) Cheng, Y. F.; Wu, S. L.; Chen, D. Y.; Dovichi, N. J. *Anal. Chem.* **1990**, *62*, 496-503.
(92) Swinney, K.; Bornhop, D. *Crit. Rev. Anal. Chem.* **2000**, *30*, 1-30.
(93) Cheng, Y. F.; Dovichi, N. J. *Science* **1988**, *242*, 562-564.
(94) Parsons, L. H.; Justice, J. B. *Crit. Rev. Neurobiol.* **1994**, *8*, 189-220.
(95) Davies, M. I. *Anal. Chim. Acta* **1999**, *379*, 227-249.

(96) Bal-Price, A. K.; Sunol, C.; Weiss, D. G.; van Vliet, E.; Westerink, R. H. S.; Costa, L. G. *Neurotoxicology* **2008**, *29*, 520-531.
(97) Westerink, B. H. C.; Damsma, G.; Rollema, H.; Devries, J. B.; Horn, A. S. *Life Sci.* **1987**, *41*, 1763-1776.
(98) Andren, P. E.; Caprioli, R. M. *J. Mass Spectrom.* **1995**, *30*, 817-824.
(99) Church, J. *Journal of Physiology-London* **1992**, *455*, 51-71.
(100) Westerink, R. H. S. *Neurotoxicology* **2013**, *39*, 169-172.
(101) Khan, S. N. H.; Shuaib, A. *Methods* **2001**, *23*, 3-9.
(102) Richards, D. A.; Silva, M. A.; Murphy, N.; Wigmore, S. J.; Mirza, D. F. *Amino Acids* **2007**, *33*, 429-437.
(103) Gilinsky, M. A.; Faibushevish, A. A.; Lunte, C. E. *J. Pharm. Biomed. Anal.* **2001**, *24*, 929-935.
(104) Woo, K. L.; Lunte, C. E. *J. Pharm. Biomed. Anal.* **2008**, *48*, 85-91.
(105) Zhu, T.; Cheung, B. W. Y.; Cartier, L. L.; Giebink, G. S.; Sawchuk, R. J. *J. Pharm. Sci.* **2003**, *92*, 1947-1956.
(106) Lindekens, N.; Smolders, I.; Khan, G. M.; Bialer, M.; Ebinger, G.; Michotte, Y. *Pharm. Res.* **2000**, *17*, 1408-1413.
(107) Smolders, I.; Khan, G. M.; Lindekens, H.; Prikken, S.; Marvin, C. A.; Manil, J.; Ebinger, G.; Michotte, Y. *J. Pharmacol. Exp. Ther.* **1997**, *283*, 1239-1248.
(108) Plock, N.; Kloft, C. *Eur. J. Pharm. Sci.* **2005**, *25*, 1-24.
(109) Kennedy, R. T.; Bowser, M. T. *Electrophoresis* **2001**, *22*, 3668-3676.
(110) Kast, B. *Nature* **2001**, *412*, 674-676.
(111) Fonslow, B. R.; Barocas, V. H.; Bowser, M. T. *Anal. Chem.* **2006**, *78*, 5369-5374.
(112) Walker, M. E.; Hatfield, J. K.; Brown, M. A. *Biochimica Et Biophysica Acta-Molecular Basis of Disease* **2012**, *1822*, 57-65.
(113) Fonslow, B. R.; Bowser, M. T. *Anal. Chem.* **2008**, *80*, 3182-3189.
(114) Fonslow, B. R.; Bowser, M. T. *Anal. Chem.* **2006**, *78*, 8236-8244.
(115) Hogerton, A. L.; Bowser, M. T. *Anal. Chem.* **2013**, *85*, 9070-9077.
(116) Adeva, M. M.; Calvino, J.; Souto, G.; Donapetry, C. *Amino Acids* **2012**, *43*, 171-181.
(117) Newgard, C. B. *Cell Metab.* **2012**, *15*, 606-614.
(118) Buse, M. G.; Biggers, J. F.; Friderici, K. H.; Buse, J. F. *J. Biol. Chem.* **1972**, *247*, 8085-8096.
(119) Birn, H. *Am. J. Physiol. Renal Physiol.* **2006**, *291*, F22-36.
(120) Meijer, A. J.; Dubbelhuis, P. F. *Biochem. Biophys. Res. Commun.* **2004**, *313*, 397–403.
(121) Yang, R.; Dong, J.; Guo, H.; Li, H.; Wang, S.; Zhao, H.; Zhou, W.; Yu, S.; Wang, M.; Chen, W. *PLoS One* **2013**, *8*, e81144.
(122) Perez-Cornago, A.; Brennan, L.; Ibero-Baraibar, I.; Hermsdorff, H. H. M.; O'Gorman, A.; Zulet, M. A.; Alfredo Martinez, J. *J. Physiol. Biochem.* **2014**, *70*, 593-602.
(123) Adams, R. F. *J. Chromatogr.* **1974**, *95*, 189-212.
(124) Matsumura, S.; Kataoka, H.; Makita, M. *J. Chromatogr. B Biomed. Appl.* **1996**, *681*, 375-380.

(125) Mayers, J. R.; Wu, C.; Clish, C. B.; Kraft, P.; Torrence, M. E.; Fiske, B. P.; Yuan, C.; Bao, Y.; Townsend, M. K.; Tworoger, S. S.; Davidson, S. M.; Papagiannakopoulos, T.; Yang, A.; Dayton, T. L.; Ogino, S.; Stampfer, M. J.; Giovannucci, E. L.; Qian, Z. R.; Rubinson, D. A.; Ma, J.; Sesso, H. D.; Gaziano, J. M.; Cochrane, B. B.; Liu, S. M.; Wactawski-Wende, J.; Manson, J. E.; Pollak, M. N.; Kimmelman, A. C.; Souza, A.; Pierce, K.; Wang, T. J.; Gerszten, R. E.; Fuchs, C. S.; Vander Heiden, M. G.; Wolpin, B. M. *Nat. Med.* **2014**, *20*, 1193-1198.
(126) Robitaille, L.; Hoffer, L. J. *Can. J. Physiol. Pharmacol.* **1988**, *66*, 613-617.
(127) Tuma, P.; Gojda, J. *Electrophoresis* **2015**, *36*, 1969-1975.
(128) Chang, P. L.; Chiu, T. C.; Wang, T. E.; Hu, K. C.; Tsai, Y. H.; Hu, C. C.; Bair, M. J.; Chang, H. T. *Electrophoresis* **2011**, *32*, 1080-1083.
(129) Lorenzo, M. P.; Navarrete, A.; Balderas, C.; Garcia, A. *J. Pharm. Biomed. Anal.* **2013**, *73*, 116-124.
(130) O'Brien, K. B.; Esguerra, M.; Klug, C. T.; Miller, R. F.; Bowser, M. T. *Electrophoresis* **2003**, *24*.
(131) Ciriacks, C. M.; Bowser, M. T. *Anal. Chem.* **2004**, *76*.
(132) Thompson, J. E.; Vickroy, T. W.; Kennedy, R. T. *Anal. Chem.* **1999**, *71*, 2379-2384.
(133) O'Brien, K. B.; Bowser, M. T. *Electrophoresis* **2006**, *27*, 1949-1956.
(134) O'Brien, K. B.; Esguerra, M.; Miller, R. F.; Bowser, M. T. *Anal. Chem.* **2004**, *76*, 5069-5074.
(135) Wu, S.; Dovichi, N. J. *J. Chromatogr.* **1989**, *480*, 141–155.
(136) Shackman, J. G.; Watson, C. J.; Kennedy, R. T. *J. Chromatogr.* **2004**, *1040*, 273-282.
(137) Fajans, S. S. *N. Engl. J. Med.* **1965**, *272*, 1224-1227.
(138) Cota, D.; Proulx, K.; Smith, K. A. B.; Kozma, S. C.; Thomas, G.; Woods, S. C.; Seeley, R. J. *Science* **2006**, *312*, 927-930.
(139) She, P.; Reid, T. M.; Bronson, S. K.; Vary, T. C.; Hajnal, A.; Lynch, C. J.; Hutson, S. M. *Cell Metab.* **2007**, *6*, 181-194.
(140) Buse, M. G.; Reid, S. S. *J. Clin. Invest.* **1975**, *56*, 1250-1261.
(141) Fulks, R. M.; Li, J. B.; Goldberg, A. L. *J. Biol. Chem.* **1975**, *250*, 290-298.
(142) Platell, C.; Kong, S.-E.; McCauley, R.; Hall, J. C. *J. Gastroenterol. Hepatol.* **2000**, *15*, 706-717.
(143) Brosnan, J. T.; Brosnan, M. E. *J. Nutr.* **2006**, *136*, 207S-211S.
(144) Holeček, M. *Nutrition* **2002**, *18*, 130-133.
(145) Herman, M. A.; She, P.; Peroni, O. D.; Lynch, C. J.; Kahn, B. B. *J. Biol. Chem.* **2010**, *285*, 11348-11356.
(146) Student, A. K.; Hsu, R. Y.; Lane, M. D. *J. Biol. Chem.* **1980**, *255*, 4745-4750.
(147) Chang, T. H.; Polakis, S. E. *J. Biol. Chem.* **1978**, *253*, 4693-4696.
(148) Harstad, R. K.; Bowser, M. T. *Anal. Chem.* **2016**, *88*, 8115–8122.
(149) Shackman, J.; Watson, C.; Kennedy, R. *J. Chromatogr.* **2004**, *1040*, 273-282.
(150) Yoshizawa, F. *J. Pharmacol. Sci.* **2012**, *118*, 149-155.

(151) Halama, A.; Horsch, M.; Kastenmueller, G.; Moller, G.; Kumar, P.; Prehn, C.; Laumen, H.; Hauner, H.; de Angelis, M. H.; Beckers, J.; Suhre, K.; Adamski, J. *Arch. Biochem. Biophys.* **2016**, *589*, 93-107.
(152) Newgard, C. B.; An, J.; Bain, J. R.; Muehlbauer, M. J.; Stevens, R. D.; Lien, L. F.; Haqq, A. M.; Shah, S. H.; Arlotto, M.; Slentz, C. A. *Cell Metab.* **2009**, *9*, 311-326.
(153) Chen, X.; Yang, W. *J. Diabetes Invest.* **2015**, *6*, 369-370.
(154) Saltiel, A. R.; Kahn, C. R. *Nature* **2001**, *414*, 799-806.
(155) Patti, M.-E.; Kahn, C. R. *J. Basic Clin. Physiol. Pharmacol.* **1998**, *9*, 89-110.
(156) Klip, A.; Pâquet, M. R. *Diabetes Care* **1990**, *13*, 228-243.
(157) Aronoff, S. L.; Berkowitz, K.; Shreiner, B.; Want, L. *Diabetes Spectr.* **2004**, *17*, 183-190.
(158) Jiang, G.; Zhang, B. B. *Am. J. Physiol. Endocrinol. Metab.* **2003**, *284*, E671-E678.
(159) Nauck, M. A.; Heimesaat, M. M.; Orskov, C.; Holst, J. J.; Ebert, R.; Creutzfeldt, W. *J. Clin. Invest.*, *91*, 301-307.
(160) Nishitani, S.; Takehana, K.; Fujitani, S.; Sonaka, I. *Am. J. Physiol. Gastrointest. Liver Physiol.* **2005**, *288*, G1292-G1300.
(161) Swithers, S. E. *Trends Endocrinol. Metab.* **2013**, *24*, 431-441.
(162) Yamamoto, K.; Ishimaru, Y. *Semin. Cell Dev. Biol.* **2013**, *24*, 240-246.
(163) Lindsley, J. E.; Rutter, J. *Comp. Biochem. Physiol. B: Biochem. Mol. Biol.* **2004**, *139*, 543-559.
(164) Kroger, M.; Meister, K.; Kava, R. *Compr. Rev. Food Sci. Food Saf.* **2006**, *5*, 35-47.
(165) Sardesai, V. M.; Waldshan, T. H. *J. Nutr. Biochem.* **1991**, *2*, 236-244.
(166) Simon, B. R.; Parlee, S. D.; Learman, B. S.; Mori, H.; Scheller, E. L.; Cawthorn, W. P.; Ning, X. M.; Gallagher, K.; Tyrberg, B.; Assadi-Porter, F. M.; Evans, C. R.; MacDougald, O. A. *J. Biol. Chem.* **2013**, *288*, 32475-32489.
(167) Geiger, M.; Frost, N. W.; Bowser, M. T. *Anal. Chem.* **2014**, *86*, 5136-5142.

Appendix

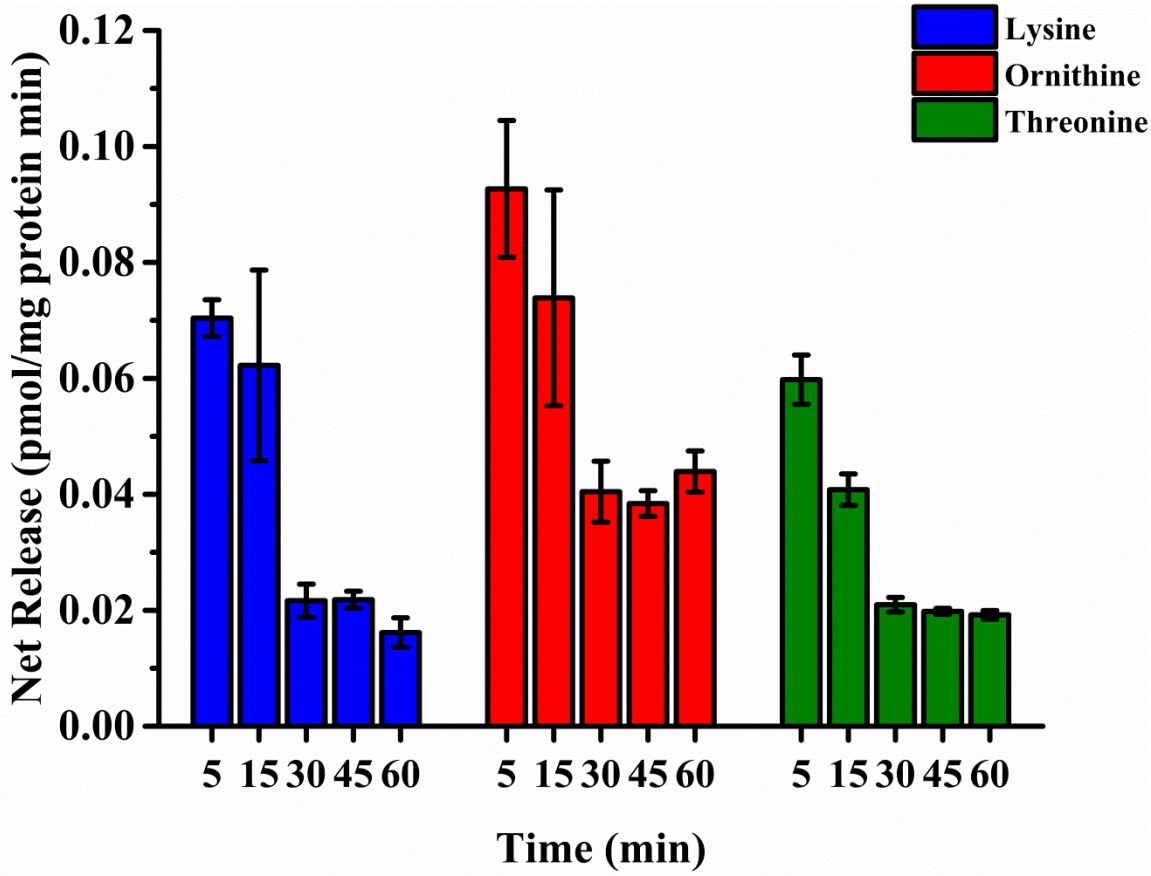

Figure A.1. Net rate of lysine, ornithine, and threonine efflux by 3T3-L1 cells incubated with Ringer's solution + 5 mM glucose and 200 μM isoleucine, leucine and valine for time periods ranging from 5 to 60 minutes. Rates were normalized to cell protein content as determined by BCA assay. Error bars are SE for n=3 samples.

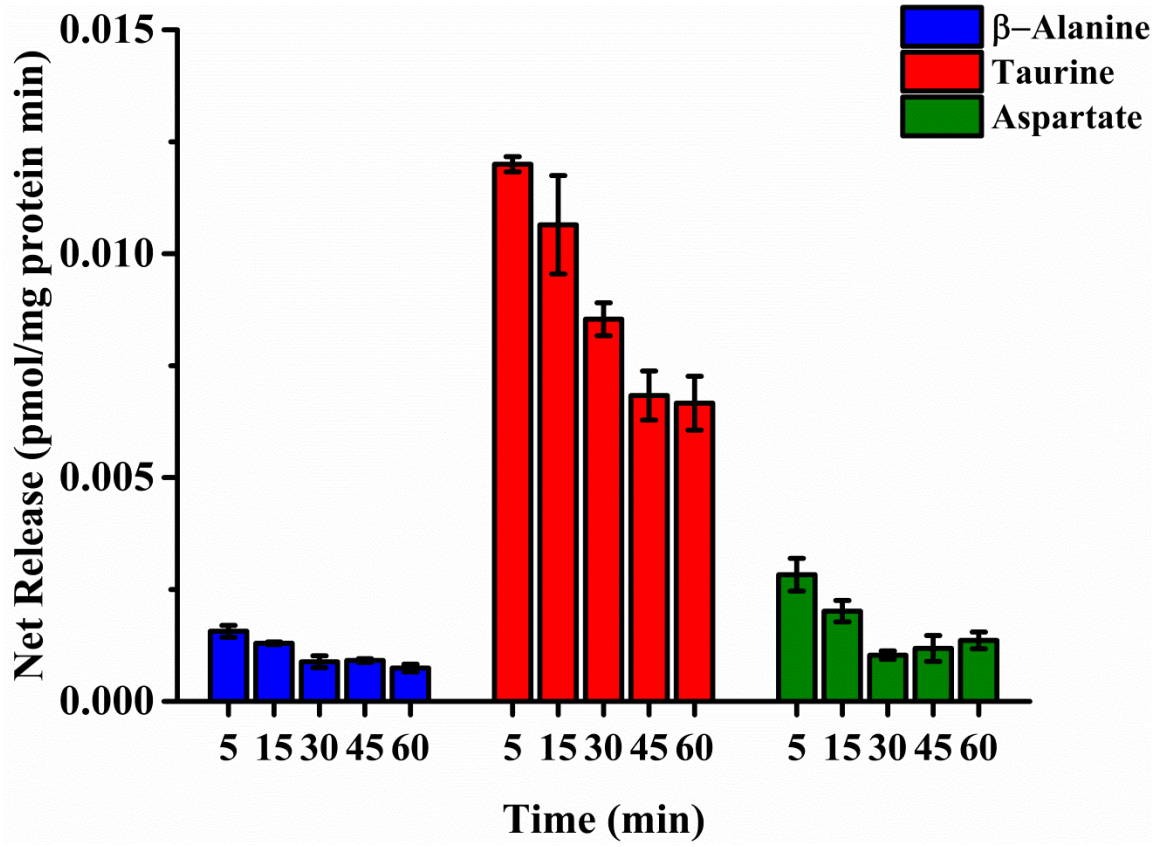

Figure A.2. Net rate of β-alanine, taurine, and aspartate efflux by 3T3-L1 cells incubated with Ringer's solution + 5 mM glucose and 200 µM isoleucine, leucine and valine for time periods ranging from 5 to 60 minutes. Rates were normalized to cell protein content as determined by BCA assay. Error bars are SE for n=3 samples.

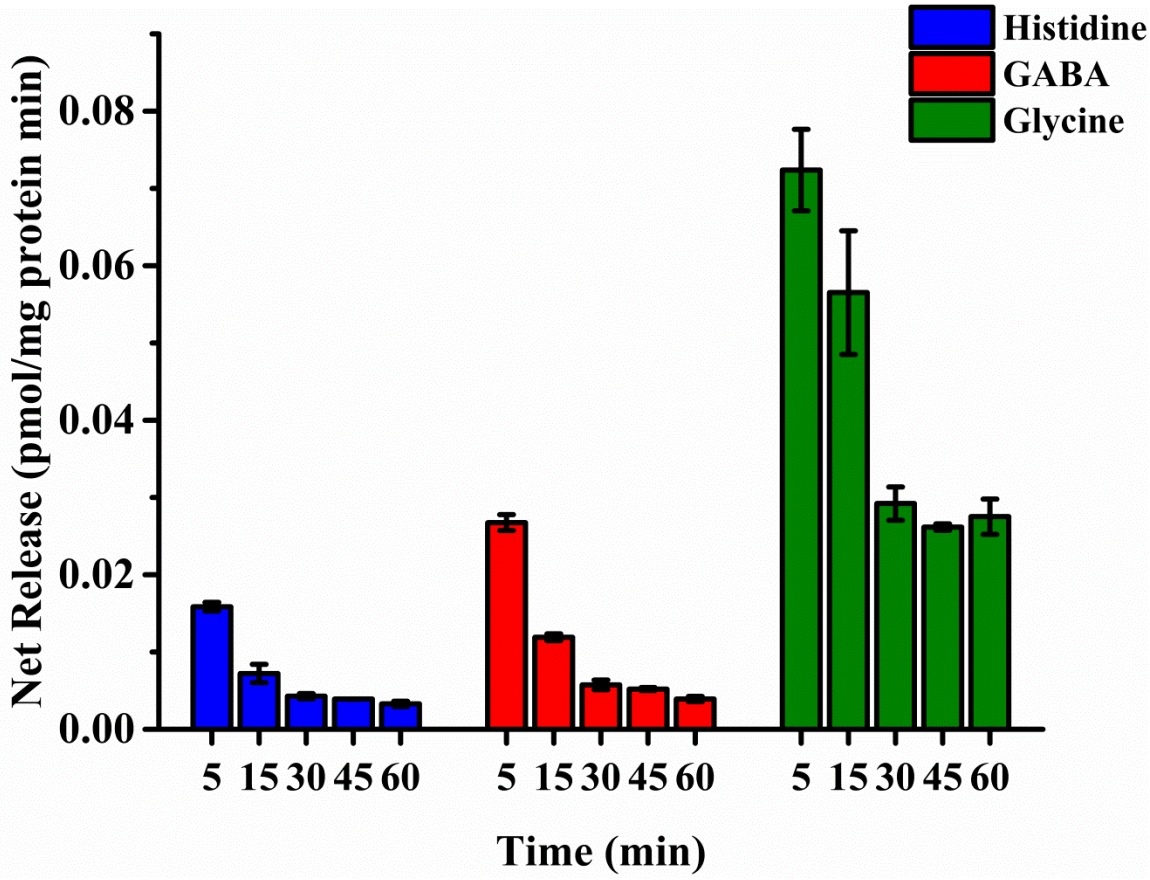

Figure A.3. Net rate of histidine, GABA, and glycine efflux by 3T3-L1 cells incubated with Ringer's solution + 5 mM glucose and 200 μM isoleucine, leucine and valine for time periods ranging from 5 to 60 minutes. Rates were normalized to cell protein content as determined by BCA assay. Error bars are SE for n=3 samples.

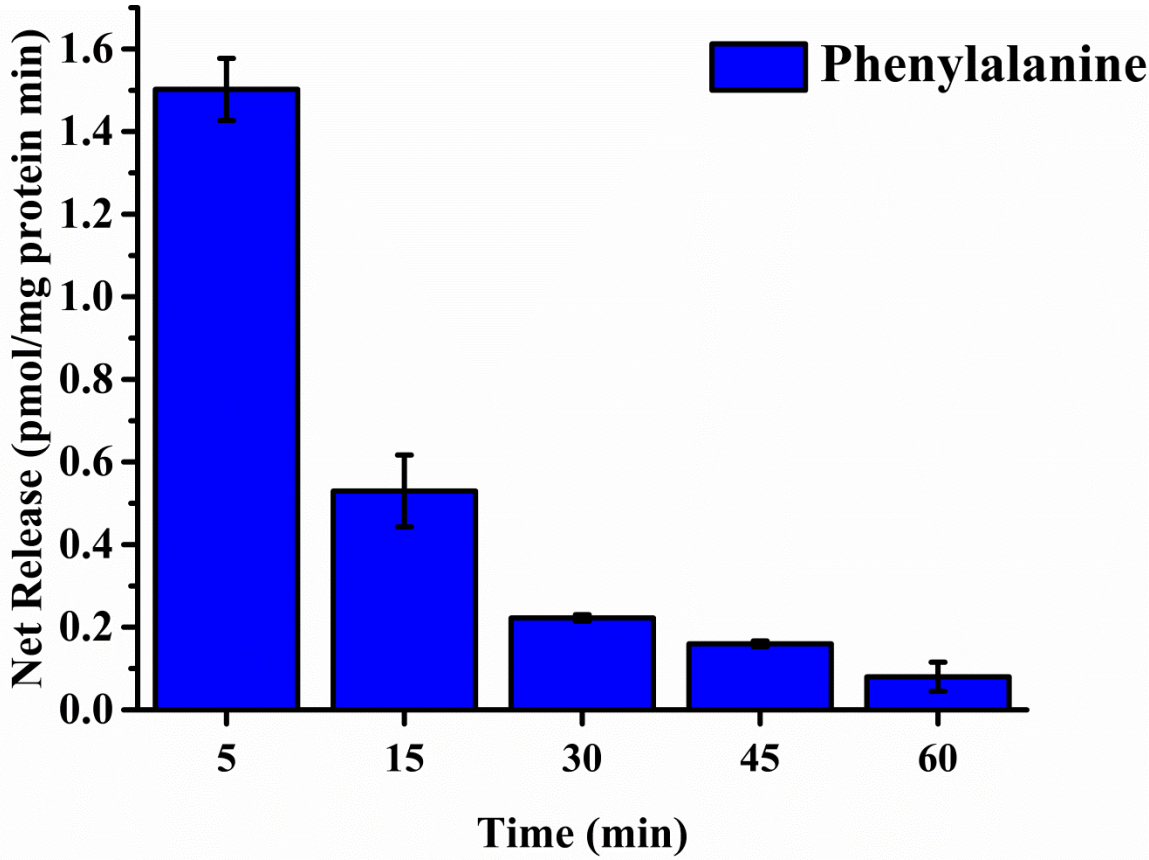

Figure A.4. Net rate of phenylalanine efflux by 3T3-L1 cells incubated with Ringer's solution + 5 mM glucose and 200 µM isoleucine, leucine and valine for time periods ranging from 5 to 60 minutes. Rate was normalized to cell protein content as determined by BCA assay. Error bars are SE for n=3 samples.

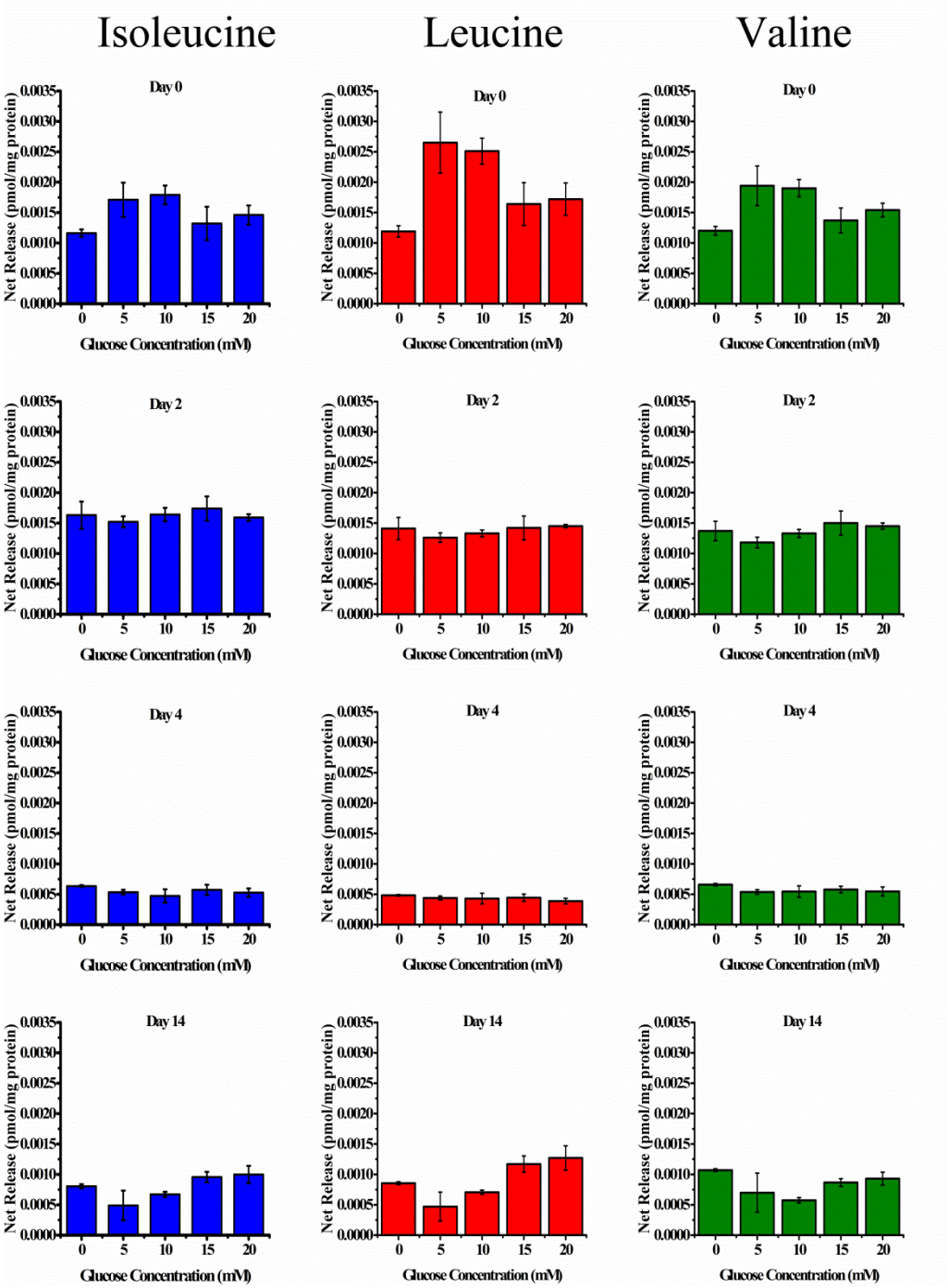

Figure A.5. Rate of isoleucine, leucine, and valine release at each stage of differentiation by 3T3-L1 cells incubated with Ringer's solution, 200 μM BCAAs, and varying concentrations of glucose. Rates were normalized to cell protein content as determined by BCA assay. Error bars are SE for n=3 samples.

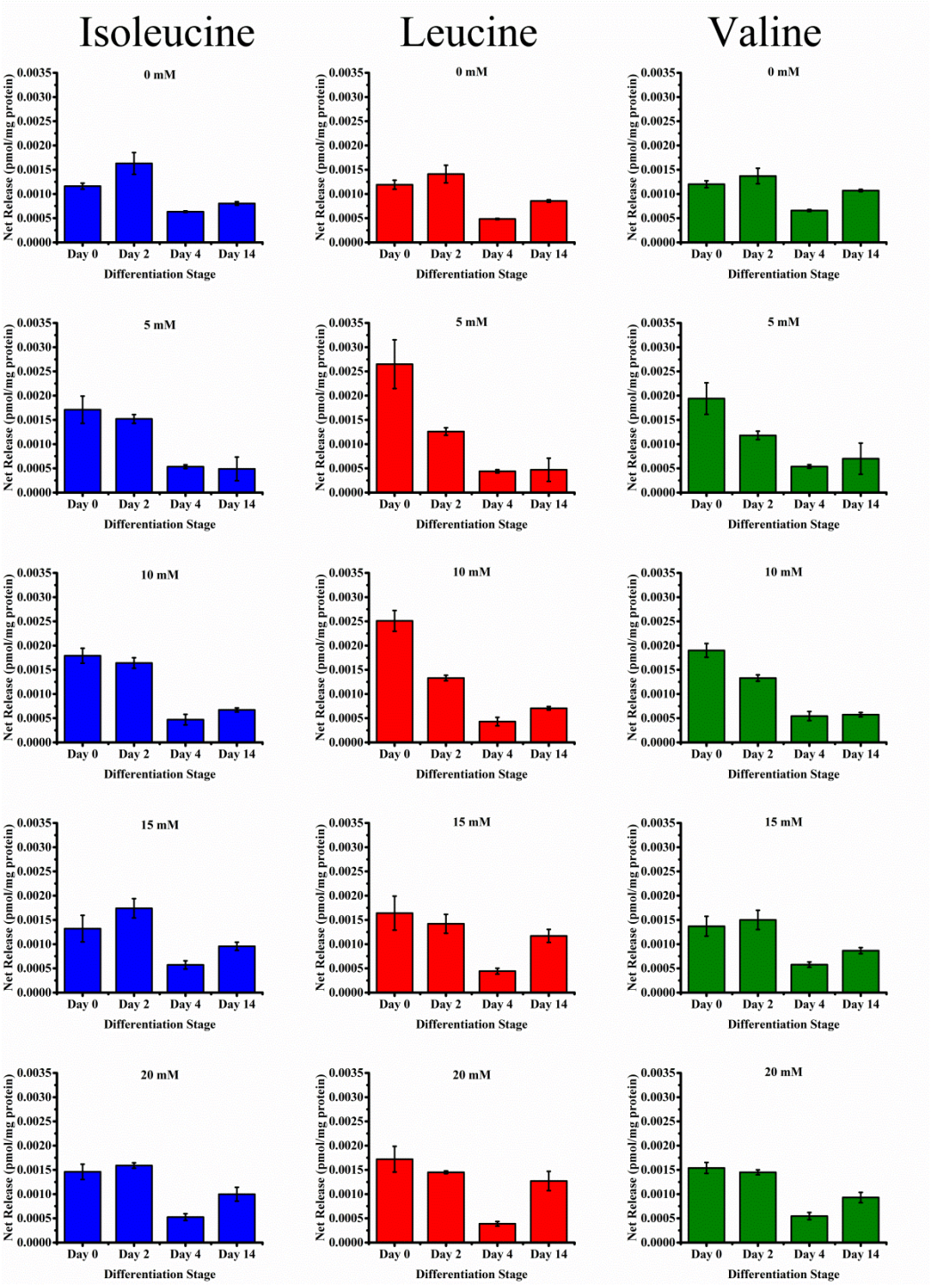

Figure A.6 . Rate of isoleucine, leucine, and valine uptake after incubation with varying concentrations of glucose, at each stage of differentiation by 3T3-L1 cells incubated with Ringer's solution, 200 μM BCAAs, and varying concentrations of glucose. Rates were normalized to cell protein content as determined by BCA assay. Error bars are SE for n=3 samples.

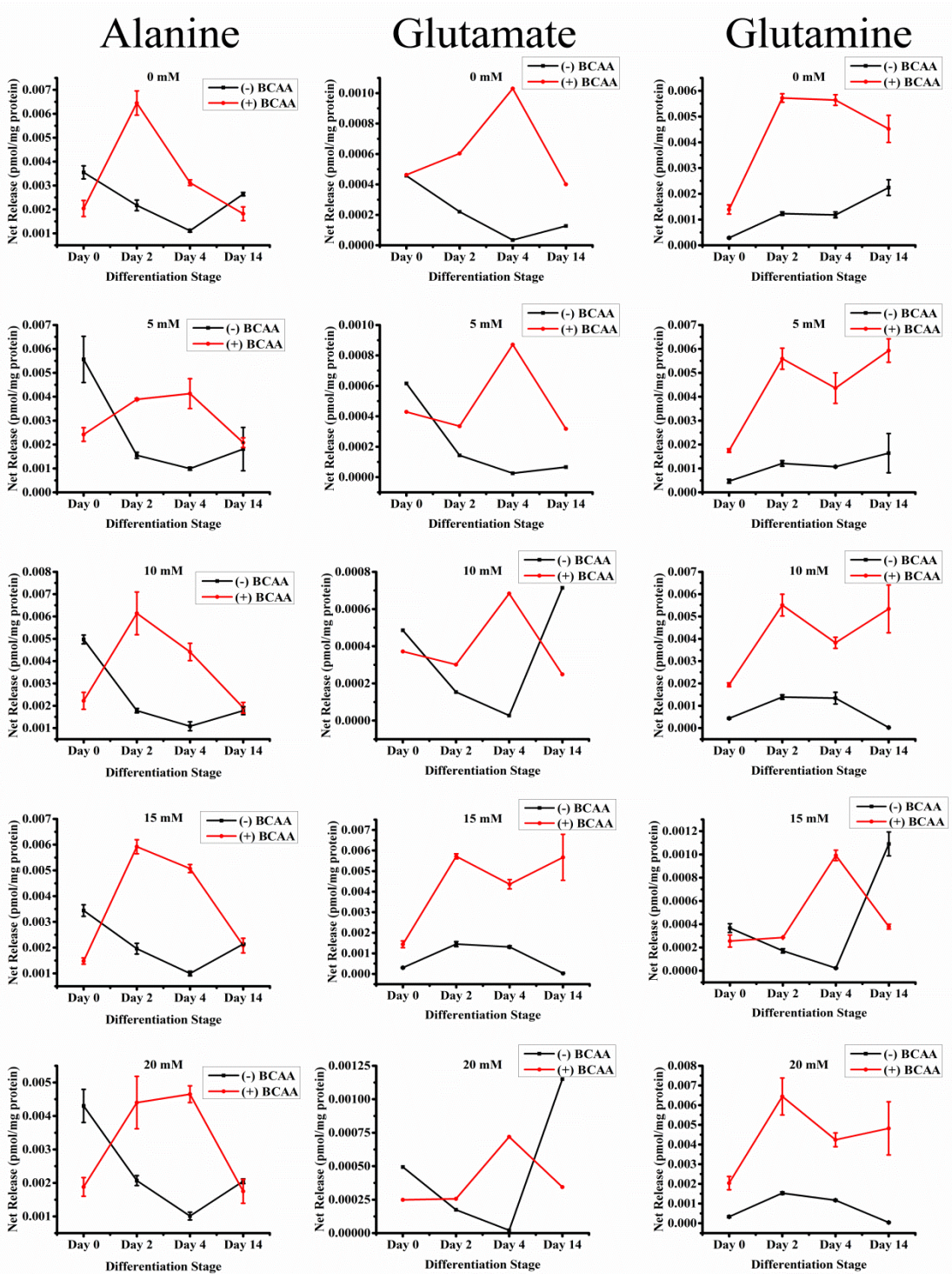

Figure A.7. Rate of alanine, glutamate, and glutamine release at each stage of differentiation after incubation with varying concentrations of glucose by 3T3-L1 cells incubated with Ringer's solution, with (red) and without (black) 200 µM BCAAs, and varying concentrations of glucose (0-20 mM). Amounts were normalized to cell protein content as determined by BCA assay. Error bars are SE for n=3 samples.

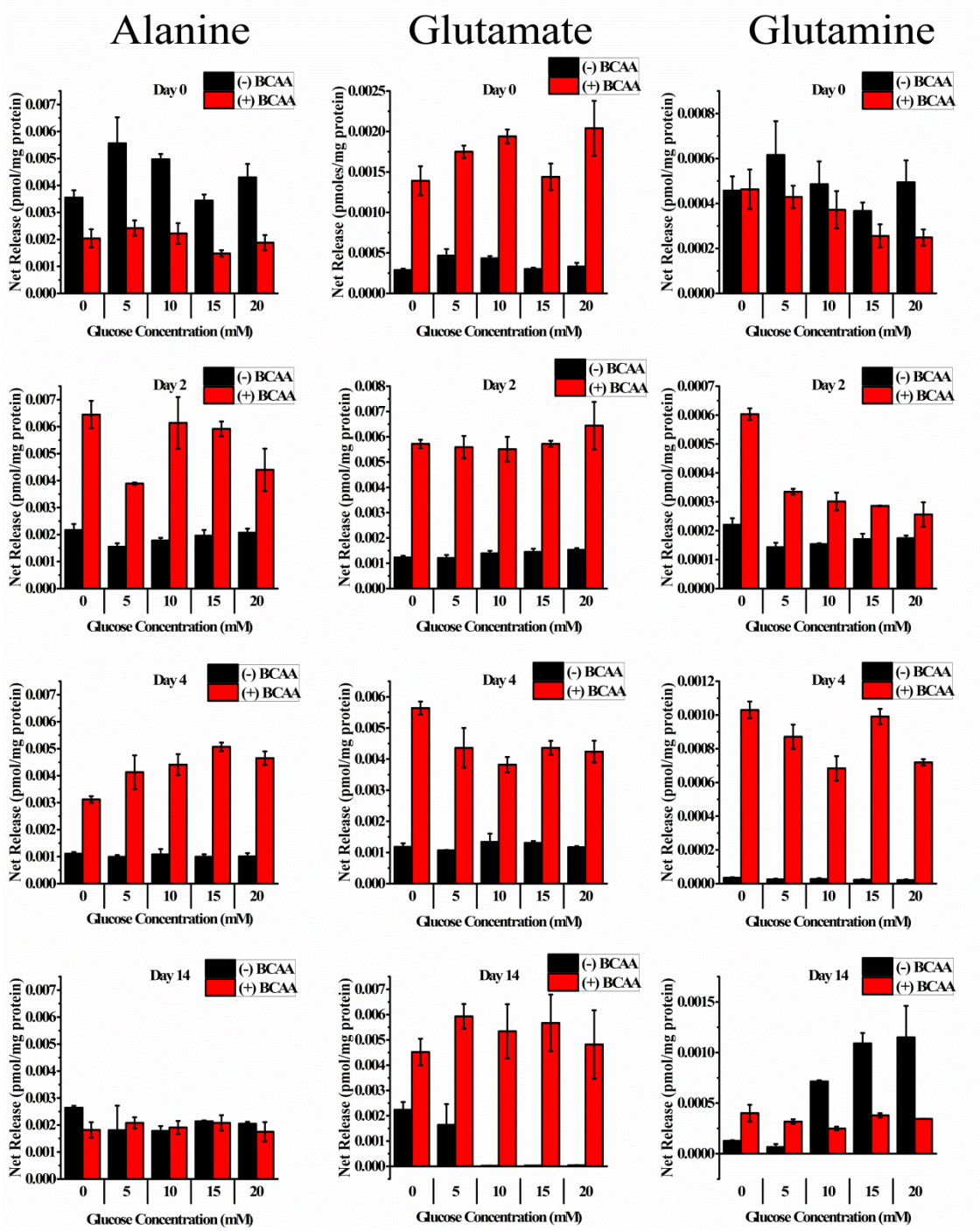

Figure A.8. Rate of alanine, glutamate, and glutamine release after incubation with varying concentrations of glucose, at each stage of differentiation, by 3T3-L1 cells incubated with Ringer's solution, with (red) and without (black) 200 µM BCAAs, and varying concentrations of glucose (0-20 mM). Amounts were normalized to cell protein content as determined by BCA assay. Error bars are SE for n=3 samples.

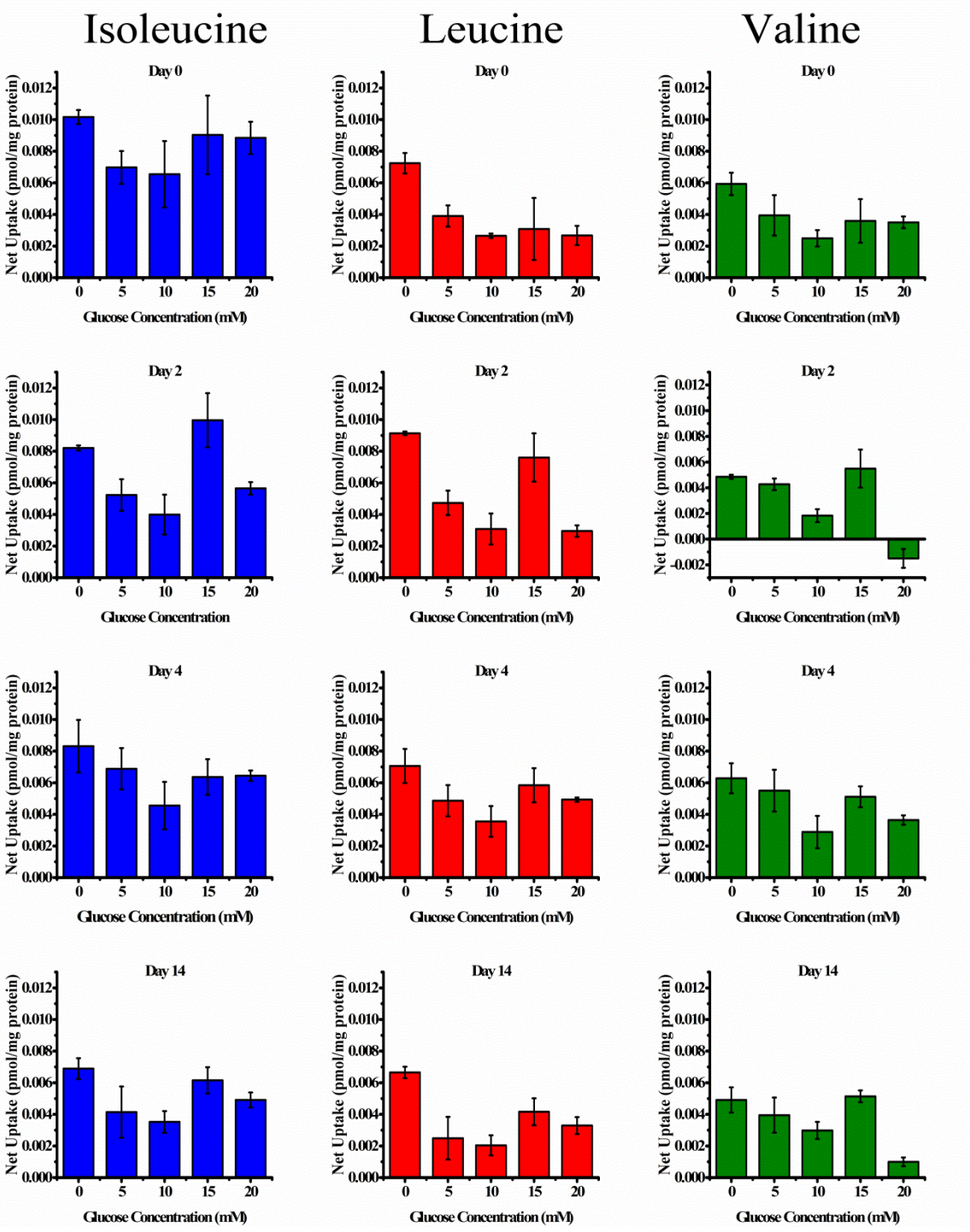

Figure A.9. Rate of isoleucine, leucine, and valine uptake at each stage of differentiation by 3T3-L1 cells incubated with Ringer's solution, 200 µM BCAAs, and varying concentrations of glucose. Rates were normalized to cell protein content as determined by BCA assay. Error bars are SE for n=3 samples.

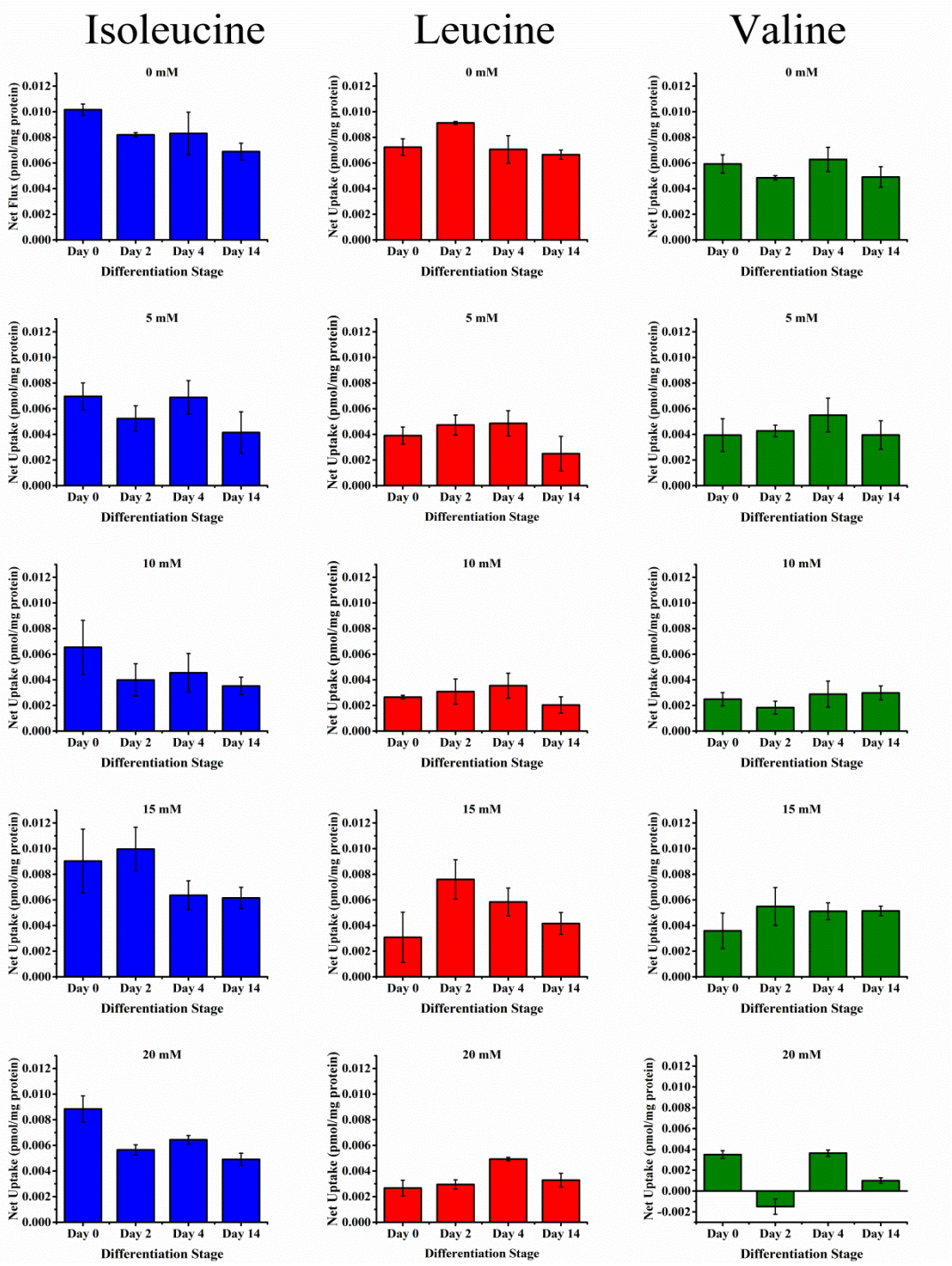

Figure A.10. Rate of isoleucine, leucine, and valine uptake after incubation with varying concentrations of glucose, at each stage of differentiation by 3T3-L1 cells incubated with Ringer's solution, 200 μM BCAAs, and varying concentrations of glucose. Rates were normalized to cell protein content as determined by BCA assay. Error bars are SE for n=3 samples.

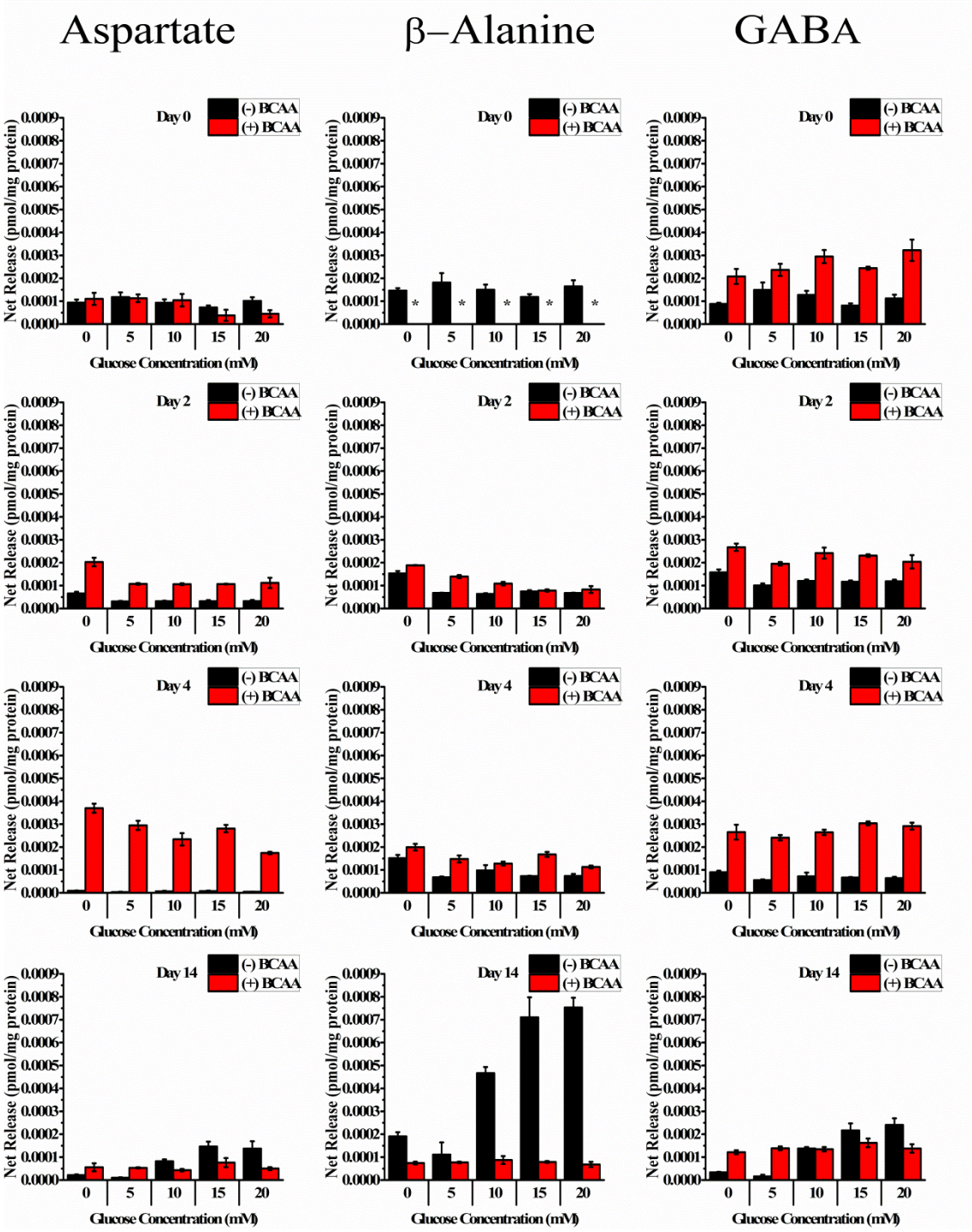

Figure A.11. Rate of aspartate, β-alanine, and GABA release after incubation with varying concentrations of glucose, at each stage of differentiation, by 3T3-L1 cells incubated with Ringer's solution, with (red) and without (black) 200 μM BCAAs, and varying concentrations of glucose (0-20 mM). Amounts were normalized to cell protein content as determined by BCA assay. Error bars are SE for n=3 samples.

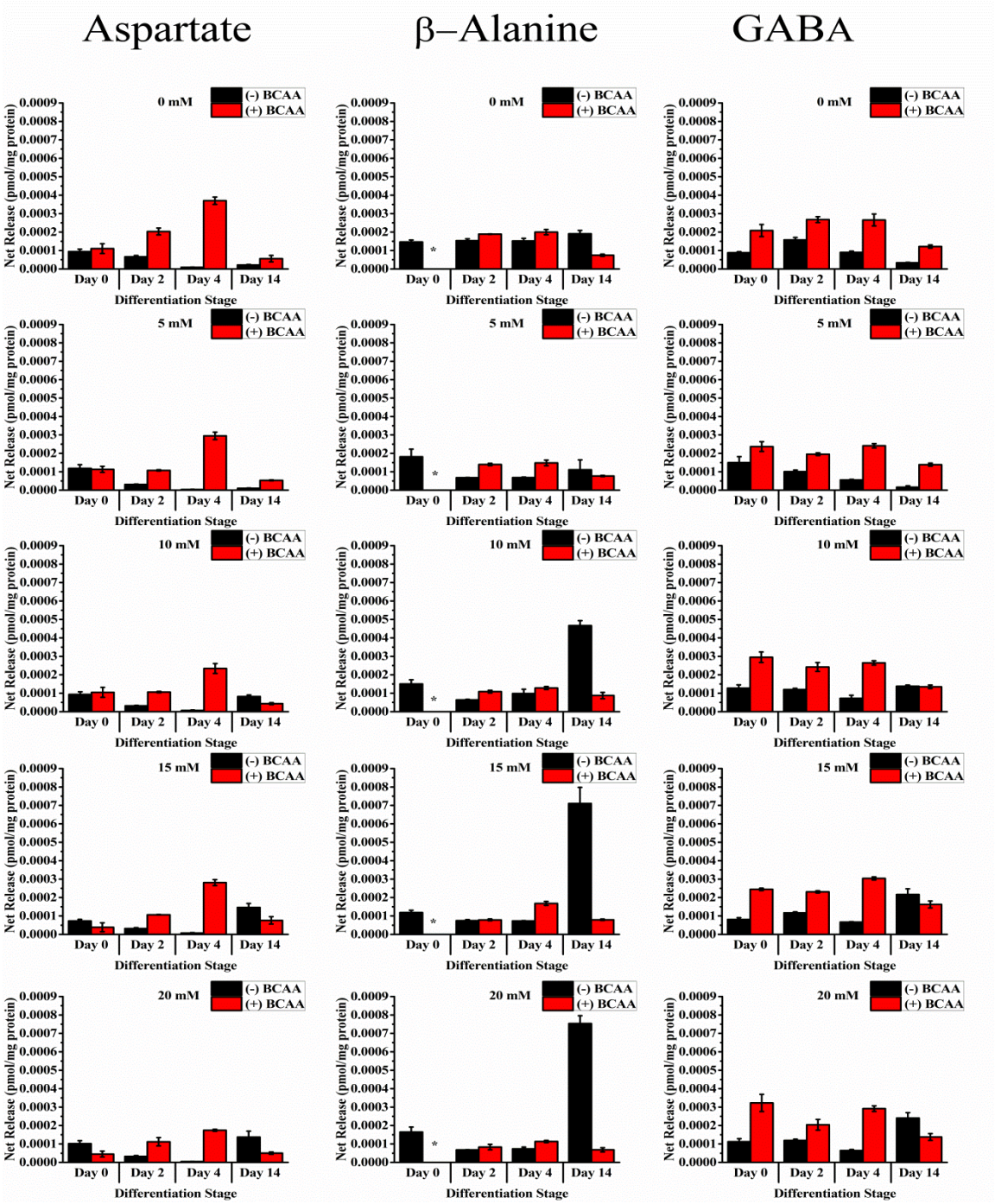

Figure A.12. Rate of aspartate, β- alanine, and GABA release at each stage of differentiation after incubation with varying concentrations of glucose by 3T3-L1 cells incubated with Ringer's solution, with (red) and without (black) 200 μM BCAAs, and varying concentrations of glucose (0-20 mM). Amounts were normalized to cell protein content as determined by BCA assay. Error bars are SE for n=3 samples.

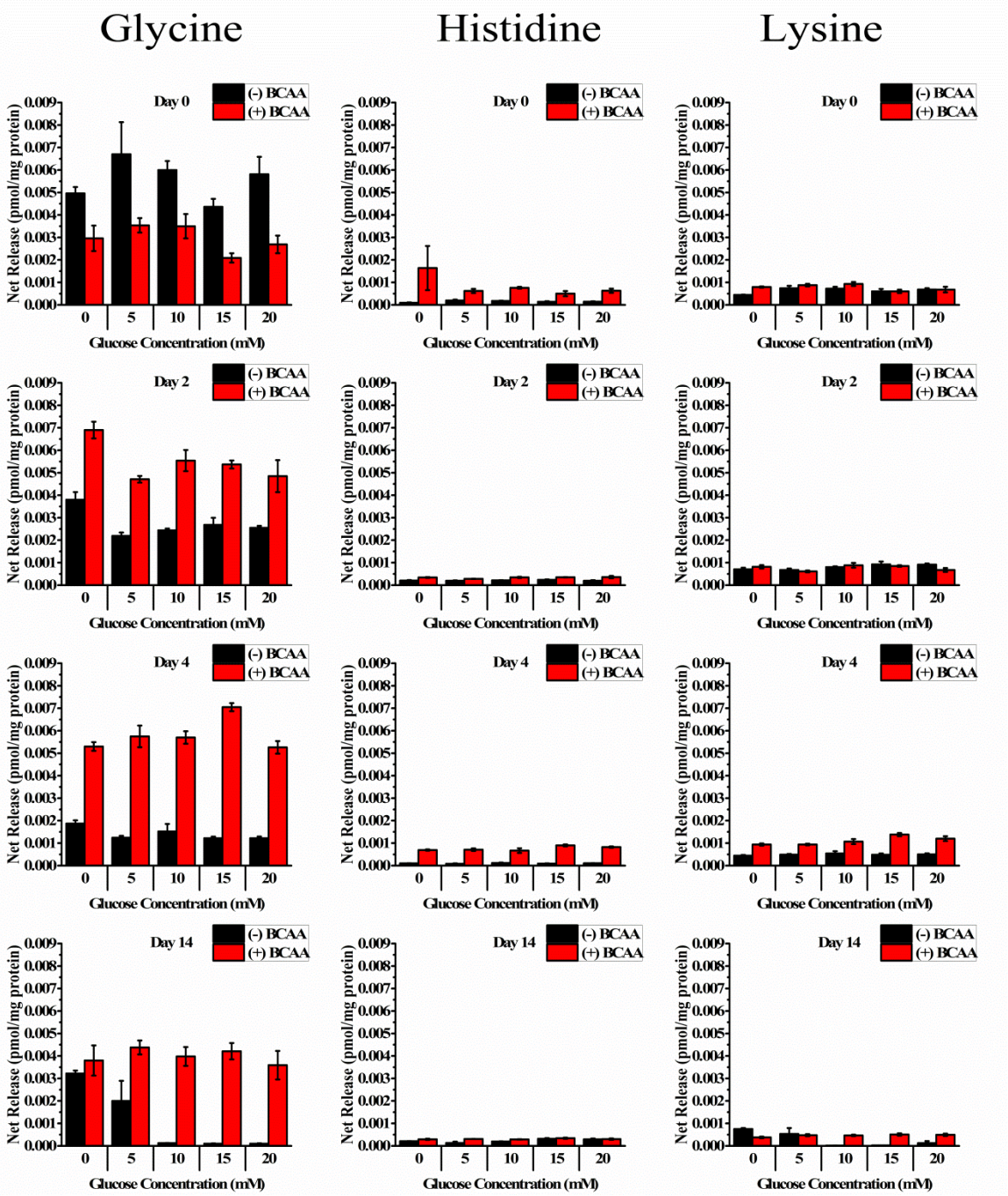

Figure A.13. Rate of glycine, histidine, and lysine release after incubation with varying concentrations of glucose, at each stage of differentiation, by 3T3-L1 cells incubated with Ringer's solution, with (red) and without (black) 200 µM BCAAs, and varying concentrations of glucose (0-20 mM). Amounts were normalized to cell protein content as determined by BCA assay. Error bars are SE for n=3 samples.

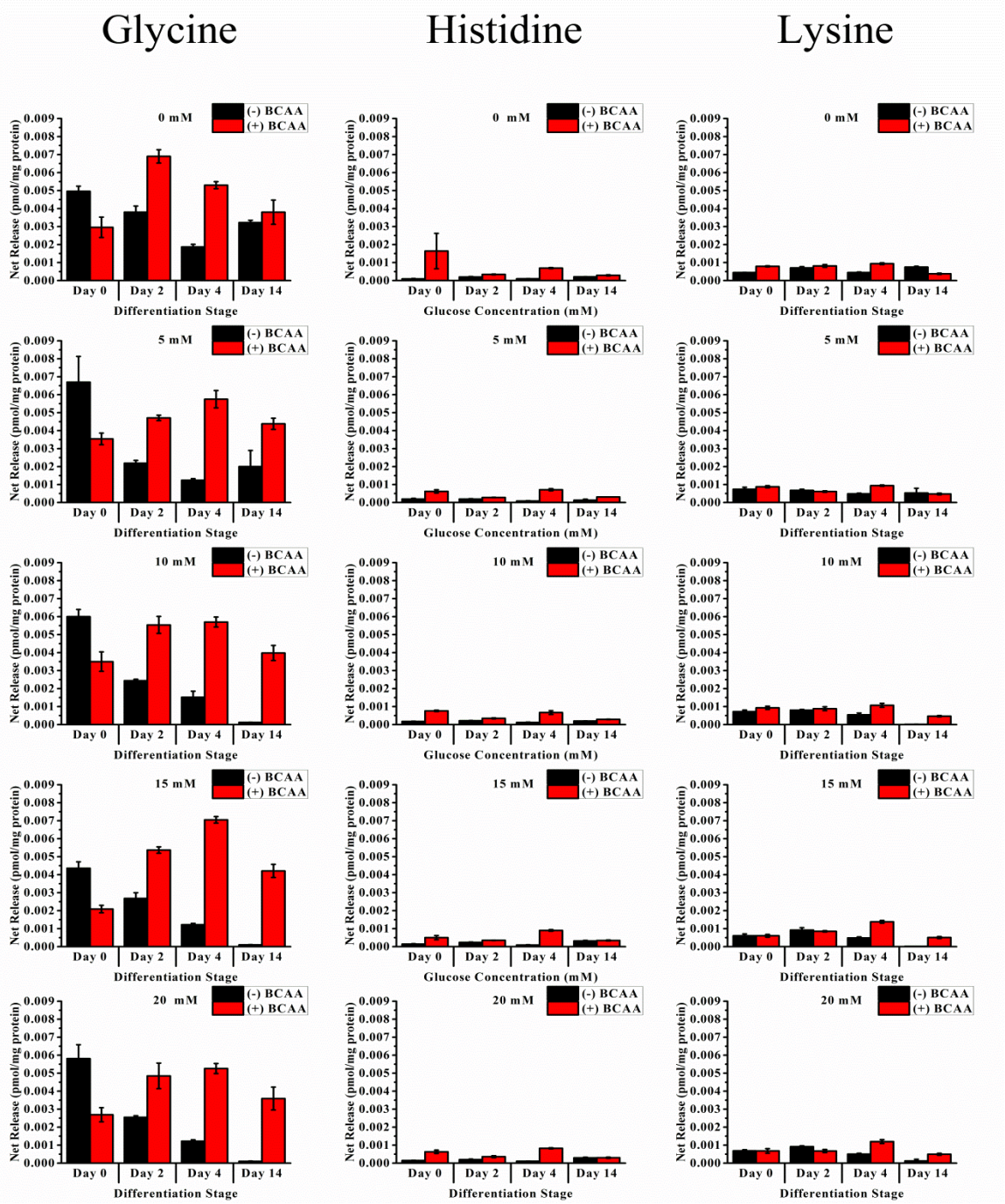

Figure A.14. Rate of glycine, histidine, and lysine release at each stage of differentiation after incubation with varying concentrations of glucose by 3T3-L1 cells incubated with Ringer's solution, with (red) and without (black) 200 µM BCAAs, and varying concentrations of glucose (0-20 mM). Amounts were normalized to cell protein content as determined by BCA assay. Error bars are SE for n=3 samples.

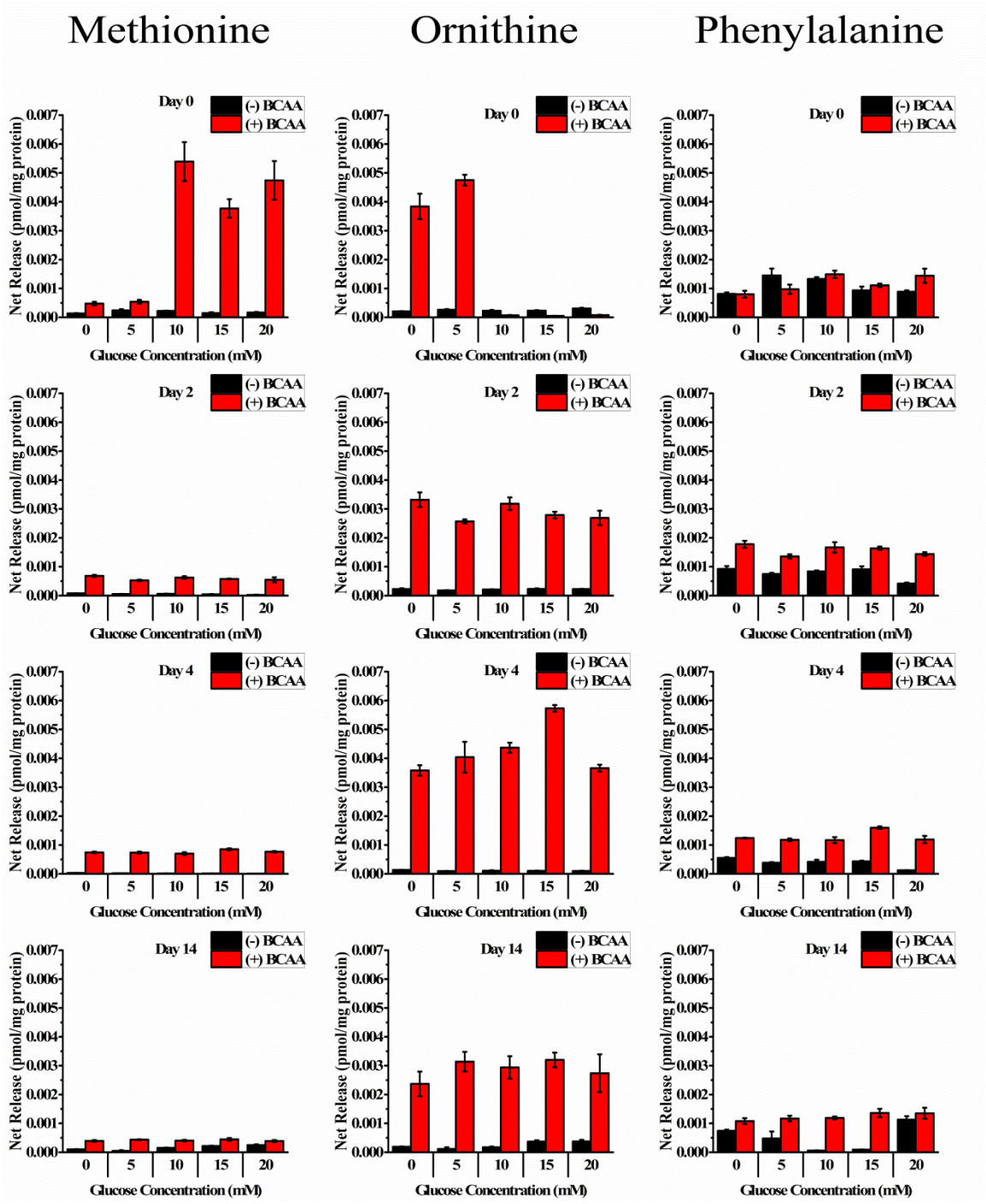

Figure A.15 Rate of methionine, ornithine, and phenylalanine release after incubation with varying concentrations of glucose, at each stage of differentiation, by 3T3-L1 cells incubated with Ringer's solution, with (red) and without (black) 200 μM BCAAs, and varying concentrations of glucose (0-20 mM). Amounts were normalized to cell protein content as determined by BCA assay. Error bars are SE for n=3 samples.

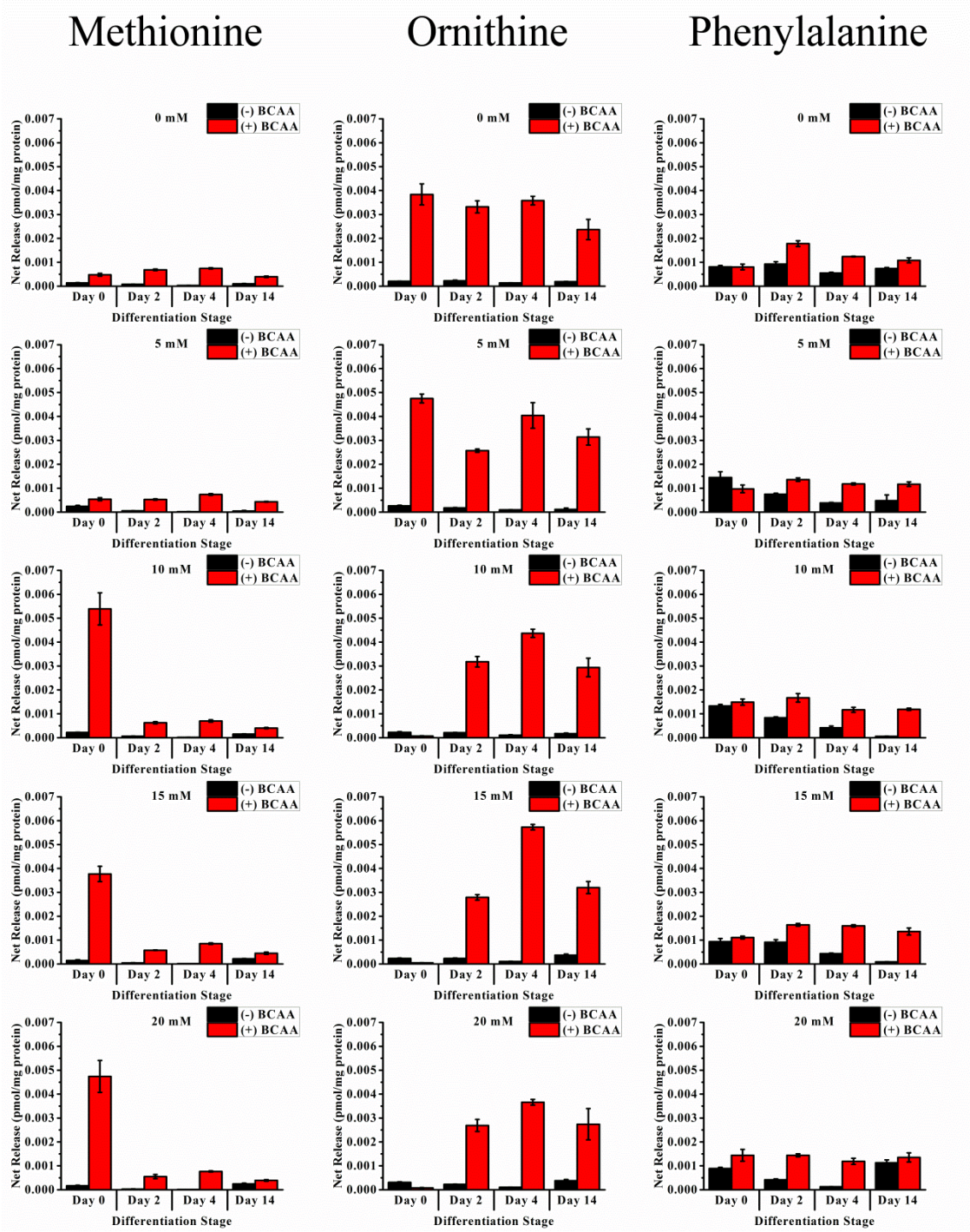

Figure A.16 Rate of methionine, ornithine, and phenylalanine release at each stage of differentiation after incubation with varying concentrations of glucose by 3T3-L1 cells incubated with Ringer's solution, with (red) and without (black) 200 µM BCAAs, and varying concentrations of glucose (0-20 mM). Amounts were normalized to cell protein content as determined by BCA assay. Error bars are SE for n=3 samples.

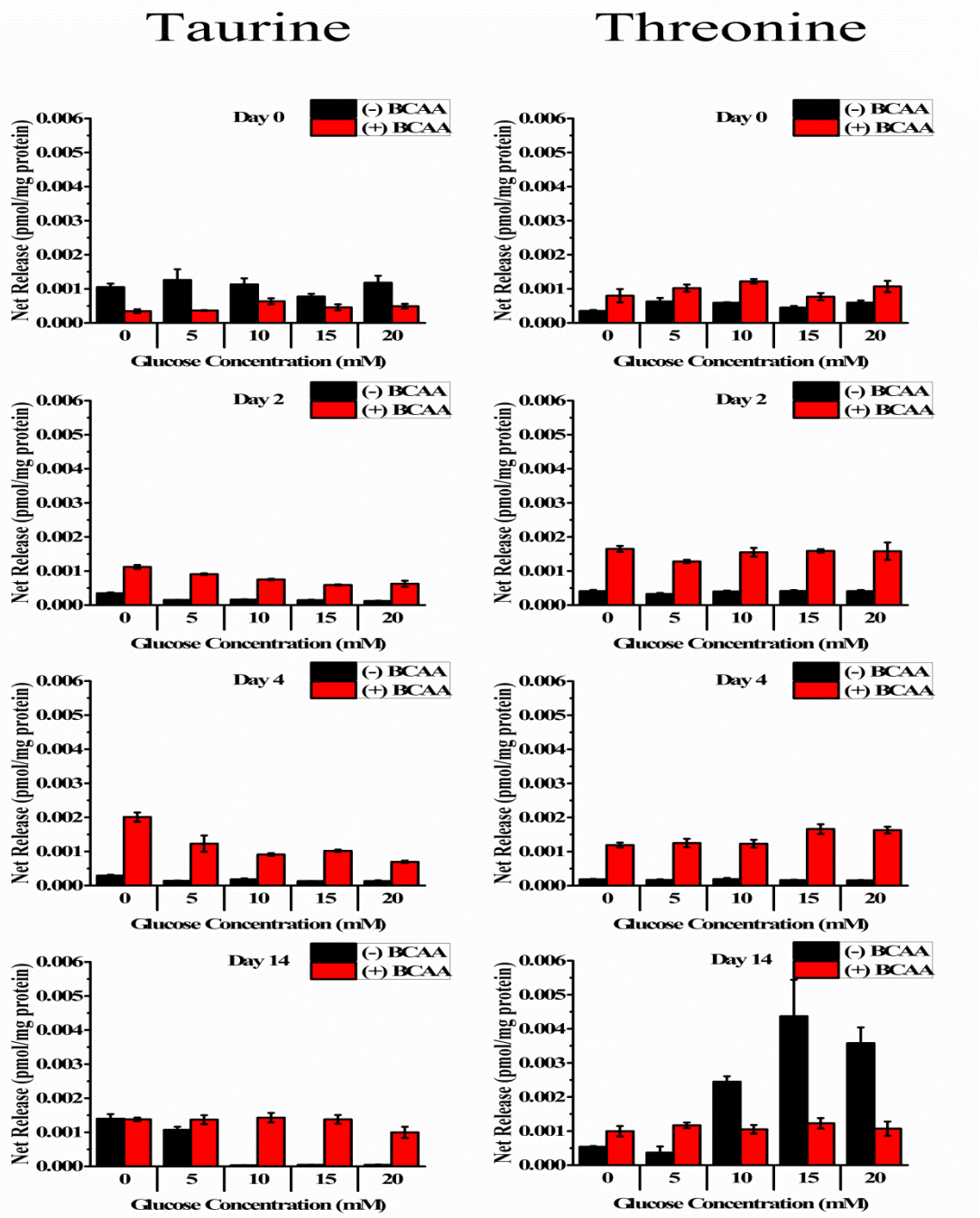

Figure A.17. Rate of taurine and threonine release after incubation with varying concentrations of glucose, at each stage of differentiation, by 3T3-L1 cells incubated with Ringer's solution, with (red) and without (black) 200 µM BCAAs, and varying concentrations of glucose (0-20 mM). Amounts were normalized to cell protein content as determined by BCA assay. Error bars are SE for n=3 samples.

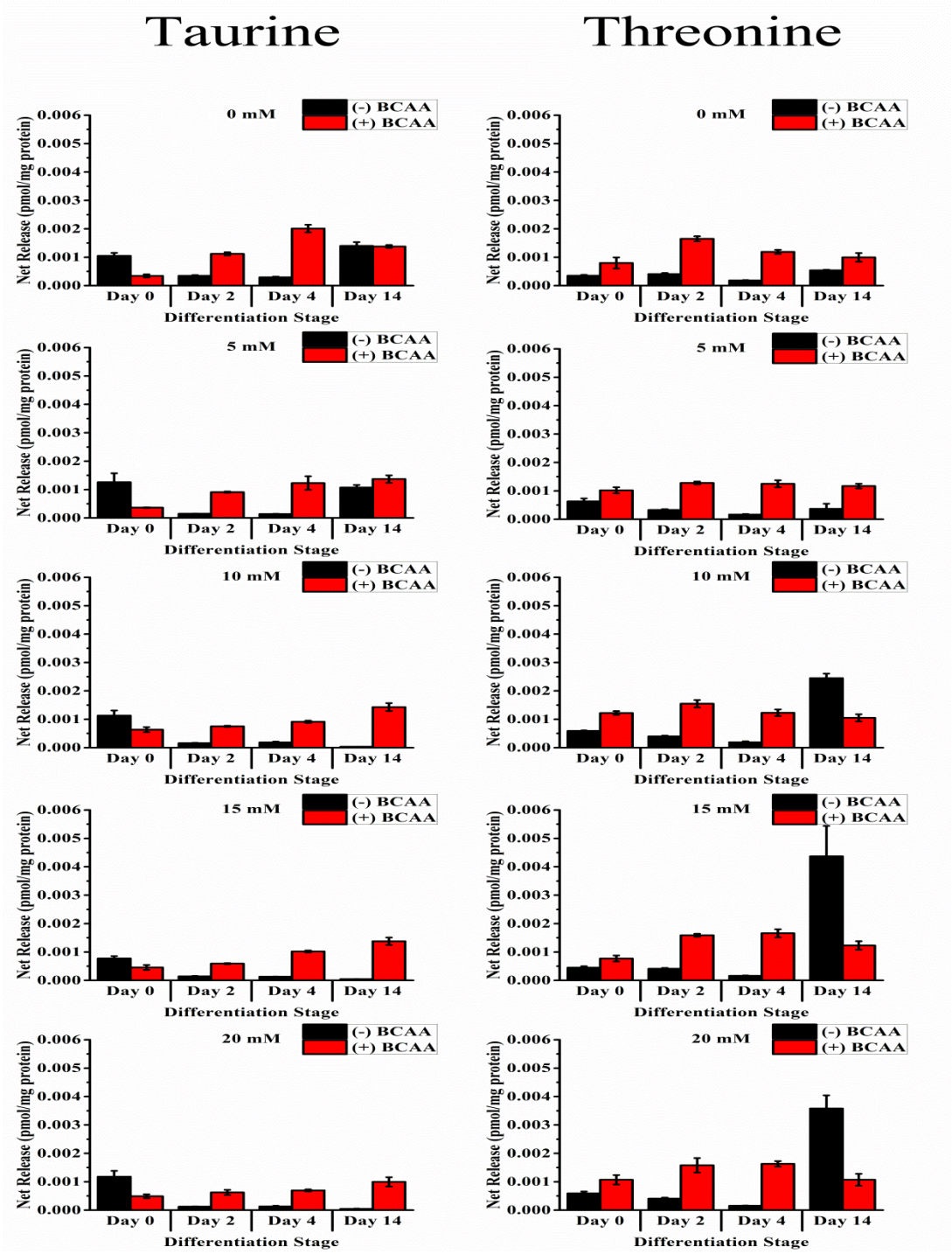

Figure A.18. Rate taurine and threonine release at each stage of differentiation after incubation with varying concentrations of glucose by 3T3-L1 cells incubated with Ringer's solution, with (red) and without (black) 200 µM BCAAs, and varying concentrations of glucose (0-20 mM). Amounts were normalized to cell protein content as determined by BCA assay. Error bars are SE for n=3 samples.

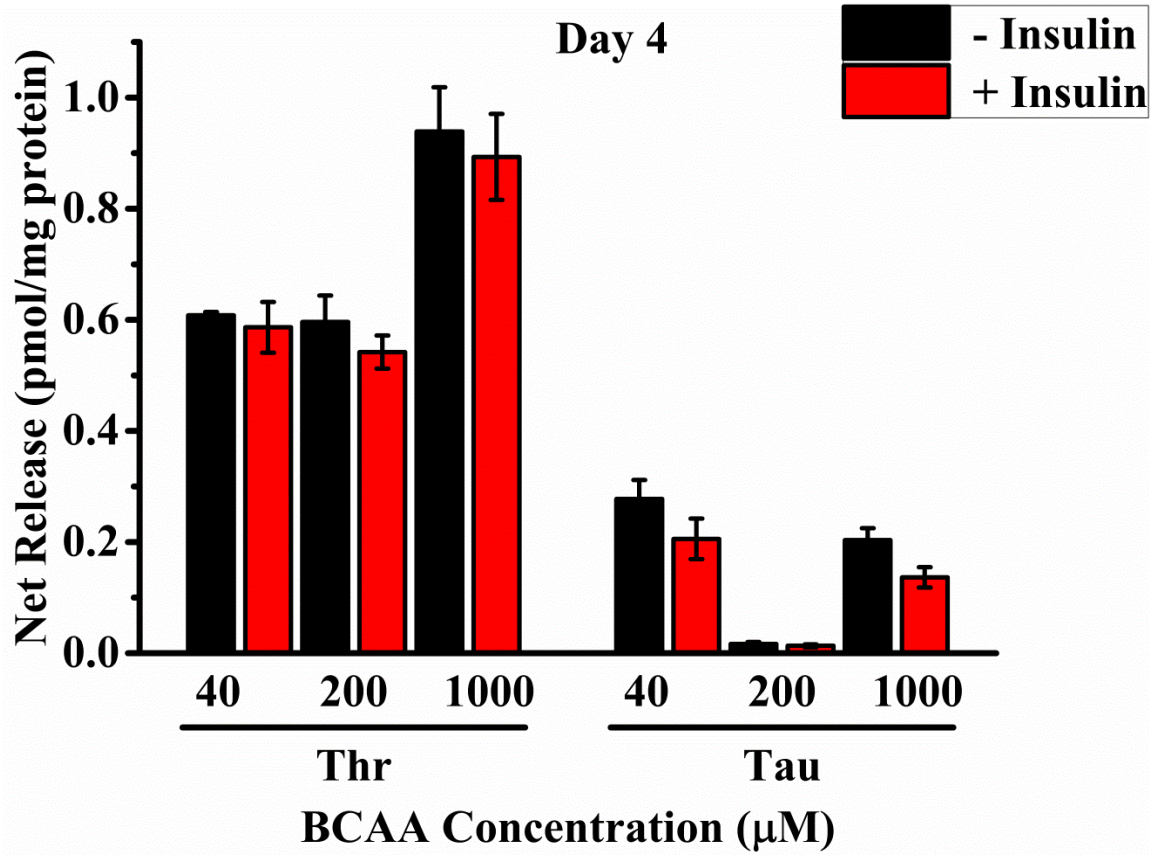

Figure A.19. Release of threonine (Thr) and taurine (Tau) on Day 4 when incubated in Ringer's solution with (red) and without (black) 10 nM insulin, 5 mM glucose, and either 40, 200, or 1000 μM BCAAs for 30 minutes. Error bars are SEM; n=3.

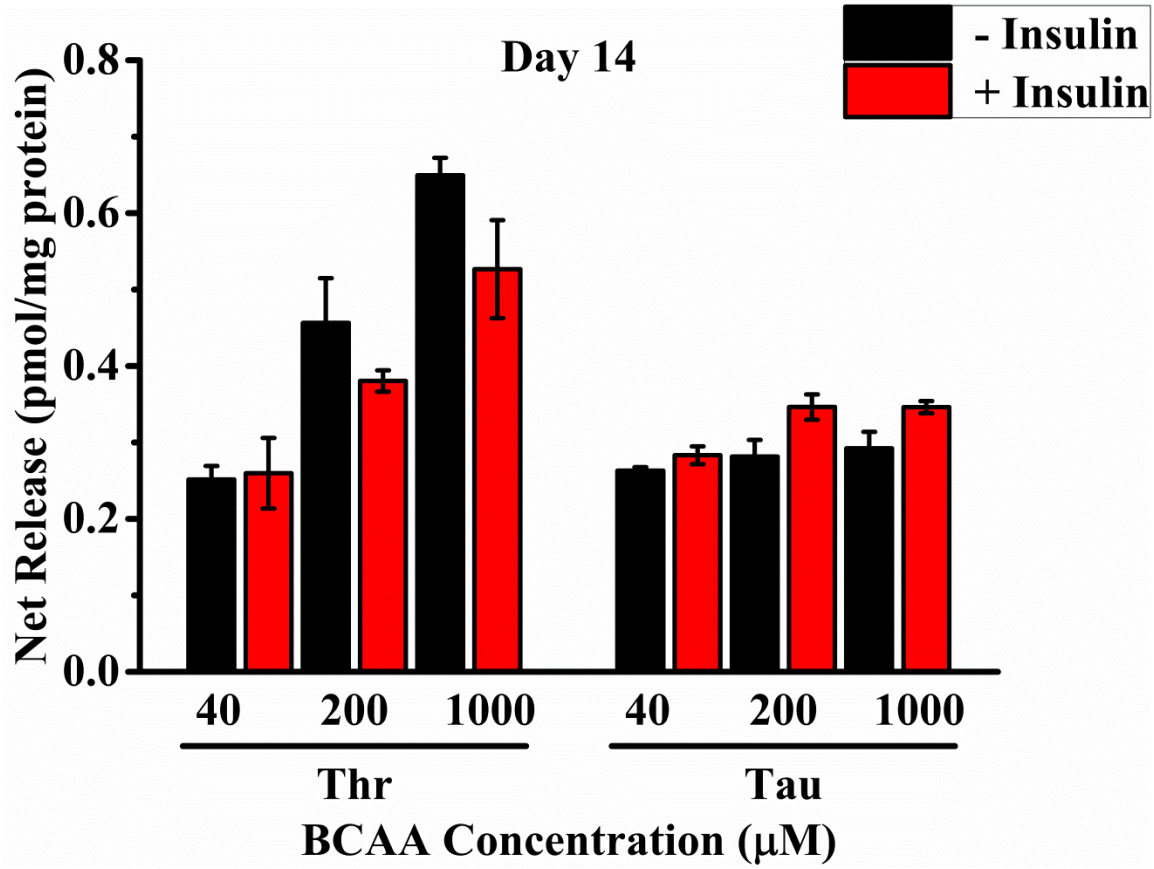

Figure A.20. Release of threonine (Thr) and taurine (Tau) on Day 14 when incubated in Ringer's solution with (red) and without (black) 10 nM insulin, 5 mM glucose, and either 40, 200, or 1000 μM BCAAs for 30 minutes. Error bars are SEM; n=3

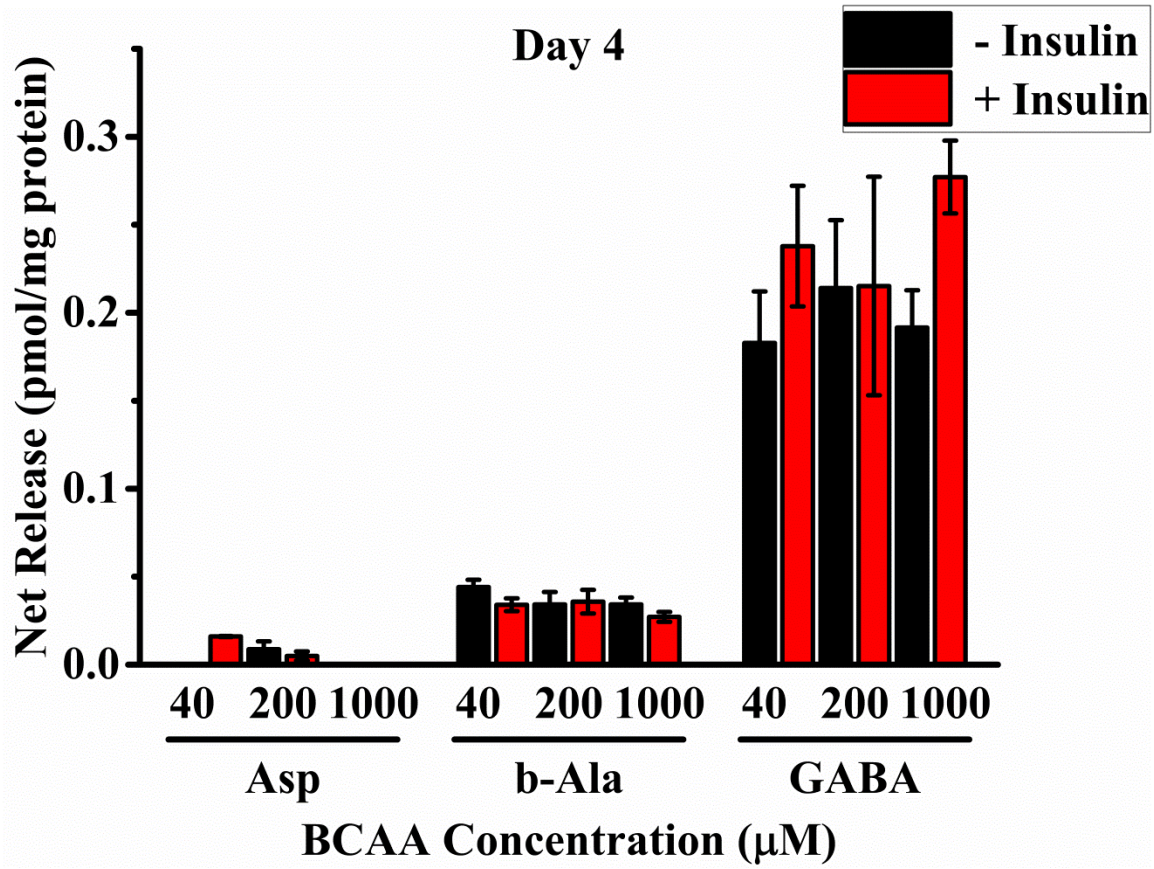

Figure A.21. Release of aspartate (Asp), β-alanine (b-Ala), and GABA on Day 4 when incubated in Ringer's solution with (red) and without (black) 10 nM insulin, 5 mM glucose, and either 40, 200, or 1000 μM BCAAs for 30 minutes. Error bars are SEM; n=3.

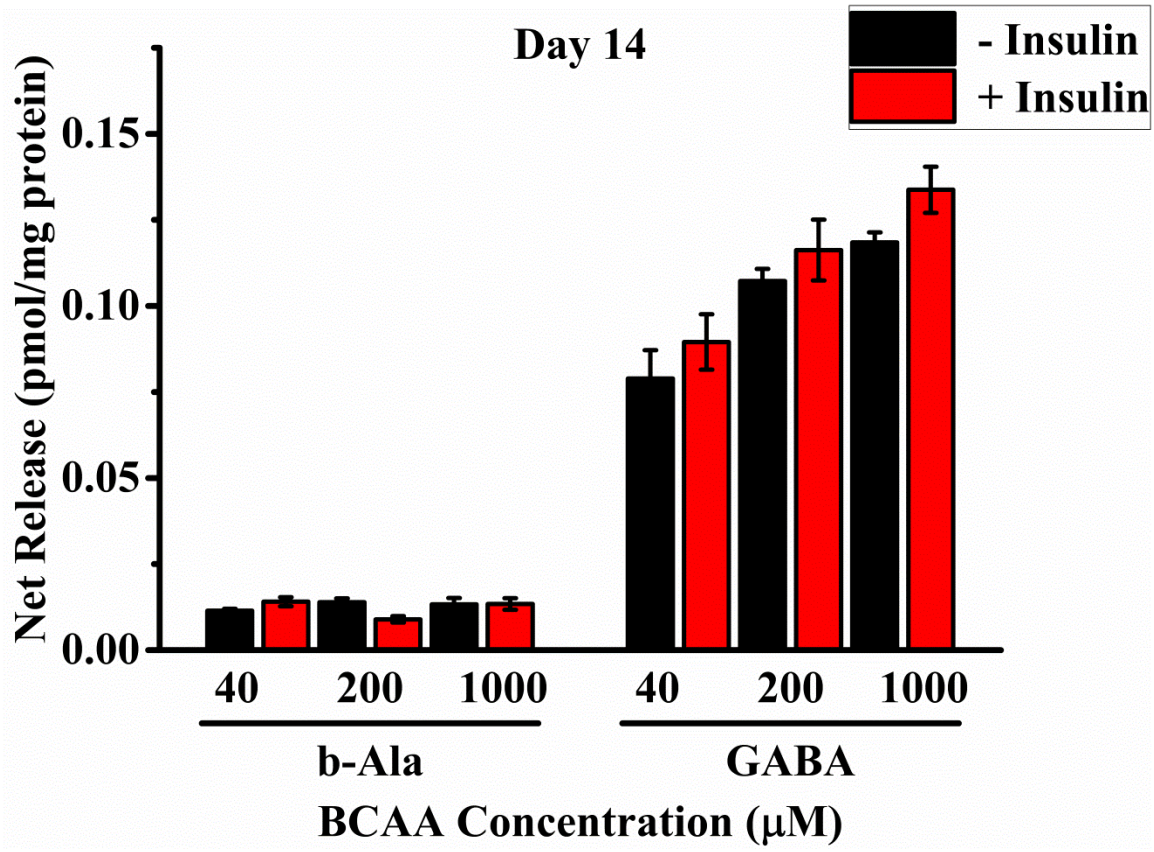

Figure A.22. . Release of β-alanine (b-Ala), and GABA on Day 14 when incubated in Ringer's solution with (red) and without (black) 10 nM insulin, 5 mM glucose, and either 40, 200, or 1000 μM BCAAs for 30 minutes. Error bars are SEM; n=3

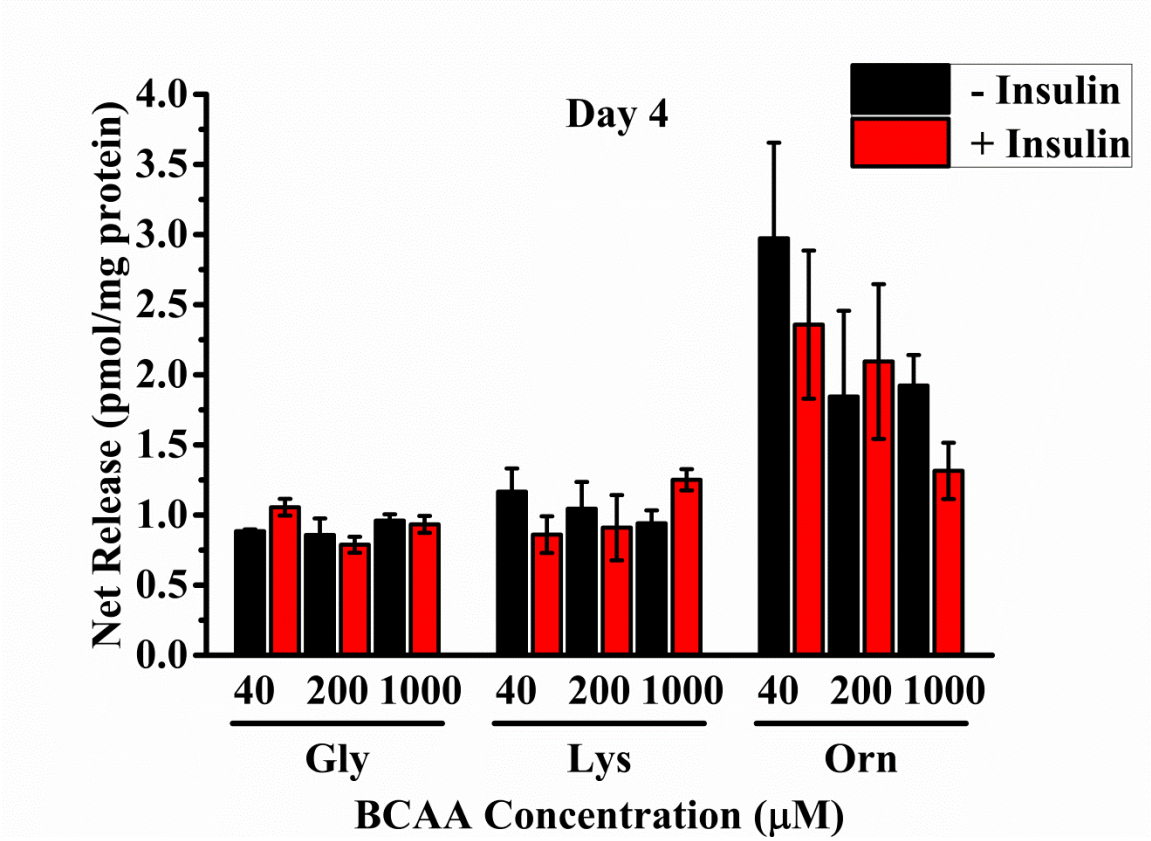

Figure A.23. Release of glycine (Gly), lysine (Lys), and ornithine (Orn) on Day 4 when incubated in Ringer's solution with (red) and without (black) 10 nM insulin, 5 mM glucose, and either 40, 200, or 1000 μM BCAAs for 30 minutes. Error bars are SEM; n=3

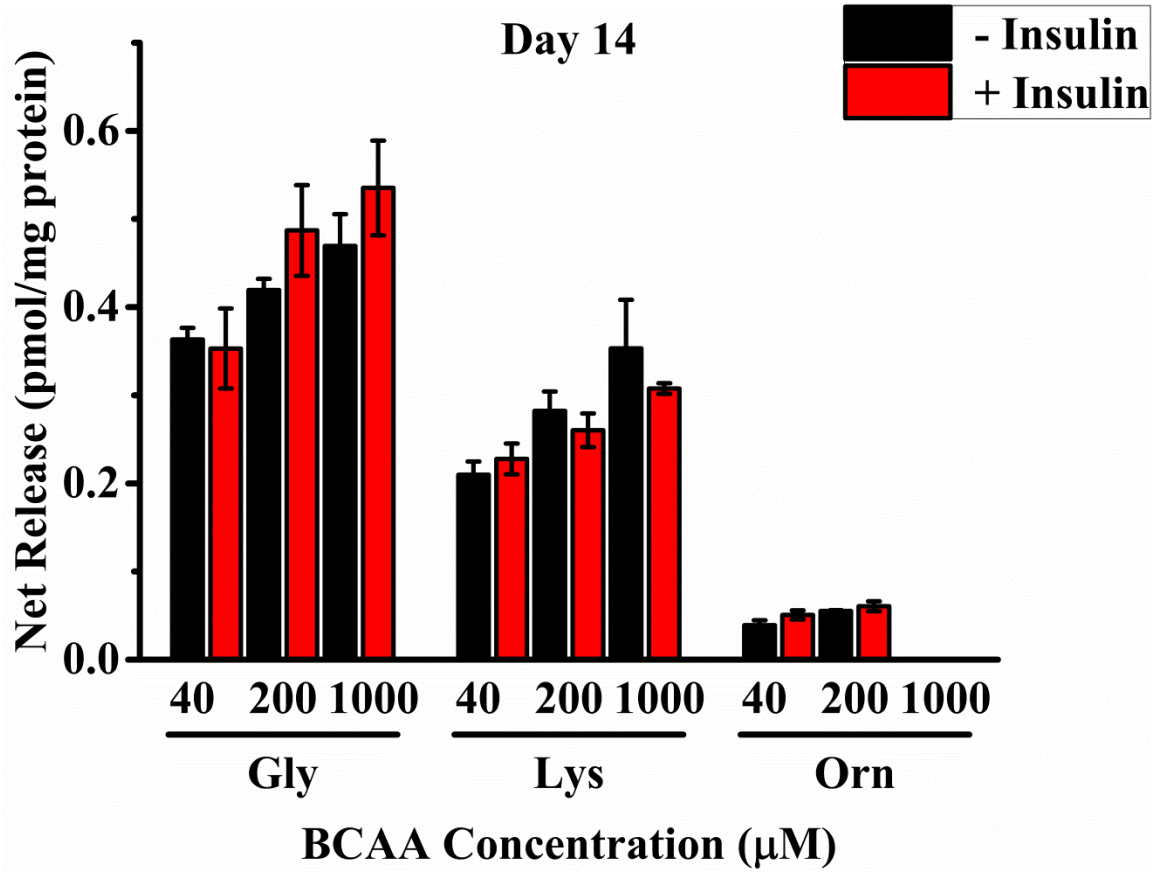

Figure A.24. . Release of glycine (Gly), lysine (Lys), and ornithine (Orn) on Day 14 when incubated in Ringer's solution with (red) and without (black) 10 nM insulin, 5 mM glucose, and either 40, 200, or 1000 μM BCAAs for 30 minutes. Error bars are SEM; n=3

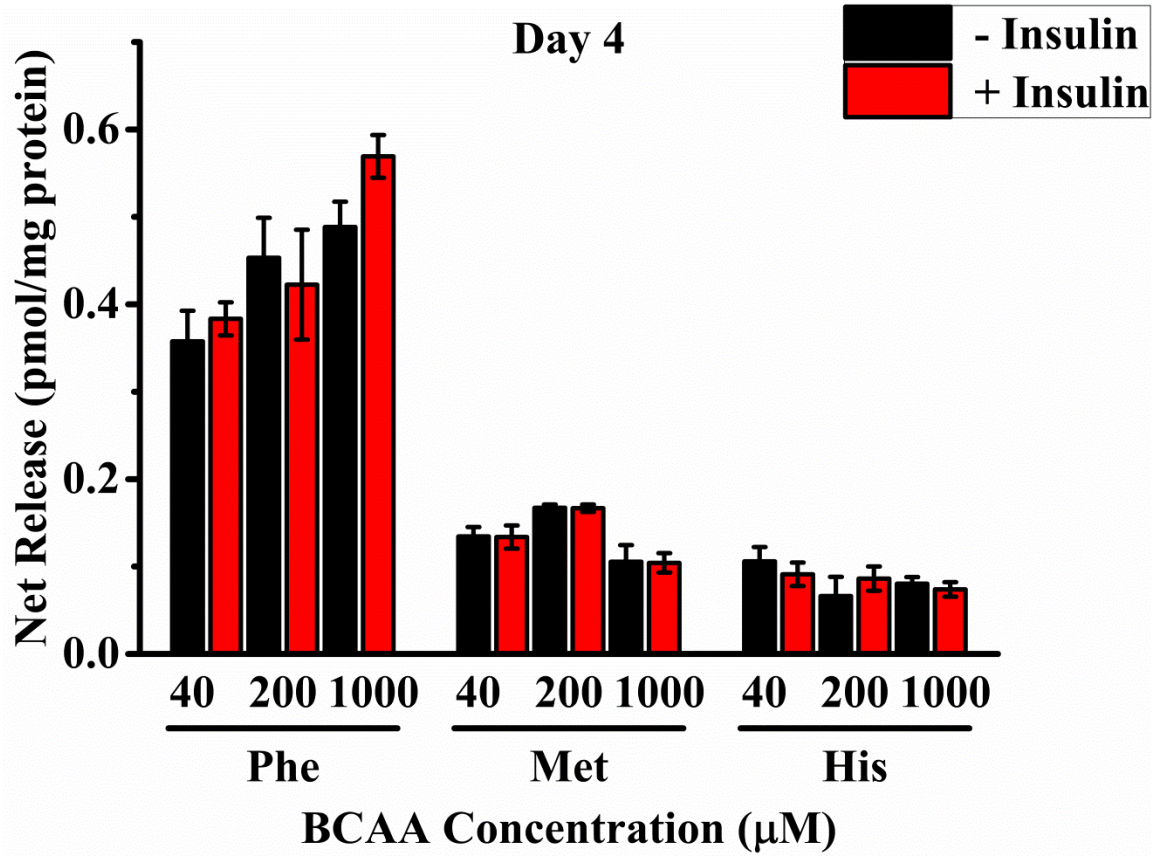

Figure A.25. Release of phenylalanine (Phe), methionine (Met), and histidine (His) on Day 4 when incubated in Ringer's solution with (red) and without (black) 10 nM insulin, 5 mM glucose, and either 40, 200, or 1000 μM BCAAs for 30 minutes. Error bars are SEM; n=3.

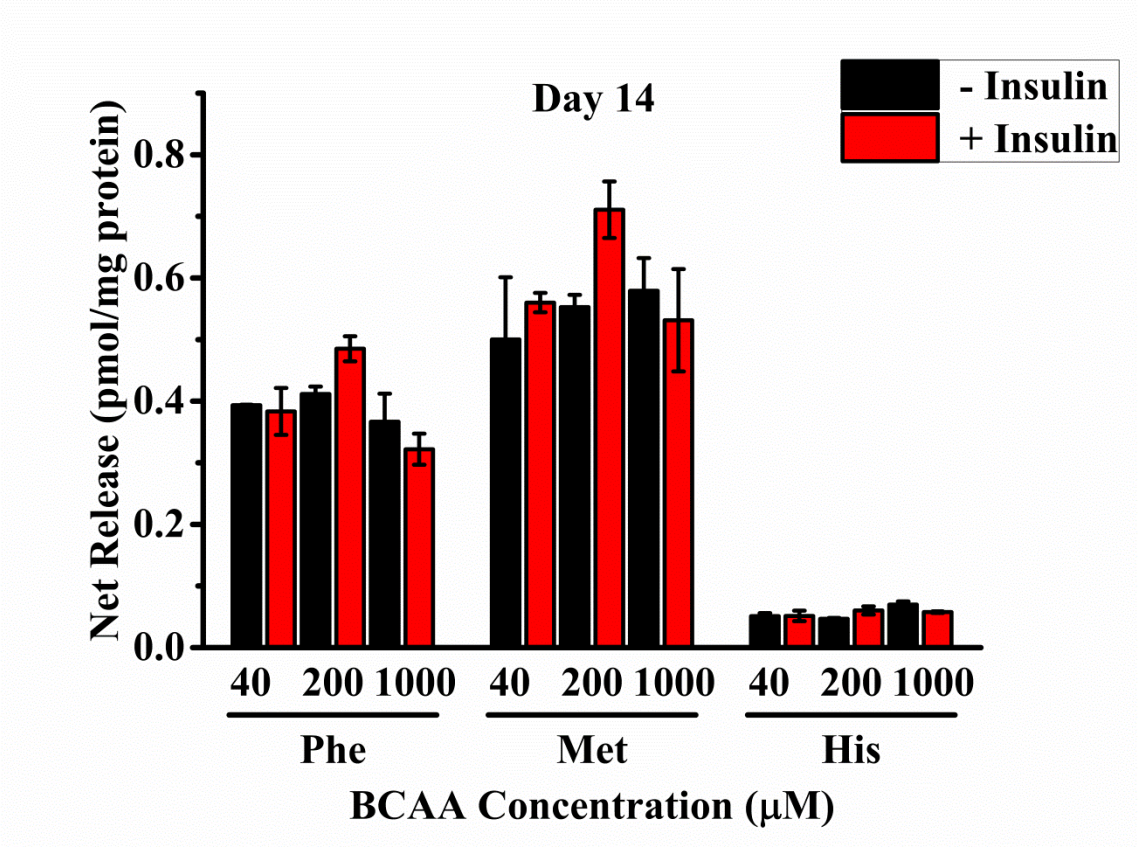

Figure A.26. . Release phenylalanine (Phe), methionine (Met), and histidine (His) on Day 14 when incubated in Ringer's solution with (red) and without (black) 10 nM insulin, 5 mM glucose, and either 40, 200, or 1000 μM BCAAs for 30 minutes. Error bars are SEM; n=3

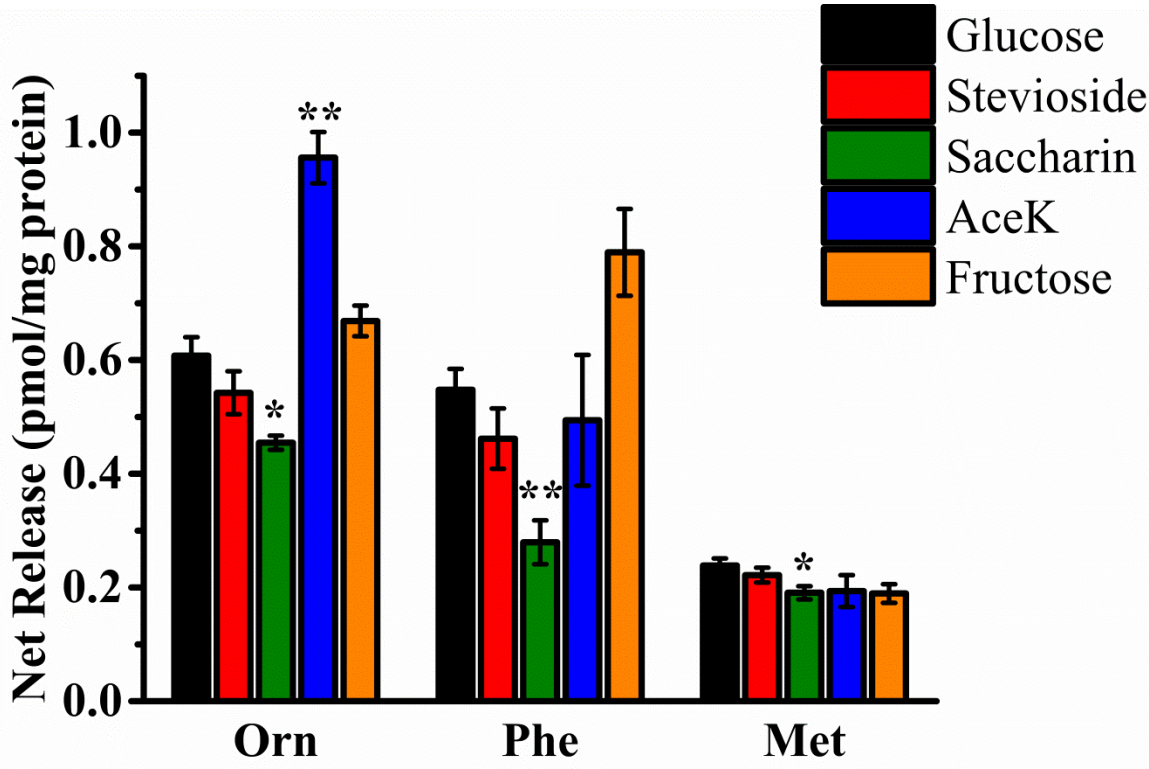

Figure A.27 Release of ornithine (Orn), phenylalanine (Phe), and methionine (Met) on Day 4 when incubated in Ringer's solution, 200 µM BCAAs, and either glucose (5 mM, black), or 5 mM glucose plus one of the following: stevioside (64.5µM, red), saccharin (350 µM, green), AceK (968 µM, blue), or fructose (30 mM, orange) for 30 minutes. Error bars are SEM; n = 3 samples. *, p-value < 0.05, **, p-value < 0.01 compared to incubation with 5 mM glucose only (black).

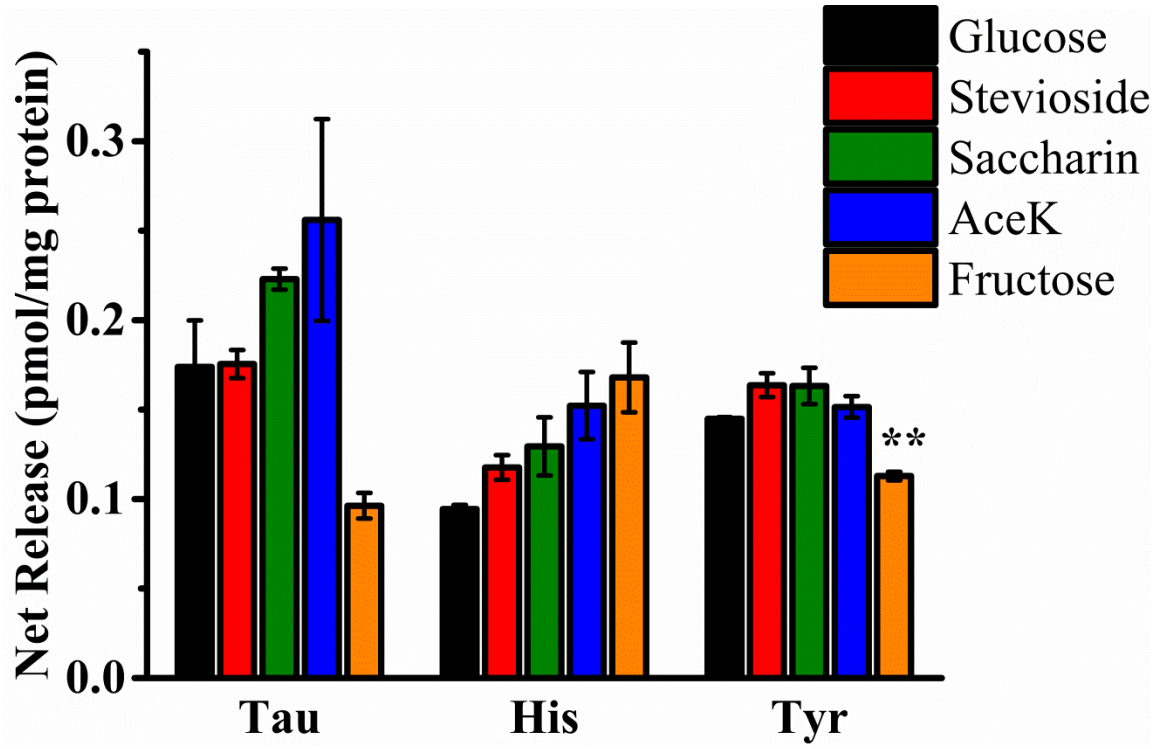

Figure A.28 Release of taurine (Tau), histidine (His), and tyrosine (Tyr) on Day 4 when incubated in Ringer's solution, 200 µM BCAAs, and either glucose (5 mM, black), or 5 mM glucose plus one of the following: stevioside (64.5µM, red), saccharin (350 µM, green), AceK (968 µM, blue), or fructose (30 mM, orange) for 30 minutes. Error bars are SEM; n = 3 samples. *, p-value < 0.05, **, p-value < 0.01 compared to incubation with 5 mM glucose only (black).

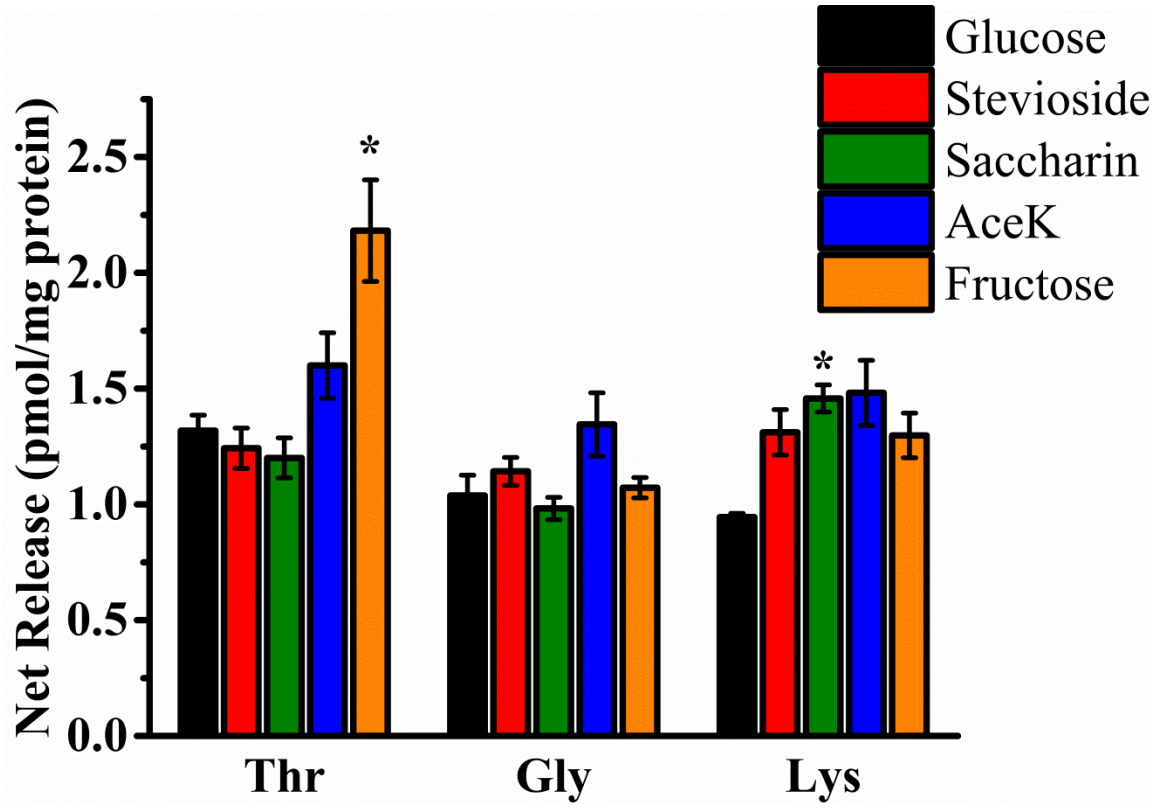

Figure A.29. Release of threonine (Thr), glycine (Gly), and lysine (Lys) on Day 4 when incubated in Ringer's solution, 200 µM BCAAs, and either glucose (5 mM, black), or 5 mM glucose plus one of the following: stevioside (64.5µM, red), saccharin (350 µM, green), AceK (968 µM, blue), or fructose (30 mM, orange) for 30 minutes. Error bars are SEM; n = 3 samples. *, p-value < 0.05, **, p-value < 0.01 compared to incubation with 5 mM glucose only (black).

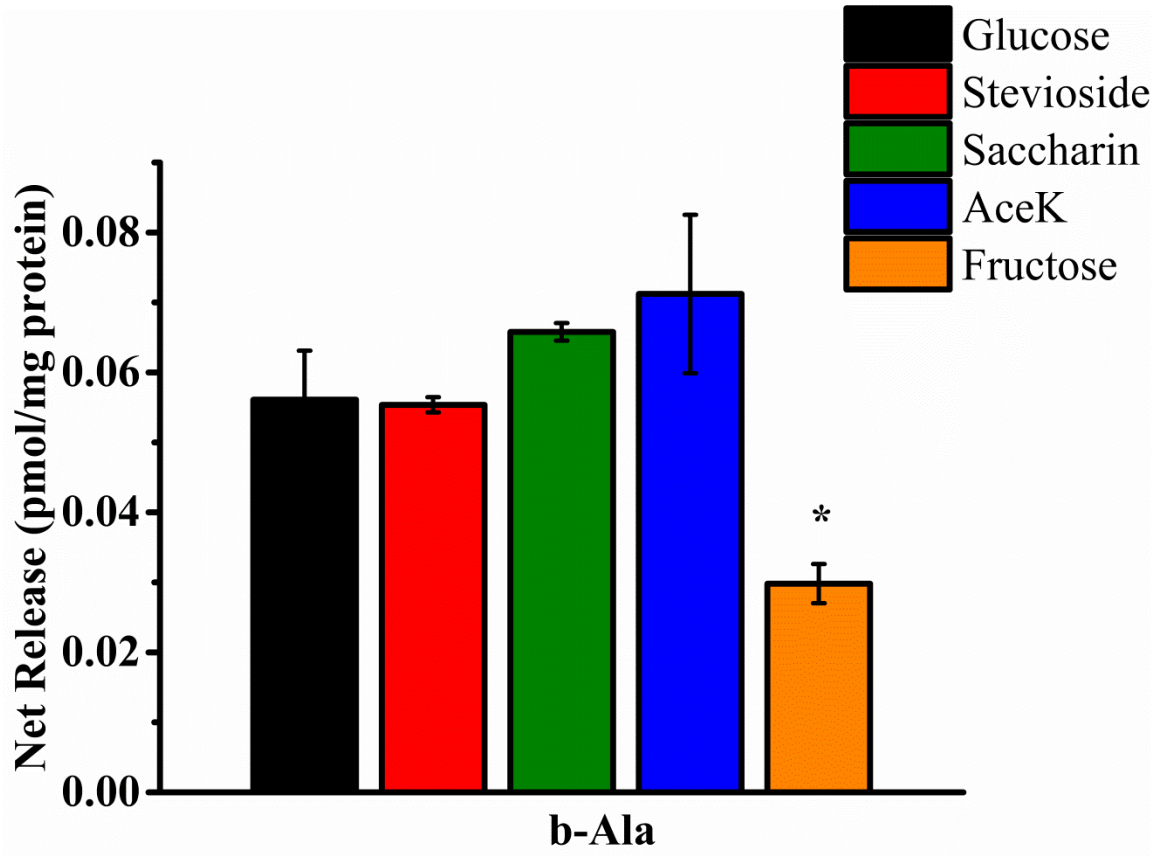

Figure A.30. Release of β-alanine (b-Ala) on Day 4 when incubated in Ringer's solution, 200 µM BCAAs, and either glucose (5 mM, black), or 5 mM glucose plus one of the following: stevioside (64.5µM, red), saccharin (350 µM, green), AceK (968 µM, blue), or fructose (30 mM, orange) for 30 minutes. Error bars are SEM; n = 3 samples. *, p-value < 0.05, **, p-value < 0.01 compared to incubation with 5 mM glucose only (black).